DEVELOPMENT OF A SEMIVOLATILE AEROSOL DICHOTOMOUS SAMPLER

A DISSERTATION
SUBMITTED TO THE FACULTY OF THE GRADUATE SCHOOL
OF THE UNIVERSITY OF MINNESOTA
BY

Seung Won Kim

IN PARTIAL FULFILLMENT OF THE REQUIREMENTS
FOR THE DEGREE OF
DOCTOR OF PHILOSOPHY

Peter C. Raynor, Ph.D., Advisor

December 2008

Acknowledgements

I would like to thank Dr. Raynor, my advisor, for his academic and research guidance as well as for his encouragement. The idea of developing a new sampler, SADS, was shaky at the start of this study. I have been discouraged by SAD outcomeS a lot of times. Each time he encouraged me to keep going. I could not have made it through my studies without his encouragement and guidance.

I gratefully acknowledge Dr. Ramachandran for his nice introduction to optimization procedure and Xiaoliang Wang for his kind consultation on Fluent software. For their helpful advice, I wish to thank my other thesis committee members: Matt Simcik, Virgil Maple, Claudiu Lungu, and Peter McMurry. I also would like to acknowledge the NIOSH-sponsored Midwest Center for Occupational Health and Safety at the University of Minnesota for providing seed grants to this study and the University of Minnesota Supercomputing Institute for providing access to nice computers and useful software.

I also want to thank my fellow coworkers and friends who made my life enjoyable: Girard Griggs, Sook Ja Cho, Tara Oberg, Jodi Quam, Jo Anne Goot,

Sumati Dhawan, Mira Grice, Soo Jae Chae, Andrea Bartekova, Kenjiro Iida, James Farnsworth, Weihua Tang, M. A. Rama, Senthil Anatharaman, and Nick Stanley.

And finally, I'm grateful to my beautiful wife, Ji Young Park, and our cheerful son, Aidan, for their patience and love. Special thanks are extended to my family and friends in Korea.

Abstract

This dissertation consists of three main sections which report the procedures used to develop the semivolatile aerosol dichotomous sampler (SADS) and their results. The first section describes the theoretical background of SADS and the validation of its performance using numerical simulations and experimental data. SADS was proposed as an alternative method to overcome some of the problems of existing personal sampling methods such as evaporative loss during filter sampling. The main difference between virtual impactors and the SADS was the inverted flow ratio between the major and the minor flow. Sampling in the SADS settings gave a lower cutsize in both numerical simulations and experimental results.

The second section reports the results of an optimization procedure for SADS and experimental confirmation with the optimized sampler. Using numerical modeling, the relationships between four major design and operating parameters significantly affecting the performance of the SADS and four performance parameters were expressed in polynomial equations. Utilizing an optimization procedure, values for the major parameters giving the best performance were determined and used as the base model for optimizing minor parameters. Five minor parameters were then investigated for their possible contribution to better performance of the SADS. Experimental tests

confirmed that the performance of the new sampler was improved although not as much as expected from the numerical simulation.

In the third section, the sampling performance of SADS was compared with existing vapor and particle sampling methods. Seven different test fluids were used to generate test droplets and the concentrations and composition in each phase were evaluated using gas chromatography. Combined vapor and particle concentrations for each test aerosol were not statistically different from one another as a function of test method. However, the particle concentrations estimated using the SADS were statistically higher than those from the other methods. In the tests of a chemical mixture and oil mists, a similar pattern of vapor/particle concentration ratio to the individual compounds was observed. SADS worked better than a filtration method and measured higher particle concentrations than other methods.

Table of Contents

List of Tables

List of Figures

Chapter I

Chapter II

Chapter III

Chapter IV

CHAPTER I

Overview

SOCs and Semivolatile Aerosols

In workplace environments, some hazardous materials can exist in the vapor and particle phases simultaneously. One example of this is semivolatile organic compounds (SOCs). SOCs are substances which have a relatively low vapor pressure, roughly between 10^{-4} and 10^{-11} atm (Bidleman, 1988). Thus, at room temperature they do not evaporate as readily as volatile organic compounds (VOCs). Examples of common semivolatile materials include metalworking fluids (MWFs) mist, pesticides, polycyclic aromatic hydrocarbons (PAHs) in diesel exhaust, asphalt fumes, polychlorinated biphenyls (PCBs), dioxins, and environmental tobacco smoke (ETS) (CONCAWE, 1986; Lioy and Daisey, 1986; Woskie et al., 1988; Norseth et al., 1991; Zaebst et al., 1991; Hawthorne et al., 1996; Pankow, 2001, Kriech et al., 2002).

MWF mists pose a potential hazard to more than 1.2 million workers in the United States (NIOSH, 1998). Epidemiological studies have linked MWF mist exposure to cancer (Calvert et al., 1998), respiratory ailments (Rosenmann et al., 1995; Kreiss and Cox-Ganser, 1997), and dermatitis (Alomar, 1994; Sprince et al., 1996).

Pesticides are substances or mixtures of substances used to control pests including weeds and microbes. Humans can be exposed to pesticides during

production and distribution of pesticides as well as their application (Garcia, 1998). The World Health Organization (WHO) estimated that 3 million workers in agriculture in the developing world experience severe poisoning from pesticides each year, about 18,000 of whom die (Miller, 2004). The health effects of pesticide exposure vary from headaches to cancers depending on the type of pesticide. IARC (1991) listed more than 20 pesticides as probable or possible human carcinogens. Some pesticides include dioxins as by-products (IARC, 1997).

PAHs are organic compounds that consist of multiple fused aromatic rings. Benzo[a]pyrene is well known for its carcinogenicity and belongs to this group. PAHs are produced from smoking and fuel burning and humans are exposed to them by inhalation (Nielsen et al., 1996). Mutagenic and carcinogenic effects, bone marrow toxicity, reproductive toxicity, and immunosuppressive effects have been reported as the potential health effects from PAHs (Nebert et al., 1980; Legraverend et al., 1984; White et al., 1985).

Diesel exhaust is a mixture of particles and gases emitted by diesel engines and contains more than several hundred different organic and inorganic compounds including PAHs (Jensen and Hites, 1983; Kagawa, 2002). WHO (1996) reported elevated levels of lung cancer for railroad workers and truck drivers. Acute and chronic respiratory diseases including bronchitis and asthma have been reported to be

related to diesel emission exposure (Kagawa, 2002).

Asphalt is a dark, high-boiling point material derived from petroleum refining. Approximately 99% of asphalt use is in paving and roofing. Paving contractors employ approximately 300,000 workers in the United States (NIOSH, 2000). About 50,000 roofers are exposed to asphalt fumes in the U.S. Workers exposed to asphalt fumes often suffer from eye, nose, and throat irritation (NIOSH, 2000).

PCBs are a class of organic compounds in which 1 to 10 chlorine atoms are attached to biphenyl. Although they have not been industrially manufactured and used in United States since 1977, the opportunity for human exposure still exists because PCB-containing transformers and capacitors remain in use (Wolff, 1985). NIOSH (1977) estimated that 12,000 workers had potential occupational exposure from 1970 to 1976. The evidence for cancer and reproductive effects is inconclusive and adverse neurobehavioral effects in infants and young children have been reported (Kimbrough, 1995).

Dioxins are a group of structurally and chemically related polychlorinated dibenzo para dioxins (PCDDs) and polychlorinated dibenzofurans (PCDFs) including dioxin, 2,3,7,8- tetrachlorodibenzo para dioxin (TCDD). PCDDs are formed as inadvertent by-products during the production of several herbicides. PCDDs and PCDFs also may be produced in incinerators, thermal metal processing, and paper

pulp bleaching with free chlorine (IARC, 1997). From short-term exposure to dioxins, skin lesions and altered liver function may be caused. Long-term exposure is linked to several types of cancer and impairment of the immune system, the developing nervous system, the endocrine system, and reproductive functions. TCDD was classified by IARC as a known human carcinogen (IARC, 1997).

ETS, sometimes called secondhand smoke, includes more than 4,000 chemical compounds, many of which are carcinogenic, toxic, or irritating. Nonsmokers can be exposed to ETS in homes, workplaces, and public places. Musicians and employees in bars, nightclubs, and lounges have been exposed to high levels of ETS (Bergman et al., 1996). The health effects from exposure to ETS include developmental disorders, respiratory symptoms, cardiovascular diseases, and cancers (Aviado, 1996).

When a SOC consists of one component, a significant fraction of the material can be expected to exist in the vapor phase if the material's saturated vapor concentration (SVC) is greater than its total airborne concentration (Figure 1a). Perez and Soderholm (1991) reported 41 substances for which SVCs are greater than their threshold limit values (TLVs). A substance that has a SVC that is much less than its total airborne concentration can be found predominantly in the particle phase (Figure 1b). In multicomponent SOCs, some compounds are more volatile than others. The more volatile a compound is, the greater fraction of that compound that exists as

vapor. Therefore, mixed SOCs have a different composition or different ingredients in each phase (Figure 1c). Vapor and particles can also coexist when VOCs are present with solid particles of another substance that may adsorb or solubilize the vapor (Figure 1d). In this situation, a significant fraction of VOCs may exist in the particle phase (Perez and Soderholm, 1991). In all of these instances, sampling only one phase will bias the measured concentration. The separation of vapors and particles, therefore, is important. The Chemical Substances Threshold Limit Values Committee (1983) of American Conference of Governmental Industrial Hygienists (ACGIH) suggested the possible need for separate TLVs for both phases of a substance.

Separate sampling of vapor and particles is important because the intake and uptake mechanisms of the two phases are different. Particle deposition in the lungs is a function of aerodynamic diameter, whereas gas deposition is a function of tissue solubility, which is related to the air-lung partitioning ratio (Volckens and Leith, 2003). In the case of SOCs, mass distributes between the two phases according to a gas-particle partitioning ratio. Therefore, deposition to the lungs will vary with these two ratios. Pankow (2001) explained the deposition of SOCs in the respiratory tract using four different mechanisms: (1) direct gas deposition (DGD) of the portion of the compound that is initially in the gas phase of the inhaled SOCs; (2) evaporative gas deposition (EGD) from the particle phase compound by evaporation to the gas phase,

then deposition; (3) particle deposition with evaporation (PDE) from the deposited particle, then deposition from the gas phase; and (4) particle deposition with diffusion (PDD) into the respiratory tract tissue. Three of the mechanisms (DGD, EGD, and PDE) involve volatilization from the particle phase. The relative importance of all the mechanisms is greatly affected by the volatility of the compound from the particle phase, which is set by the compound's gas-particle partitioning constant through the compound's vapor pressure.

The separation of vapor and particles is also important when VOCs and solid particles coexist. VOCs are used in many industrial spraying processes. The particle phase and vapor phase of VOCs often coexist in these environments. Malek et al. (1986) found that the styrene in aerosol droplets could contribute up to 30% of the total styrene concentration in air during a resin spraying process in the reinforced plastic industry. Cohen et al. (1992) demonstrated that xylene contained in paint droplets during automobile paint spray operations could represent up to 50% of the total airborne xylene concentration. Perez and Soderholm (1991) listed 46 substances that could be underestimated when they coexist with vapor-adsorbing particles. Therefore, the actual worker exposure to VOCs may require measuring not only the total airborne concentration but also the phase distribution in certain workplace conditions.

Sampling Semivolatile Aerosols

Several different types of sampling devices are available to evaluate semivolatile aerosols concentrations. Devices sampling only one phase are sometimes not appropriate for measuring semivolatile aerosols due to the characteristics of SOCs described previously. Depending on the principles of the sampling mechanism, some methods are more subject to evaporative loss than others. For dichotomous sampling, the cutsize of sampling devices is important. Cutsize, sometimes called cutpoint or cutoff size, is the hypothetical aerodynamic particle diameter for which all particles greater than this diameter are collected and all particles less than this size pass through in a particulate sampling device (Hinds, 1999). The real cutsize differs from hypothetical diameter partly because particles are not complete spheres and have different densities. There is always an imperfect efficiency curve rather than a step function. Portability of sampling instruments should be considered in the industrial hygiene field when personal exposure is assessed.

Particle Phase

Filtration

Filter media remove particles from air by several mechanisms which include impaction, interception, diffusion, electrical attraction, and sedimentation (Lippmann, 2001). The collection efficiency of a given filter media varies with face velocity and particle size. Sampling semivolatile aerosols using filtration methods is subject to large evaporative losses because filter media have large effective surface areas.

Currently, standard methods for measuring aerosol concentrations of SOCs depend primarily on sampling using various filter media. Table 1 shows the National Institute for Occupational Safety and Health (NIOSH) sampling methods for some mixed SOCs (NIOSH, 1998). Sampling methods using filter media only (0500, 5026, 5042, and 0600) have a high possibility of evaporative loss for the particles captured on filter media. In the case of metalworking fluid mist, Volckens et al. (1999) showed that concentrations determined by sampling with filters were up to 75-80% lower than the true concentrations. In the case of ETS respirable particulate fraction sampling using method 0600, the possibility of evaporative loss depends on the sampling situation. Samples taken near smokers might experience more evaporation than samples taken far from smokers. This is because volatile materials can evaporate from particles within seconds to minutes after ETS is emitted into the air (NRC, 1986). Two methods for nicotine use sorbent tubes only. Other methods for pesticides in Table 1 do not have the probability of underestimation from evaporative loss because

they attach sorbent tubes after filters. However, they provide total airborne concentrations and not the amounts in each phase.

In contrast to the evaporation artifact, there is also a possibility that the vapor molecules of SOCs can be adsorbed on the filter media or on accumulated particulate and/or organic matter on the surface of the filter media (Peters et al., 2000). This would result in an apparent increase in the particle phase loading of the SOCs in question.

ESPs

Electrostatic precipitators (ESPs) electrically charge particles and attract them to a substrate with opposite polarity. ESPs can collect particles with diameters down to the nanometer range (Hering, 2001). Since Tolman et al. (1919) collected smoke particles employing electrostatic precipitation, ESPs have long been used to collect samples of general aerosols, bioaerosols, and radioactive aerosols (Bergstedt, 1956; Wilkening, 1962; Decker et al., 1969; Mainelis et al., 2002). More commonly, ESPs are now used to collect samples for analysis by microscopy (Dixkens and Fissan, 1999). Leith et al. (1996) compared the oil mist concentration measured using filters and an ESP. They found that an ESP had several times less loss of sampled mass during air aspiration than filters did, but they still had the evaporative loss problem.

Samples of semivolatile aerosols collected by ESPs are susceptible to reactions and degradation due to ozone generated by corona (Kaupp and Umlauf, 1992; Cardello et al., 2002; Volckens and Leith, 2003). The fact that they require power supplies to provide the high voltage at which they operate adds extra weight to the equipment which workers need to wear for personal sampling.

Impactors

Simple inertial impactors have been used extensively for collecting airborne particles. The origin of the inertial impactor was in the period from 1860 to 1870 (Marple, 2004). Currently, impactors usually have more than one stage to differentiate the sizes of particles. Impactors separate particles from aerosol using the inertia that the accelerated particles carry (Hering, 2001). The characteristics of impactors and the fluid flow in them have been studied thoroughly (Fuchs, 1964; Marple, 1970; Marple and Liu, 1974; Marple and Liu, 1975). Evaporative loss from impactors occurs from the pressure drop in impactors and from continuous aspiration of air though impactors (Zhang and McMurry, 1987).

Virtual impactors

Instead of a collection plate in impactors, a virtual impactor has an axial probe below the impactor jet. In a virtual impactor, large particles are concentrated in the flow passing to the collection probe whereas the large particles are depleted in the main flow. One major advantage of virtual impactors is that they minimize the errors from particle bounce or re-entrainment and concentrate airborne particles. A limitation is that they have significant wall losses for liquid particles near the cutpoint (Hering, 2001).

Hounam and Sherwood (1965) proposed the first type of round nozzle virtual impactors. The impaction plates in a cascade impactor were replaced with "centripeter" stages in which a filter was mounted at the bottom of each stage. The flow inside the cascade centripeter was not dichotomous because the small fraction of air that passed through the filter media rejoined the main air flow. One variant of the original centripeter was the multi-orifice centripeter, which was a dichotomous sampler. Although it did not have air nozzles to accelerate air flow, it had the other components that modern virtual impactors have.

Conner (1966) introduced a single-stage dichotomous sampler and this was the prototype of modern virtual impactors. This sampler had an acceleration nozzle and a collection nozzle and was further developed by Dzubay and Stevens (1975).

McFarland et al. (1978) described the efficiency curve and the effect of flow ratio between the large and small particle flows on the cutsize of the sampler.

Marple and Chien (1980) studied virtual impactors employing the numerical solution of the Navier-Stokes equations and of the equations of motion for particles. They described the effects of the nozzle Reynolds number, the flow split ratio, the diameter ratio between the acceleration nozzle and the collection probe, and the distance between the acceleration nozzle and the collection probe on particle collection efficiencies and wall losses. Loo and Cork (1988) studied these factors by experiments and established a standard for virtual impactor design.

Several virtual impactors different from conventional designs were also studied. Slit nozzle virtual impactors were studied by Ravenhall et al. (1978) and Forney et al. (1982) and further developed by Sioutas et al. (1994) and Ding and Koutrakis (2000). Masuda and Nakasita (1988) investigated a rectangular jet virtual impactor. Chein and Lundgren (1993) and Li and Lundgren (1997) studied virtual impactors with a clean air core for better separation characteristics. Noone et al. (1988) developed a counterflow virtual impactor as an aircraft sampling device for cloud droplets, and Boulter et al. (2006) modified this to be operated without depending on an outside air current.

Virtual impactors separate particles from air instantly and keep them airborne. Most virtual impactors currently available are large and require such a high airflow rate, 1 cfm or higher, that they can not be used for personal sampling. They have large internal losses of particles with diameters near the cutoff size. For personal sampling, Xiong et al. (1998) designed a portable vapor/particle sampler for use by industrial hygienists, but it still allowed some sampled mist to evaporate. In their paper, Xiong et al. discussed the possibility of loss of volatile components from the particulate portion collected on a filter. In a situation where ambient VOC concentrations change greatly during the sampling process, they found that particle-bound VOCs may volatilize not only into the airstreams passing through the filter but also into the side airstreams. In their experiments with liquid styrene, they estimated that in general 10-20% of styrene was lost at their recommended flow ratio ($Q_{particle}$:Q_{vapor}). Accordingly, their sampler can still yield large sampling errors.

Marple et al. (1995) developed a virtual impactor personal aerosol sampler (VIPAS) for dichotomous sampling of diesel exhaust and mine dust. VIPAS was designed for sampling solid particles and had a fixed cutsize of 0.8 μm. Particles were collected on 37-mm filter cassettes and the sampling flow rate was 2 lpm. The losses on the collection probe and in the major flow cavity were reported to be 0.1% -12.1% and 0.3% - 1.6%, respectively, for particles with aerodynamic diameters of 0.77 –

1.16 μm.

Other methods

Other sampling devices such as impingers, cyclone samplers, aerosol centrifuges, elutriators, and thermal precipitators are available for sampling particles (Hering, 2001). Among them, cyclone samplers, aerosol centrifuges, elutriators, and thermal precipitators are subject to evaporative loss like the other devices described above. From the perspective of personal exposure assessment, impingers and aerosol centrifuges are generally not appropriate for personal sampling. These devices seldom have been used for semivolatile aerosol sampling except cyclones. In most cases, cyclones have been used as a preseparator to obtain a specific size fraction of particles such as the thoracic fraction (Piacitelli et al., 2001; O'Brian et al., 2001; Verma et al., 2006).

Direct-reading instruments are also available for analyzing airborne particles. However, they only can count and/or size particles. The compositions of particles need to be analyzed by separate methods.

Vapor Phase

Sorbent tubes

Activated carbon is an excellent sorbent for most organic vapors (Brown and Monteith, 2001). The vapor molecules diffuse and are adsorbed onto the carbon. Activated carbon tubes (ACTs) are recommended by NIOSH for sampling airborne vapors of volatile hydrocarbons. However, sorbent tubes can sample particles both on the filter plugs inside them and potentially on the sorbent material as well. Cohen et al. (1992) found that the air concentrations of xylene sampled by ACTs were higher than those determined by 3M diffusion monitors at paint spray operations. This finding was attributed to the ACTs capturing not only vapor molecules but also particles.

Diffusive samplers

Diffusive samplers take samples of vapor from air by diffusion or permeation through a membrane without the active movement of air. Ambient air velocity and orientation can affect the performance of a diffusive sampler (Brown and Monteith, 2001). Most diffusive samplers require minimum face velocities in order to take representative samples. In paint spray applications where vapor and particles coexist, airborne droplets containing solvent can damage the membrane of diffusive samplers

causing an increase in the sampling rate for the solvent vapor and can make the sampler significantly overestimate the vapor concentration (Cohen et al., 1992). Recently, Simpson and Wright (2008) measured mixed C_7-C_{16} hydrocarbon vapors using diffusive samplers and found that as molecular weight increased, the diffusive uptake rate decreased and their standard uncertainty increased. In the same study, it was found that a small amount of SOCs were adsorbed on the internal metal surface of thermal desorption tube samplers. The authors of this study recommended not using diffusive samplers when mist concentration is lower than 3 mg/m^3.

Diffusion denuders

A diffusion denuder is a tube or set of tubes through which the atmospheric sample is passed. The inside of the tube is coated with a material which collects the components of interest. Because the diffusion coefficients of particles and vapor-phase molecules differ by 10^3-10^6, the particles tend to pass through the tube while the vapor phase components tend to diffuse to the wall and accumulate (Krieger and Hites, 1992). The design of denuders has been changed from glass or metallic hollow tubes into the shape of annular tubes, honeycomb, compact coil, a bundle of gas chromatographic columns, and compact porous-metal (Durham et al., 1978; Possanzini et al., 1983; Gunderson and Anderson, 1987; Krieger and Hites, 1992;

Koutrakis et al., 1993; Poon et al., 1994). The selectivity of coating materials can be a strength or a weakness depending on the situation. In mixed SOCs sampling, this selectivity can bias the measured concentrations because some components of SOCs may not be captured by a coating. Turpin et al. (1993) developed a diffusion separator that uses clean airflow instead of a coating. However, this device is sensitive to the air temperature and not appropriate for contaminants which normally have low airborne concentrations.

Other methods

Cold traps put gaseous contaminants into liquid or solid form, commonly for chemical identification purposes (Brown and Monteith, 2001). When vapor passes though a cooling system, it can be separated by condensation. This method is used when other techniques are not efficient.

Sampling bags can also be employed for integrated air sampling (Brown and Monteith, 2001). Personal sampling is also possible with this method. However, particles might deposit on the surface of bags depending on the size of the particle and the sampling time.

Direct-reading instruments are also available for evaluating vapor concentration. However, in many cases the compounds in the vapor must be known

first to use this method.

Objectives

Some SOCs are important inhalation hazards and SOCs can exist as both vapor and particles. Sampling one phase of SOCs may underestimate the real exposure to SOCs and the exposure mechanism of each phase is different. Therefore, both phases may need to be sampled at the same time. Current methods do not always sample one or both phases accurately.

The long-range goal of this research was to evaluate the exposure of workers to particles and vapors more accurately. The objective for this study was to develop a new personal sampler that can separate vapor phase contaminants and particle phase contaminants based on the greater inertia that particles possess. The rationale for this study was that a more accurate evaluation of vapor/particle concentration will allow for better exposure analysis of workers in the field and contribute to the better understanding of health effect mechanisms of SOCs and VOCs. To achieve the objective, the specific aims for this study were:

1. Evaluate the possible benefits of a new dichotomous sampler using computer simulation and confirm the findings with experiments,

2. Optimize the new sampler using computer simulation and statistical procedures and confirm the findings with experiments, and

3. Compare the new sampler with existing SOC sampling methods in a laboratory test using both single and multicomponent SOCs.

Structure of Dissertation

This dissertation consists of five chapters including the current introductory chapter. The next three chapters each contain a separate manuscript and are followed by the last chapter containing overall conclusions and recommendations for future work. A bibliography and appendices are attached at the end.

Each manuscript has been submitted or is ready to be sent to a journal for review. Chapter II, submitted to the *Annals of Occupational Hygiene*, explains the principle of the new sampler and describes the procedure for evaluating a prototype sampler using numerical simulations and experiments. Chapter III describes the optimization procedure for obtaining better performance and the experimental procedure for validating the findings. Chapter IV describes how the new sampler was compared with existing semivolatile aerosol methods utilizing real SOC particles and vapors.

References

Alomar A. (1994) Occupational skin disease from cutting fluids. Dermatol Clin; 12(3) 537-546.

Aviado DM. (1996) Cardiovascular Disease and Occupational Exposure to Environmental Tobacco Smoke. Am Ind Hyg Assoc J; 57(3) 285-294.

Bergman TA, Johnson DL, Boatright DT, Smallwood KG, Rando RJ. (1996) Occupational exposure of nonsmoking nightclub musicians to environmental tobacco smoke. Am Ind Hyg Assoc J; 57(8) 746-752.

Bergstedt BA. (1956) Application of the electrostatic precipitator to the measurement of radioactive aerosols. J Sci Instr; 33 142-148.

Barr EB, Hoover MD, Kanapilly GM, Yeh HC, Rothenberg SJ. (1983) Aerosol concentrator. Aerosol Sci Technol; 2 437-442.

Bidleman TE. (1988) Atmospheric processes – wet and dry deposition of organic compounds are controlled by their vapor-particle partitioning. Environ Sci Technol; 22 361-367.

Boulter JE, Cziczo DJ, Middlebrook AM, Thomson DS, Murphy DM. (2006) Design and performance of a pumped counterflow virtual impactor. Aerosol Sci Technol; 40 969–976.

Brown RH, Monteith LE. (2001) Gas and vapor sample collectors. In Cohen BS, McCammon CS Jr., editors. Air sampling instruments for evaluation of atmospheric contaminants. Cincinnati: American Conference of Governmental Industrial Hygienists. p. 421-424. ISBN 1 882417 39 9.

Calvert GM, Ward E, Schnorr TM, Fine LJ. (1998) Cancer risk among workers exposed to metalworking fluids: a systematic review. Am J Ind Med; 33 282-292.

Cardello N, Volckens J, Tolocka MP, Wiener R, Buckley TJ. (2002) Technical note: performance of a personal electrostatic precipitator particle sampler. Aerosol Sci Technol; 36(2) 162-165.

Chein H, Lundgren DA. (1993) A virtual impactor with clean air core for the generation of aerosols with narrow size distributions. Aerosol Sci Technol; 18 376-388.

Chemical Substances Threshold Limit Values Committee. (1983) Separate TLVs for vapor and particulate. Ann Am Conf Govt Ind Hyg; 4 153-155.

Cohen BS, Brosseau LM, Fang CP, Bower A, Snyhder C. (1992) Measurement of air concentrations of volatile aerosols in paint spray applications. Appl Occup Environ Hyg; 7 514-521.

CONCAWE. (1986) Health aspects of worker exposure to oil mists. Brussels 86/89.

Conner WD. (1966) An inertial-type particle separator for collecting large samples. J

Air Pollut Control Assoc; 16(1) 35-8.

Decker HM, Buchanan LM, Frisque DE, Filler ME, Dahlgren CM. (1969) Advances in large-volume air sampling. Contamination Cot; 8: 13-17.

Ding Y, Koutrakis C. (2000) Development of a dichotomous slit nozzle virtual impactor. J Aerosol Sci; 31(12) 1421-1431.

Dixkens J, Fissan H. (1999) Development of an Electrostatic Precipitator for Off-Line Particle Analysis. Aerosol Sci Technol; 30(5) 438-453.

Durham JL, Wilson WE, Bailey EB. (1978) Application of an SO2 denuder for continuous measurement of sulfur in submicrometer aerosols. Atmos Environ; 12 883-886.

Dzubay TG, Stevens RK. (1975) Ambient air analysis with dichotomous sampler and x-ray fluorescence spectrometer. Environ Sci Technol; 9 663-668.

Forney LJ, Ravenhall DG, Lee SS. (1982) Experimental and theoretical study of a two-dimensional virtual impactor. Environ Sci Technol; 16 492-497.

Fuchs NA. (1964) The Mechanics of Aerosols. New York: Pergamon Press. p. 151-159.

Garcia AM. (1998) Occupational exposure to pesticides and congenital malformations: a review of mechanisms, methods, and results. Am J Ind Med; 33 232-240.

Guidotti TL, Yoshida K, Clough V. (1994) Personal exposure to pesticide among workers engaged in pesticide container recycling operations. Am Ind Hyg Assoc J; 55 1154-1163.

Gunderson EC, Anderson CC. (1987) Collection Device for Separating Airborne Vapor and Particulates. Am Ind Hyg Assoc J; 48(7) 634 – 638.

Hawthorne SB, Miller DJ, Louie PKK, Butler RD, Mayer GG. (1996) Vapor-phase and particulate-phase pesticides and PCB concentrations in eastern North Dakota air samples. J Environ Qual; 25 594-600.

Hering SV. (2001) Impactors, cyclones, and other particle collectors. In Cohen BS, McCammon CS Jr., editors. Air sampling instruments for evaluation of atmospheric contaminants. Cincinnati: American Conference of Governmental Industrial Hygienists. p. 315-354. ISBN 1 882417 39 9.

Hinds WC. (1999) Aerosol Technology. 2nd ed. Wiley-Interscience, New York, NY.

Hounam RF, Sherwood RJ. (1965) The cascade centripeter: a device for determining the concentration and size distribution of aerosols. Am Ind Hyg Assoc J; 26 122-131.

IARC. (1991) Occupational Exposures in Insecticide Application, and Some Pesticides. Lyon, France. IARC: IARC Monographs on the Evaluation on the Carcinogenic Risks to Humans, Volume 53.

IARC. (1997) Polychlorinated Dibenzo-para-Dioxins and Polychlorinated Dibenzofurans. Lyon, France. IARC: IARC Monographs on the Evaluation on the Carcinogenic Risks to Humans, Volume 69.

Jensen TE, Hites RA. (1983) Aromatic diesel emissions as a function of engine conditions. Anal Chem; 55 594-599.

Kagawa J. (2002) Health effects of diesel exhaust emissions—a mixture of air pollutants of worldwide concern. Toxicol; 181-182 349-353.

Kaupp H, Umlauf G. (1992) Atmospheric gas-particle portioning of organic compounds: comparison of sampling methods. Atmos Environ; 26 2259-2267.

Kimbrough RD. (1995) Polychlorinated biphyenyls (PCBs) and human health: an update. Crit Rev Toxicol; 25(2) 133-163

Kriech AJ, Kurek JT, Wissel HL, Osborn LV, Blackburn GR. (2002) Evaluation of worker exposure to asphalt paving fumes using traditional and nontraditional techniques. Am Ind Hyg Assoc J; 63 628-635.

Krieger MS, Hites RA. (1992) Diffusion denuder for the collection of semivolatile organic compounds. Environ Sci Technol; 26 1551-1555.

Koutrakis P, Sioutas C, Ferguson ST, Wolfson JM. (1993) Development and Evaluation of a glass honeycomb denuder/filter pack system to collect atmospheric gases and particles. Environ Sci Technol; 27 2497-2501.

Kreiss K, Cox-Ganser J. (1997) Metalworking fluid-associated hypersensitivity pneumonitis: a workshop summary. Am J Ind Med; 32 423-432.

Legraverend C, Guenthner TM, Nebert DW. (1984) Importance of the route of administration for genetic differences in benzo[a]pyrene-induced in utero toxicity and tetratogenicity. Teratology; 29 35-47.

Leith D, Leith FA, Boundy MG. (1996) Laboratory measurements of oil mist concentrations using filters and an electrostatic Precipitator. Am Ind Hyg Assoc J; 57 1137-1141.

Li S-N, Lundgren DA. (1997) Effect of clean air core geometry on fine particle contamination and calibration of a virtual impactor. Aerosol Sci Technol; 27 625-635.

Lioy PJ, Daisey JM. (1986) Airborne toxic elements and organic substances. Environ Sci Technol; 20 8-14.

Lippmann M. (2001) Filters and filter holders. In Cohen BS, McCammon CS Jr., editors. Air sampling instruments for evaluation of atmospheric contaminants. Cincinnati: American Conference of Governmental Industrial Hygienists. p. 281-284. ISBN 1 882417 39 9.

Loo BW, Cork CP. (1988) Development of high efficiency virtual impactors. Aerosol Sci Technol; 9 167-176.

Mainelis G, Adhikari A, Willeke K, Lee S-A, Reponen T, Grinshpun SA. (2002) Collection of airborne microorganisms by a new electrostatic precipitator. J Aerosol Sci; 33 1417–1432.

Malek RF, Daisey JM, Cohen BS. (1986) The effect of aerosol on estimates of inhalation exposure to airborne styrene. Am Ind Hyg Assoc J; 47 524-529.

Marple VA. (1970) A fundamental study of inertial impactors. PhD Thesis, Mechanical Engineering Department, University of Minnesota: Particle Technology Laboratory Publ. No. 144.

Marple VA, Liu BYH. (1974) Characteristics of laminar jet impactors. Environ Sci Technol; 8 648-654.

Marple VA, Liu BYH. (1975) On fluid flow and aerosol impaction in inertial impactors. J Colloid interface Sci; 53 31-34.

Marple VA, Chien CM. (1980) Virtual impactors: a theoretical study. Environ Sci Technol; 14 976-984.

Marple VA, Rubow KL, Olson BA. (1995) Diesel exhaust / mine dust virtual impactor personal aerosol sampler: design, calibration and field evaluation. Aerosol Sci Technol; 22 140-150.

Marple VA. (2004) History of Impactors—The First 110 Years. Aerosol Sci Technol; 38 247–292.

Masuda H, Nakasita S. (1988) Classification performance of a rectangular jet virtual impactor. Effect of nozzle width ratio of collection nozzle to acceleration jet. J Aerosol Sci; 19(2) 243-252.

McFarland AR, Ortiz CA, Bertch Jr RW. (1978) Particle collection characteristics of a single-stage dichotomous sampler. Environ Sci Technol; 12 679-682.

Miller GT. (2004) Sustaining the Earth. 6th ed. Thompson Learning, Inc. Pacific Grove, California. Chapter 9, p. 211-216.

National Research Council (NRC). (1986) Environmental tobacco smoke – measuring exposures and assessing health effects. Committee on Passive Smoking in NRC. p. 69-100.

Nebert DW, Jensen NM, Levitt RC, Felton JS. (1980) Toxic chemical depression of the bone marrow and possible aplastic anemia explainable on a genetic basis. Clin Toxicol; 16 99-122.

Nielsen T, Jørgensen HE, Larsen JC, Poulsen LM. (1996) City air pollution of polycyclic aromatic hydrocarbons and other mutagens: occurrence, sources and health effects. Sci Total Environ; 189/190 41-49.

NIOSH (1977). Occupational Exposure to Polychlorinated Biphenyls, USDHEW (NIOSH) Publication 77-225.

NIOSH (1998). NIOSH Manual of Analytical Methods (NMAM). 4th ed., DHHS

(NIOSH) Publication 94-113. Available from: URL: http://www.cdc.gov/niosh/nmam/nmammenu.html

NIOSH (1998). Occupational Exposure to Metalworking Fluids, DHHS (NIOSH) Publication 98-102.

NIOSH (2000). Health Effects of Occupational Exposure to Asphalt, DHHS (NIOSH) Publication 2001-110.

Noone KJ, Ogren JA, Heintzenberg J, Charlson RJ, Covert DS.(1988) Design and calibration of a counterflow virtual impactor for sampling of atmospheric fog and cloud droplets. Aerosol Sci Technol; 8(3) 235-244.

Norseth T, Waage J, Dale I. (1991) Acute effects and exposure to organic compounds in road maintenance workers exposed to asphalt. Am J Ind Med; 20 737-744.

O'Brien DM, Piacitelli GM, Sieber WK, Hughes RT, Catalano JD. (2001) An evaluation of short-term exposures to metalworking fluids in small machine shops. 62(3) 342-348.

Pankow JF. (2001) A consideration of the role of gas/particle partitioning in the deposition of nicotine and other tobacco smoke compounds in the respiratory track. Chem Res Toxicol; 14(11) 1465-1481.

Park D, Kim S, Yoon C. (2003) Loss of straight metalworking fluid samples from evaporation during sampling and desiccation. Am Ind Hyg Assoc J; 64 837-841.

Perez C, Soderholm SC. (1991) Some chemicals requiring special consideration when deciding whether to sample the particle, vapor, or both phases of an atmosphere. Appl Occup Environ Hyg; 6(10) 859-864.

Peters AJ, Lane DA, Gundel LA, Northcott GL, Jones KC. (2000) A comparison of high volume and diffusion denuder samplers for measuring semivolatile organic compounds in the atmosphere. Environ Sci Technol; 34 5001-5006.

Piacitelli GM, Sieber WK, O'Brien DM, Hughes RT, Glaser RA, Catalano JD. (2001) Metalworking fluid exposure in small machine shops: an overview. Am Ind Hyg Assoc J; 62 356-370.

Poon WS, Pui DYH, Lee CT, Liu BYH. (1994) A compact porous-metal denuder for atmospheric sampling of inorganic aerosols. J Aerosol Sci; 25(5) 923-934.

Possanzini M, Febo A, Liberti A. (1983) New design of a high-performance denuder for the sampling of atmospheric pollutants. Atmos Environ; 17(12) 2605-2601.

Ravenhall DG, Forney LJ, Jazayeri M. (1978) Aerosol sizing with a slotted virtual impactor. J Colloid Interface Sci; 65(1) 108-117.

Rosenmann KD, Reilly MJ, Kalinowski D, Watt F. (1995) Occupational asthma and respiratory symptoms among workers exposed to machining fluids. In symposium proceedings of the Industrial Metalworking Environment. p. 143-146.

Rounds SA, Tiffany BA, Pankow JF. (1993) Description of gas/particle sorption

kinetics with an intraparticle diffusion model: desorption experiments. Environ Sci Technol; 27(2) 366-377.

Simpson AT, Groves JA, Unwin J, Piney M. (2000) Mineral oil metal working fluids (MWFs) – development of practical criteria for mist sampling. Ann Occup Hyg; 44 165-172.

Simpson AT. (2003) Comparison of methods for the measurement of mist and vapor from light mineral oil-based metalworking fluids. Appl Occup Environ Hyg; 18(11) 865-876.

Simpson AT, Wright MD. (2008) Diffusive sampling of C7-C16 hydrocarbons in workplace air: uptake rates, wall effects and use in oil mist measurements. Ann Occup Hyg; 52(4) 249-257.

Sioutas C, Koutrakis P, Burton PM. (1994) A high-volume small cutpoint virtual impactor for separation of atmospheric particulate from gases pollutants. Particulate Sci Technol; 12 207-221.

Sprince NL, Palmer JA, Popendorf W, Thorne PS, Selim MI, Zwerling C, Miller ER. (1996) Dermatitis among automobile production machine operators exposed to metalworking fluids. Am J Ind Med; 30 421-429.

Tolman RC, Reyerson LH, Brooks AP, Smyth HD. (1919) An electrical precipitator for analyzing smokes. J Am Chem Soc; 41 587-589.

Turpin BJ, Liu S, Podolske KS, Gomes MSP, Eisenreich SJ, McMurry PH. (1993) Design and evaluation of a novel diffusion separator for measuring gas/particle distributions of semivolatile organic compounds. Environ Sci Technol; 27 2441-2449.

Verma DK, Shaw DS, Shaw ML, Julian JA, McCollin S-A, Tombe KD. (2006) An evaluation of analytical methods, air sampling techniques, and airborne occupational exposure of metalworking fluids. J Occup Environ Hyg; 3(2) 53-66.

Volckens J, Boundy M, Leith D, Hands D. (1999) Oil mist concentration: a comparison of sampling methods. Am Ind Hyg Assoc J; 60 684-689.

Volckens J, Leith D. (2002) Electrostatic Sampler for Semivolatile Aerosols: Chemical Artifacts. Environ Sci Technol; 36 4608-4612.

Volckens J, Leith D. (2003) Partitioning theory for respiratory deposition of semivolatile aerosols. Ann Occup Hyg; 47(2) 157-164.

White KLJ, Lysy HH, Holsapple MP. (1985) Immunosuppression by polycyclic aromatic hydrocarbons: a structure-activity relationship in B6C3F1 and DBA/2 mice. Immunopharmacology; 9 155-164.

Wilkening MH. (1962) A monitor for natural atmospheric radioactivity. Nucleonics; 10(6) 36-39.

Wolff MS. (1985) Occupational exposure to polychlorinated biphenyls (PCBs).

Environ Health Perspectives; 60 133-138.

World Health Organization. (1996) Diesel fuel and exhaust emissions. International Program on Chemical Safety. Environmental Health Criteria 171, Geneva, Switzerland.

Woskie SR, Smith TJ, Hammond SK, Schenker MB, Garshick E, Speizer FE. (1988) Estimation of the diesel exhaust exposures of railroad workers: I. current exposures. Am J Ind Med; 13(3) 381-394.

Woskie SR, Smith TJ, Hammond SK, Hallock MH. (1994) Factors affecting worker exposures to metal-working fluids during automotive component manufacturing. Appl Occup Environ Hyg; 9 612-21.

Xiong JQ, Fang C, Cohen BS. (1998) A portable vapor/particle sampler. Am Ind Hyg Assoc J; 58 614-621.

Zhang X, McMurry PH. (1987) Theoretical analysis of evaporative losses from impactor and filter deposits. Atmos Environ; 21 1779-1789.

Zaebst DD, Clapp DE, Blade LM. (1991) Quantitative determination of trucking industry workers exposures to diesel exhaust particles. Am Ind Hyg Assoc J; 52(12) 529-541.

Table 1. NIOSH sampling methods for mixed semivolatile organic compounds

Semivolatile organic compounds		NIOSH sampling method	Possibility of evaporative loss
MWFs		# 0500	O
		# 5026	O
Asphalt fume		# 5042	O
ETS[a]	Respirable particulate fraction	# 0600	Δ
	Nicotine	# 2544	X
		# 2551	X
Pesticides	Organophosphorus	# 5600	X
	Organonitrogen	# 5601	X
	Chlorinated Organonitrogen	# 5602	X

O: significant, Δ: possible, X: not likely

[a] Environmental Tobacco Smoke (ETS) itself is not a substance regulated by Occupational Safety and Health Administration (OSHA)

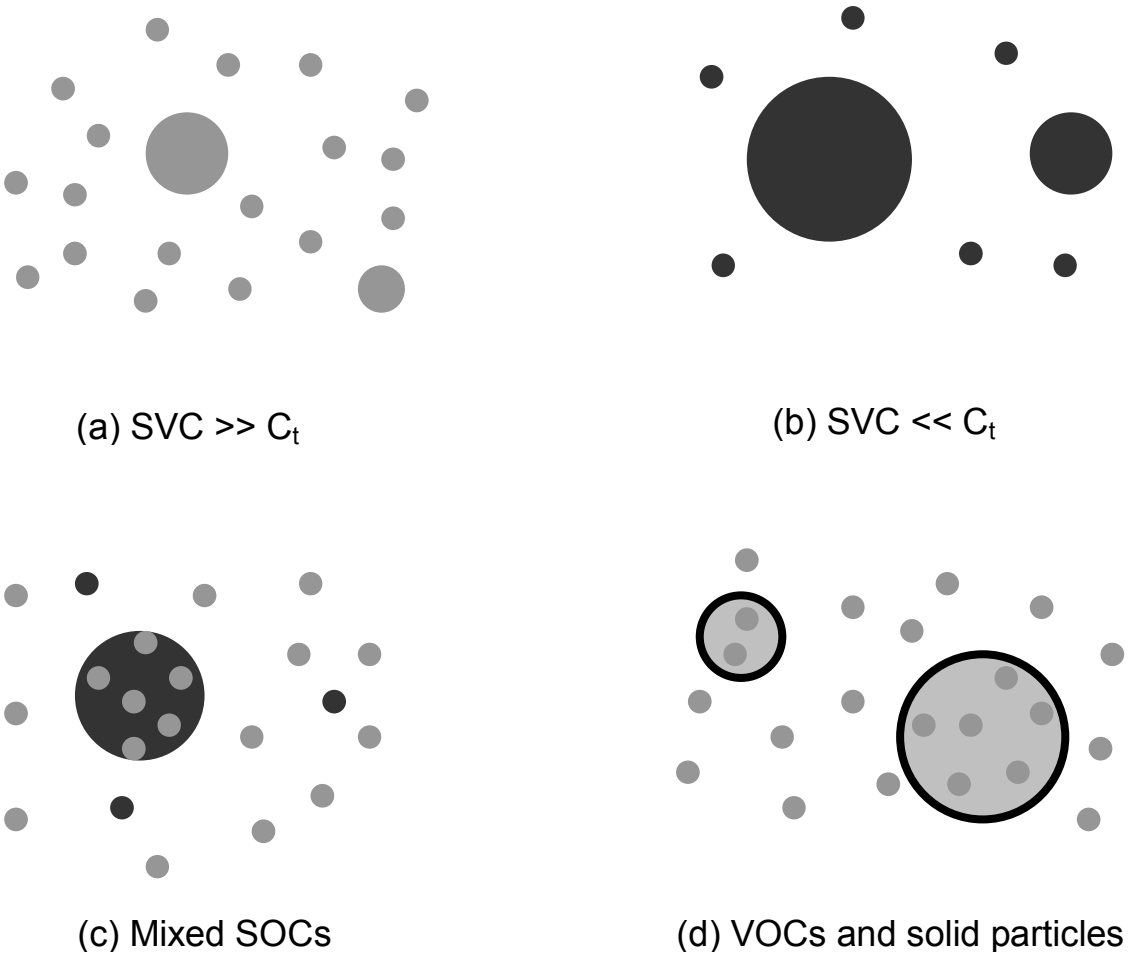

Figure 1. Situations of chemicals existing in the vapor phase and particle phases. Small dots are vapor molecules and bigger ones are particles. (SVC: saturated vapor concentration, C_t: total air concentration)

CHAPTER II

New Approach for Sampling Semivolatile Aerosol Using a Virtual Impactor

ABSTRACT

This study reports the results of a numerical investigation and an experimental study on a round nozzle virtual impactor operated in two different modes. The newly proposed sampler, the semivolatile aerosol dichotomous sampler (SADS), was studied to overcome some of the problems of existing personal sampling methods such as evaporative loss during filter sampling. The main difference between virtual impactors and the SADS was the inverted flow ratio between the major flow and the minor flow. Sampling in the SADS settings gives a lower cutsize in both numerical simulations and experimental results. Whereas the 50% separation efficiency for a virtual impactor occurred in numerical simulations when the square root of Stokes number equaled 0.97, the 50% efficiency for the same sampler run in the SADS settings occurred when the square root of the Stokes number was 0.27. The back pressure on each flow direction was studied and greater pressure drop was observed through the vapor flow in SADS settings. Sampling using a SADS was more effective than traditional filter methods because of its smaller cutsize, instant separation of vapor from particles, and reduced particles losses.

INTRODUCTION

In workplace environments, some hazardous materials can exist in the vapor and particle phases simultaneously. One group of chemicals for which this situation is common is semivolatile organic compounds (SOCs). SOCs are substances which have a relatively low vapor pressure, approximately between 10^{-4} and 10^{-11} atm (Bidleman, 1988). Thus, at room temperature they do not evaporate as readily as volatile organic compounds (VOCs). Metalworking fluid (MWF) mists, pesticides, asphalt fumes, and environmental tobacco smoke are well known health-related semivolatile aerosols in workplaces (Woskie et al., 1994; Guidotti et al., 1994; Kriech et al., 2002; Bergman et al., 1996).

SOCs consist of one or more compounds. In mixed SOCs, some compounds are more volatile than others. Therefore, each phase of coexisting vapor and liquid particles has a different composition. In this instance, sampling only one phase will bias the measurement of concentrations to which workers are potentially exposed. The separation of vapor and particles, therefore, is important.

Separate sampling of vapor and particles is also important because the intake and uptake mechanisms of the two phases are different. Particles deposit in the lungs according to their aerodynamic diameter, whereas gases absorb into lungs depending

on their tissue solubility, which is related to the air-lung partitioning ratio (Volckens and Leith, 2003). In the case of SOCs, mass distributes between the two phases according to a gas-particle partitioning ratio. Therefore, deposition to the lungs will vary with these two ratios.

For sampling airborne vapors of volatile hydrocarbons, carbon sorbent tubes (ACTs) are recommended by the National Institute for Occupational Safety and Health (NIOSH) (1998). When vapor and particles coexist in the air, some particles can be captured by ACTs during sampling. The penetration efficiency of ACTs for particles with diameters ranging from 0.3 μm to 5.7 μm has been reported by Fairchild and Tillery (1977) and the largest penetration was reported to be approximately 30% for 1 μm particles at 0.05 lpm. The ACT collection efficiency for particles of 0.5 μm to 50 μm diameter has been reported by Brosseau et al. (1992) and the smallest collection efficiency was approximately 10% for 0.5 μm particles at 0.4 lpm. In both studies, the collection efficiency was affected by the flow rate through ACTs. Due to the presence of these captured particles on ACTs, the vapor concentrations of some SOCs can be overestimated.

When VOCs coexist with particles of another substance that may adsorb or solubilize the VOCs, the exposure assessment for the VOCs can be biased due to those particles (Cohen et al., 1992). In the same study, prefiltered ACTs were

recommended when vapor and particles coexist. However, this method does not provide individual concentrations of each phase of SOCs or VOCs, but only provides overall exposure level.

A diffusive sampler is a device sampling gas or vapor molecules into adsorbents by diffusion without mechanically pumping the air through the sampler. Ambient air velocity and orientation can affect the performance of a diffusive sampler (Brown and Monteith, 2001). Most diffusive samplers require minimum face velocities in order to take representative samples. In paint spray applications where vapor and particles coexist, airborne droplets containing solvent can damage the membrane of diffusive samplers causing an increase in the sampling rate for the solvent vapor and can make the sampler significantly overestimate the vapor concentration (Cohen et al., 1992).

A diffusion denuder is a cylindrical tube or an annular tube through which gas or vapor molecules are passed and absorbed into the wall coated with a material capturing specific molecules. The huge difference in diffusion coefficients between particles and vapor-phase molecules, a factor of 10^3-10^6, allows most of the particles to pass through the tube while the vapor-phase molecules diffuse to the wall. Diffusion denuders have not been used for sampling SOCs widely. Rather, they have primarily been used for the collection of volatile inorganic compounds in atmospheric

studies. The main reasons for this minimal use are the extremely long sampling times from the low flow rates inherent in most denuder designs and the relative non-polarity of many SOCs (Krieger and Hites, 1992). Turpin et al. (1993) developed a diffusion separator which uses clean airflow instead of coating material inside denuders to separate vapor from aerosol. However, this device was sensitive to air temperature, was not designed for personal sampling, and was not appropriate for contaminants which normally have low airborne concentrations.

Current methods for measuring aerosol concentrations of SOCs depend heavily on sampling using various filter media (NIOSH, 1998). Sampling methods using filter media have a high possibility of evaporative loss during aspiration. Because equilibrium between evaporation and recondensation is not achieved in most workplaces, the particles retained on the filter continue to evaporate from the filter into the air passing through. This evaporation leads to inaccurate measurements of mist concentration (Raynor and Leith, 1999; Park et al., 2003). There have been several studies reporting evaporative losses during filter sampling of aerosol droplets containing inorganic and organic compounds (Cheng and Tsai, 1997; Eatough et al., 1995; Van Vaeck et al., 1984; Rounds et al., 1993, Simpson et al., 2000).

In the case of MWF mist, Volckens et al. (1999) showed that sampling with filters underestimates mist concentrations by a factor of two or more compared with

the concentrations sampled using electrostatic precipitators (ESPs). ESPs have long been used to collect samples of aerosol particles (Flagan, 2001). Leith et al. (1996) compared the measured oil mist concentration using filters and an ESP. They found that an ESP had several times less loss of sampled mass during air aspiration than did filters, but they still experienced some evaporative loss. Samples of semivolatile aerosols collected by ESPs are susceptible to reactions and degradation due to ozone generated by corona (Kaupp and Umlauf, 1992).

Simple inertial impactors have been used extensively for collecting airborne particles. Their characteristics and fluid flow have been studied thoroughly (Fuchs, 1964; Marple, 1970; Marple and Liu, 1974; Marple and Liu, 1975). In order to overcome the problems of bounce and impactor overload, several alternative approaches were introduced. One was a virtual impactor in which the impaction plate from a conventional impactor was replaced with a collection probe drawing a small fraction of air, which eliminated the most prevalent particle-surface interaction problems. Since Hounam and Sherwood (1965) proposed the original prototype, virtual impactors have been modified and theoretically studied. Marple and Chien (1980) studied the effect of the nozzle Reynolds number and physical dimensions of virtual impactors on the particle collection efficiency using numerical solutions of the Navier-Stokes equations and the equations of motion of the particles. Loo and Cork

(1988) studied virtual impactors by experiments. In both studies, the most important parameters were identified to be 1) the nozzle Reynolds number, 2) the fraction of flow passing through the collection probe, 3) the ratio between the nozzle diameter and the collection probe diameter, and 4) the nozzle-to-collection probe distance.

Many virtual impactors currently available have been developed for size-fractionated aerosol sampling for air pollution study or concentrating particles for industrial applications (Sioutas et al., 1994; Barr et al., 1983). Accordingly, they were large and required such a high airflow rate, 1 cfm or higher, that they could not be used for personal sampling. Moreover, they had large internal losses of particles near the cutoff size, which was undesirable. For personal sampling, Marple et al. (1995) developed a virtual impactor personal aerosol sampler (VIPAS) for dichotomous sampling of diesel exhaust and mine dust. VIPAS was designed to sample solid particles and had a fixed cutsize of 0.8 μm. Xiong et al. (1998) designed a portable vapor/particle sampler (PVPS) for use by industrial hygienists. The particle cutsize was 0.9 μm at a sampling flow rate of 1.8 lpm and a dichotomous flow ratio between minor flow and major flow was 1:8. PVPS still allowed some sampled particles to evaporate. In their experiments with liquid styrene, Xiong et al. (1998) estimated that in general 20 – 30% of styrene was lost at their recommended flow ratio. Accordingly, their sampler could yield large sampling errors.

In this paper, we tested the possibility of a new semivolatile dichotomous sampler with the hope that it would overcome some of the problems of existing personal sampling methods. The design and theory of the proposed sampler is described. A prototype sampler was experimentally tested in two different modes and their results were compared. A numerical model was built and validated using the experimental data.

THEORY AND DESIGN

For convenience and to distinguish it from virtual impactors, the proposed sampler is called the semivolatile aerosol dichotomous sampler (SADS) throughout this paper. The principle of separating particles from air flow in SADS is basically the same as that of round nozzle virtual impactors. Virtual impactors separate particles from air flow based on the inertia that particles possess. The SADS design is similar to virtual impactor design and the prototype of SADS used in this paper was originally built as a virtual impactor. The main difference between virtual impactors and SADS is the inverted flow ratio between the major and minor flows.

Operating a virtual impactor with different flow relationships gives different performance with respect to 50% cutsize and wall loss. The definition of 50% cutsize was the size showing 50% efficiency in the particle separation efficiency curve. Particle separation efficiency (η) was computed from:

$$\eta = \frac{C_{major}}{C_{total}} \times 100(\%), \qquad (1)$$

where C_{major} and C_{total} are mean number concentrations in the major flow and the upstream flow, respectively. The wall loss was defined as the percentage of particles that collect on the inner wall of the sampler during the sampling among the total particles that enter the inlet. In this section, we explain how SADS settings can give

lower cutsize and lower wall loss compared with the same device operated as a conventional virtual impactor.

Referring to Figure 1, assume that a particle moves along the air flow and is located close to the wall of an inlet nozzle. In conventional virtual impactors [Figure 1-(a)], 90% of the air moves toward the so-called ‘major flow’ direction which is perpendicular to the air nozzle. The remaining 10% of air goes toward the ‘minor flow’ direction which is parallel to the air nozzle. Assume again that the size of the particle is small enough for the velocity vector on the particle to head toward the ‘major flow’ direction. In the SADS setting [Figure 1-(b)], the flow ratio between the ‘major flow’ and the ‘minor flow’ is inverted. To account for this difference, additional terminology was developed. In this paper, instead of using ‘major flow’ and ‘minor flow’, we use the designation ‘vapor flow’ and ‘particle flow’ respectively. For the same-sized particle in the same location as in the virtual impactor, the direction of the vector on the particle is changed. From this change, researchers could achieve a lower 50% cutsize using the same virtual impactor.

In the SADS setting, more than 50% of air directly passes through the separation area to the particle flow without significant direction change. This helps reduce the wall loss compared with the virtual impactors in which most of the air experienced directional change.

In addition to lower cutsize and lower wall loss, SADS has the advantage of instant separation of particles. This is important because instant separation minimizes the chance that captured particles evaporate and contribute to the vapor flow. SADS also does not require electrical power and can be easily utilized for personal sampling. A similar attempt was made by Xiong et al. (1998). In that study, the authors evaluated a modified virtual impactor for which the flow ratio between the particle flow and the vapor flow ($Q_{particle}/Q_{vapor}$) ranged from 0.125 to 1. Due to the design of their sampler, the particles deposited on the filer media still could evaporate to the vapor flow so that instant separation was not achieved.

In actual sampling, one filter cassette assembly and one ACT in series need to be attached to the particle flow side of the SADS and one ACT to the vapor flow side. The airborne vapor concentration (C_{vapor}) and the airborne particle concentration ($C_{particle}$) can be determined based on measured values of the masses collected on the filter (M_{filter}) and the two ACTs (M_{ACTv} and M_{ACTp}), sampling time (t), and each flow rate (Q_{vapor} and $Q_{particle}$), under the assumption of complete particle separation, as:

$$C_{vapor} = \frac{M_{ACTv}}{t \times Q_{vapor}} \tag{2}$$

$$C_{particle} = \frac{\left(M_{filter} + M_{ACTp}\right) - \left(\frac{Q_{particle}}{Q_{vapor}}\right) M_{ACTv}}{t \times \left(Q_{vapor} + Q_{particle}\right)} \tag{3}$$

It is anticipated that a minute amount of particles smaller than the cutsize of

SADS will follow the vapor flow and be captured by ACT. However, if the majority of the size distribution of airborne particles is larger than the cutsize of the SADS, this portion will be negligible when estimating the mass concentrations of each phase.

MATERIALS AND METHODS

A numerical model applicable for both the SADS and conventional virtual impactors was built using a commercially-available software package. The separation efficiency and wall losses were estimated for both schemes. For virtual impactor (VI) settings, the model was validated by comparison to a published experimental study. For SADS settings, validation was accomplished by comparison with our own experimental data.

Numerical Simulation

Numerical simulation using computational fluid dynamics (CFD) is an effective way to estimate the performance of a new sampler and identify problems before building the actual samplers. GAMBIT 2.2 and FLUENT 6.2 (FLUENT Inc., Lebanon, NH) were used for building solution domain geometries and meshes and solving flow fields, respectively. Simplified 2-dimensional axisymmetric designs were employed to build the geometries of the CFD model.

An existing virtual impactor was simulated in both SADS settings and VI settings. A schematic of that virtual impactor with key dimensions is shown in Figure 2. A nozzle diameter of 0.08 cm with an opening angle of 18.8° was used. The

geometry was based on that suggested by Loo and Cork (1988).

The inside of the SADS and one 37mm filter cassette attached to the particle flow were included in the computational domain (Figure 3). Denser meshing for the separation region and near the walls was used because the flow has large velocity gradients in these regions. The calculation domain had about 150,000 nodes and about 300,000 cells. Uniform velocity was assumed at the inlet. The two outlets had outflow boundary conditions and their split ratio was $Q_{vapor} : Q_{particle} = 9 : 1$ for VI settings and $Q_{vapor} : Q_{particle} = 1 : 6$ for SADS settings. The pressure at the inlet was assumed to be 1 atm.

The equations used for the flow field calculation were the continuity equation and the Navier-Stokes equation without the loss of continuity. For an incompressible Newtonian fluid, these equations reduce to:

$$\nabla \cdot V = 0 \tag{4}$$

$$\rho \frac{dV}{dt} = \rho g - \nabla p + \mu \nabla^2 V \tag{5}$$

where V is the two-dimensional velocity vector, ρ is the fluid density, t is time, g is the gravity field, p is the pressure, and μ is the coefficient of viscosity (White, 1994). The gravity term g was ignored in this study.

The flow in the virtual impactor was assumed to be turbulent with a Reynolds number of 3500 at the nozzle. The default standard *k-ε* model in the FLUENT

software was used for turbulent flow calculations. The initial turbulence kinetic energy was assumed to be zero. Convergence was declared when the residual of mass flow rate became less than 0.01% of the inlet mass flow rate.

After the steady flow field was obtained, the trajectory of a particle was found by integrating the equation of motion in time (Fluent Inc., 2005). Here, the particle was regarded as being deposited on an inner surface when the center of the particle reached a point less than half of the particle diameter away from the wall. FLUENT 6.2 predicted the trajectory of a discrete phase particle by integrating the force balance on the particle. For sub-micrometer particles, a form of Stokes' drag law was applied (Ounis et al., 1991).

Two hundred spherical particles were imposed with equal inter-particle distance from the inlet wall to $0.05D_{nozzle}$ away for SADS settings (Figure 4) and from the inlet wall to axis for VI settings. When the n-th particle away from the wall exited with either the particle flow or vapor flow or was deposited on a wall, any particle entering in the circular area between the *n*-th and (*n*-1)-th were considered to have the same fate. The diameters of imposed particles were between 0.1 and 2.0 μm. Uniform velocity was assumed at the inlet boundary so that the flow rate was proportional to the size of the annular area between the *n*-th and (*n*-1)-th at the inlet.

Separation efficiency is a function of particle size and was defined only for the

vapor flow. This is because particle separation occurs only for that flow. The particle flow contributes partly to wall loss and passes only through the collection probe which is coaxial with the air nozzle. Wall loss was defined as the fraction of the incoming mass that is lost on the wall between 0.1 μm to 2.0 μm.

Validation Data

The numerical model was validated by two sets of data. Validation for VI settings was performed by comparison to another computer simulation study which included experimental data. Marple and Chien (1980) studied the characteristics of virtual impactors by their numerical solutions and compared their model with experimental data. They obtained their efficiency curve by simulating at Re=5000 and compared it with the results of experiments from Loo and Cork (1978), which were performed at Re=6000. For our virtual impactor model, we simulated this case and compared our results with the experimental data from the study of Loo and Cork (1978) and Marple and Chien's (1980) numerical model.

Figure 5 shows the test system for validating the numerical model using SADS settings. To validate the SADS model, two different sets of experiments were employed. Monodisperse fluorescent polystyrene microspheres (Duke Scientific, Palo Alto, CA) in aqueous suspension were used in both sets of experiments. In the first set,

particles in the range of 0.2 to 1.0 μm were sampled from the incoming and outgoing flows using filters, eluted from the filters, and quantified using a spectrofluorometer to determine separation efficiency. However, variability increased in the spectrofluorometer readings when particles were smaller than 0.3 μm in diameter. Therefore, optical particle counters (OPCs) were used in the second set of tests to measure separation efficiency for particles 0.05 to 0.5 μm in diameter in real time.

In the first set of measurements, six different monodisperse sizes were used having physical diameters ranging from 0.2 to 1.0 μm, with a density of 1.06 g/cm^3. The red fluorescent dye had maximum excitation and emission at 542 and 612 nm, respectively. During each test run, monodisperse aerosol with a given particle size was nebulized, dried with clean dry air, and then collected from the upstream flow, vapor flow, and particle flow of a virtual impactor using 2.0 μm PTFE filters (225-27-09, SKC Inc., Eighty Four, PA). After each run, all filters were immersed in 10 ml of 0.1% Tween 80 solution (Sigma-Aldrich Co., St. Louis, MO) and then sonicated for 5 minutes to make dispersed suspensions. The fluorescence intensities of the samples were analyzed using a spectrofluorophotometer (RF-5301, Shimadzu Scientific Instruments, Columbia, MD). Relative particle concentrations were determined for each run and used to obtain separation efficiency (η) as follows:

$$\eta = \left(1 - \frac{\left(i_{vapor} - i_{blank}\right) \times DF_{vapor} / Q_{vapor}}{\left(i_{upstream} - i_{blank}\right) \times DF_{upstream} / Q_{total}}\right) \times 100(\%), \qquad (6)$$

where i and DF are intensity readings and dilution factors for each sample from blank, upstream, and vapor flow. For each particle size, the sample that had the highest intensity was diluted in series and the linearity between particle concentration and fluorescence intensity was verified.

In the second set, six different monodisperse particles suspensions having physical diameters ranging from 0.05 to 0.50 μm were nebulized and classified using an Electrostatic Classifier (TSI Model 3071, Shoreview, MN). The counts of particles were measured upstream of the sampler and at the vapor flow using a P-Trak (TSI Model 8525, Shoreview, MN) and a Condensation Particle Counter (CPC) (TSI Model 3022, Shoreview, MN), respectively. Separation efficiency (η) was calculated.

For each size of particle, experiments were repeated 3 times and averages and standard deviations were calculated. Numerical simulations were compared to these data at the same conditions. The virtual impactor performance was also modeled for the same model dimensions.

In the experiment, the back pressure at each outlet was measured using Magnehelic gauges (Dwyer Instruments, Michigan City, IN) in which the reference tab was open to room air. In the numerical simulation, the pressure at each outlet was

obtained and compared with those from experimental data.

RESULTS

Our numerical model was applied to simulate the study of Marple and Chien (1980). The separation efficiencies are shown in Figure 6. In our model, when Re=5000 and laminar flow was applied, the efficiency curve was closely overlapped with that of Marple and Chien's laminar flow model in which Re was 5000. When the turbulence model was applied at Re=6000 to compare to the data of Loo and Cork (1978) in which Re was 6000, the efficiency curve lay slightly to the left of the experimental result.

The results of experiments at SADS settings with fluorescent PSL spheres are compared with those from our numerical model (Figure 7). In SADS settings, the separation efficiency of the experimental data was slightly lower than that of the numerical model. In numerical simulations, the 50% cutsize of a virtual impactor was 0.97 $\sqrt{Stk}$ and the 50% cutsize of the same sampler ran in the SADS settings was 0.27 $\sqrt{Stk}$. The 50% cutsize for the experimental readings was 0.33 $\sqrt{Stk}$.

Pressure drops through the virtual impactor in each setting are displayed in Figure 8. The pressure drop at the vapor flow outlet was similar in both modes and the numerical estimations match well with experimental results. At the particle flow outlet, however, the difference between the two modes was significant and the numerical

model overestimated the pressure drops.

Wall losses inside the virtual impactor in each setting were estimated using the numerical model (Figure 9). In VI settings, a sharp peak was found near the 50% cutsize and the value was near 8%. In SADS settings, the peak was not distinct and wall loss was less than 0.5%. Wall losses were not evaluated experimentally.

DISCUSSION

Using experimental data, the numerical model was validated in two different tests. In both cases the numerical model slightly underestimated the 50% cutsize as compared to the experimental tests. In Figure 6, our laminar flow model fit well with the laminar flow model of Marple and Chien (1980) at Re=5000. Our turbulent model also closely matched the experimental data of Loo and Cork (1978) at Re=6000. Our laminar flow model for the SADS settings, not presented in Figure 7, matched the experimental data even better than the turbulent model. However, the laminar flow model frequently resulted in non-converging unstable solutions when Reynolds number was greater than 2000. The standard k-ε model was successfully applied in the study of virtual impactors by Asgharian and Godo (1997). For the same size of particle, our turbulence model slightly overestimated the separation efficiency compared with the experimental data of Loo and Cork (1978) in Figure 6. The differences between the model and the experimental data could partially come from the fact that initial conditions and the boundary conditions of the numerical model are not exactly matching with the experimental conditions (Munson et al., 2002). Because the differences are consistent and minor in this study, we believe that our model is valid for comparing the operation of a virtual impactor in SADS settings to operation

in VI settings.

Sampling in the SADS settings can achieve instant separation of particles from particle-laden air flow. Smaller wall loss can be expected because only a small fraction of air passes through the vapor flow and experiences the separation. The ratio of air experiencing the separation process depends on the flow ratio between the vapor flow and particle flow. In general, only a small portion of the total flow participates in the separation process in the SADS setting compared with sampling in the VI settings. Sampling in SADS settings gives lower cutsize compared with sampling in VI settings even when the same virtual impactor was used as shown in this paper.

It is clear that sampling in the SADS settings is not a completely dichotomous process. The vapor flow still contains some particles smaller than the cutsize. Nevertheless, these losses of particles to the vapor flow are expected to be much smaller than evaporative losses observed during filter sampling. Figure 10 presents a size distribution of mineral oil mist measured using an eight-stage cascade impactor in an experimental MWF study (Raynor et al., 2000). The mass median diameter and geometric standard deviation of the size distribution were 2.4 μm and 1.4, respectively (Volckens et al., 1999). The true droplet and vapor concentrations for the aerosol with this size distribution were measured using an ESP and ACTs as 0.52 and

2.8 mg/m^3, respectively. When the droplets were sampled with glass fiber, PVC, and PTFE filters, concentrations were measured as 0.15, 0.16, and 0.29 mg/m^3, respectively, suggesting evaporative losses of 44-71%. If this aerosol were sampled using the SADS evaluated in this study with the efficiency curve shown in Figure 7, the size distribution of particles in the vapor flow would be the smaller distribution in Figure 10 and the percent of incoming mass lost to the vapor flow would be only 0.5%. This demonstrates the potential for the SADS to obtain more accurate measurements of droplet and vapor concentrations for semivolatile aerosols than filters can.

In many cases for which separate sampling for the droplet and vapor phases is recommended, the mass median diameters will be larger than the above case. For example, particles generated in industrial spray processes are frequently large. The geometric mean aerodynamic diameters of aerosols generated by paint sprays range from 20-50 μm according to the data measured Brosseau et al. (1992). In case of MWFs, Woskie et al. (1994) reported that the aerodynamic mass median diameters (MMDs) for straight oil were predicted from 6.4 to 7.7 μm and MMDs for soluble oil mist varied between 6.9 and 8.0 μm. Piacitelli et al. (2001) calculated the overall mean MMD of their study data as 5.3 μm. In these conditions, sampling in the SADS settings will enable effective measurement of the particle fraction. The vapor fraction

will be slightly overestimated because the particles smaller than the cutsize will flow toward vapor flow (about 0.5 μm for the virtual impactor used in this study).

Compared with sampling in the VI settings, greater pressure drop at the outlet of vapor flow with the SADS settings was found. This could be caused by Venturi effect at the separation zone and then it can be explained by Bernoulli's equation (Munson et al., 2002). More back pressure builds up when sorbent tubes are attached to each flow to collect vapor. Still, this quantity of back pressure can be handled by personal pumps. For this reason, the SADS can be suitable for personal sampling of semivolatile aerosol exposures in workplace settings.

CONCLUSIONS

Standard sampling methods for airborne semi-volatile organic compounds have traditionally relied on filtration methods that have evaporation loss problems. While virtual impactors make instant separation of vapor and particles possible, they experience large wall losses near the cutsize of interest. A new approach to sampling aerosols using a virtual impactor was attempted using inverted flow ratios. A CFD model for VI and SADS settings was built and validated. The validated model shows that SADS settings provide much smaller cutsize and much smaller wall loss than VI settings. SADS is an approach that can lead to much more accurate sampling of the particle and vapor phases of a semivolatile aerosol.

REFERENCES

Asgharian B, Godo MN. (1997) Transportation and deposition of spherical particles and fibers in an improved virtual impactor. Aerosol Sci Technol; 27 499-506.

Barr EB, Hoover MD, Kanapilly GM, Yeh HC, Rothenberg SJ. (1983) Aerosol concentrator. Aerosol Sci Technol; 2 437-442.

Bergman TA, Johnson DL, Boatright DT, Smallwood KG, Rando RJ. (1996) Occupational exposure of nonsmoking nightclub musicians to environmental tobacco smoke. Am Ind Hyg Assoc J; 57 746–752.

Bidleman TE. (1988) Atmospheric processes – wet and dry deposition of organic compounds are controlled by their vapor-particle partitioning. Environ Sci Technol; 22 361-367.

Brosseau LM, Fang CP, Snyder C, Cohen BS. (1992) Particle size distribution of automobile paint sprays. Appl Occup Environ Hyg; 7 607–612.

Brown RH, Monteith LE. (2001) Gas and vapor sample collectors. In Cohen BS, McCammon CS Jr., editors. Air sampling instruments for evaluation of atmospheric contaminants. Cincinnati: American Conference of Governmental Industrial Hygienists. p. 421-424. ISBN 1 882417 39 9.

Cheng Y, Tsai C. (1997) Evaporation loss of ammonium nitrate particles during filter

sampling. J Aerosol Sci; 28 1553-1567.

Cohen BS, Brosseau LM, Fang CP, Bower A, Snyhder C. (1992) Measurement of air concentrations of volatile aerosols in paint spray applications. Appl Occup Environ Hyg; 7 514-521.

Eatough DJ, Lewis LJ, Eatough M, Lewis EA. (1995) Sampling artifacts in the determination of particulate sulfate and SO_2(g) in the desert Southwest using filter pack samplers. Environ Sci Technol; 29 787-791.

Fairchild CI, Tillery MI. (1977) The filtration efficiency of organic vapor sampling tubes against particulates. Am Ind Hyg Assoc J; 38 277-283.

Flagan RC. (2001) Electrical techniques. In Baron PA, Willeke K, editors. Aerosol measurement: principles, techniques, and applications. New York: Wiley-InterScience. p. 537-568. ISBN 0 471 35636 0

Fluent Inc. (2005) FLUENT 6.2 User's Guide. Fluent Inc. p. 23-5-11.

Fuchs NA. (1964) The Mechanics of Aerosols. New York: Pergamon Press. p. 151-159.

Guidotti TL, Yoshida K, Clough V. (1994) Personal exposure to pesticide among workers engaged in pesticide container recycling operations. Am Ind Hyg Assoc J; 55 1154-1163.

Hounam RF, Sherwood RJ. (1965) The cascade centripeter: a device for determining

the concentration and size distribution of aerosols. Am Ind Hyg Assoc J; 26 122-131.

Kaupp H, Umlauf G. (1992) Atmospheric gas-particle portioning of organic compounds: comparison of sampling methods. Atmos Environ; 26 2259-2267

Kriech AJ, Kurek JT, Wissel HL, Osborn LV, Blackburn GR. (2002) Evaluation of worker exposure to asphalt paving fumes using traditional and nontraditional techniques. Am Ind Hyg Assoc J; 63 628-635.

Krieger MS, Hites RA. (1992) Diffusion denuder for the collection of semivolatile organic compounds. Environ Sci Technol; 26 1551-1555.

Leith D, Leith FA, Boundy MG. (1996) Laboratory measurements of oil mist concentrations using filters and an electrostatic Precipitator. Am Ind Hyg Assoc J; 57 1137-1141.

Loo BW, Cork CP. (1978) Paper LBL-8204.University of California, Berkeley, California: Lawrence Berkeley Labs.

Loo BW, Cork CP. (1988) Development of high efficiency virtual impactors. Aerosol Sci Technol; 9 167-176.

Marple VA. (1970) A fundamental study of inertial impactors. PhD Thesis, Mechanical Engineering Department, University of Minnesota: Particle Technology Laboratory Publ. No. 144.

Marple VA, Liu BYH. (1974) Characteristics of laminar jet impactors. Environ Sci Technol; 8 648-654.

Marple VA, Liu BYH. (1975) On fluid flow and aerosol impaction in inertial impactors. J Colloid interface Sci; 53 31-34.

Marple VA, Chien CM. (1980) Virtual impactors: a theoretical study. Environ Sci Technol; 14 976-984.

Marple VA, Rubow KL, Olson BA. (1995) Diesel exhaust / mine dust virtual impactor personal aerosol sampler: design, calibration and field evaluation. Aerosol Sci Technol; 22 140-150.

Munson BR, Young DF, Okiishi TH. (2002) Fundamentals of Fluid Mechanics. Danvers, MA: John Wiley & Sons, Inc. ISBN 0 471 44250 X.

NIOSH (1998). NIOSH Manual of Analytical Methods (NMAM). 4th ed., DHHS (NIOSH) Publication 94-113. Available from: URL: http://www.cdc.gov/niosh/nmam/nmammenu.html

Ounis H, Ahmadi G, McLaughlin JB. (1991) Brownian diffusion of submicrometer particles in the viscous sublayer. J Colloid Interface Sci; 143(1) 266-277.

Park D, Kim S, Yoon C. (2003) Loss of straight metalworking fluid samples from evaporation during sampling and desiccation. Am Ind Hyg Assoc J; 64 837-841.

Piacitelli GM, Sieber WK, O'Brien DM, Hughes RT, Glaser RA, Catalano JD. (2001)

Metalworking fluid exposure in small machine shops: an overview. Am Ind Hyg Assoc J; 62 356-370.

Raynor PC, Leith D. (1999) Evaporation of accumulated multicomponent liquids from fibrous filters. Ann Occup Hyg; 43(3) 181-192.

Raynor PC, Volckens J, Leith D. (2000) Modeling evaporative loss of oil mist collected by sampling filters. Appl Occup Environ Hyg; 15 90-96.

Rounds SA, Tiffany BA, Pankow JF. (1993) Description of gas/particle sorption kinetics with an intraparticle diffusion model: desorption experiments. Environ Sci Technol; 27(2) 366-377.

Simpson AT, Groves JA, Unwin J, Piney M. (2000) Mineral oil metal working fluids (MWFs) – development of practical criteria for mist sampling. Ann Occup Hyg; 44 165-172.

Sioutas C, Koutrakis P, Burton PM. (1994) A high-volume small cutpoint virtual impactor for separation of atmospheric particulate from gases pollutants. Particulate Sci Technol; 12 207-221.

Turpin BJ, Liu S, Podolske KS, Gomes MSP, Eisenreich SJ, McMurry PH. (1993) Design and evaluation of a novel diffusion separator for measuring gas/particle distributions of semivolatile organic compounds. Environ Sci Technol; 27 2441-2449.

Van Vaeck L, Van Cauwenberghe K, Janssens J. (1984) The gas-particle distribution of organic aerosol constituents: measurement of the volatilization artifact in Hi-Vol cascade impactor sampling. Atmos Environ; 18(2) 417-430.

Volckens J, Boundy M, Leith D, Hands D. (1999) Oil mist concentration: a comparison of sampling methods. Am Ind Hyg Assoc J; 60 684-689.

Volckens J, Leith D. (2003) Partitioning theory for respiratory deposition of semivolatile aerosols. Ann Occup Hyg; 47(2) 157-164.

White FM. (1994) Fluid mechanics. 3rd ed., McGraw-Hill. p. 213.

Xiong JQ, Fang C, Cohen BS. (1998) A portable vapor/particle sampler. Am Ind Hyg Assoc J; 58 614-621.

Woskie SR, Smith TJ, Hammond SK, Hallock MH. (1994) Factors affecting worker exposures to metal-working fluids during automotive component manufacturing. Appl Occup Environ Hyg; 9 612-21.

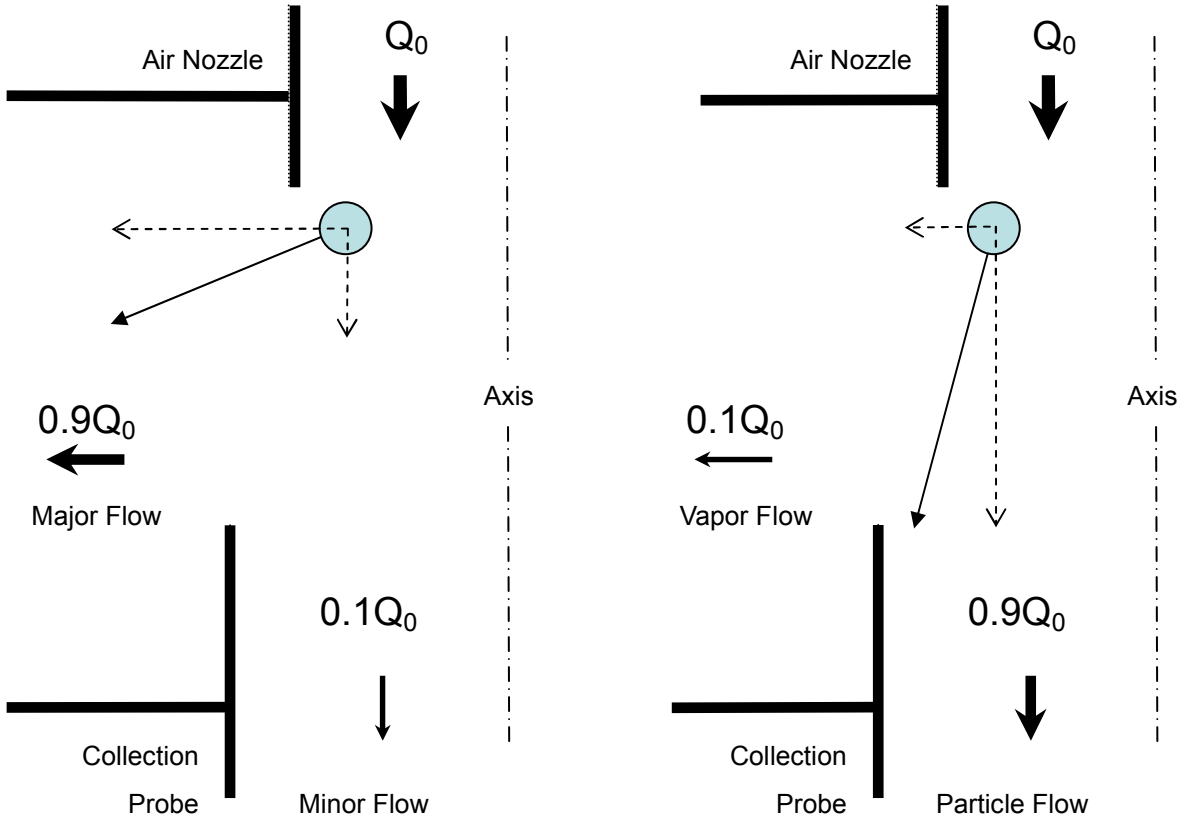

(a) Virtual Impactor

(b) SADS

Figure 1. Diagram illustrating the principle of decreasing the cutsize in the SADS settings as compared to the virtual impactor settings.

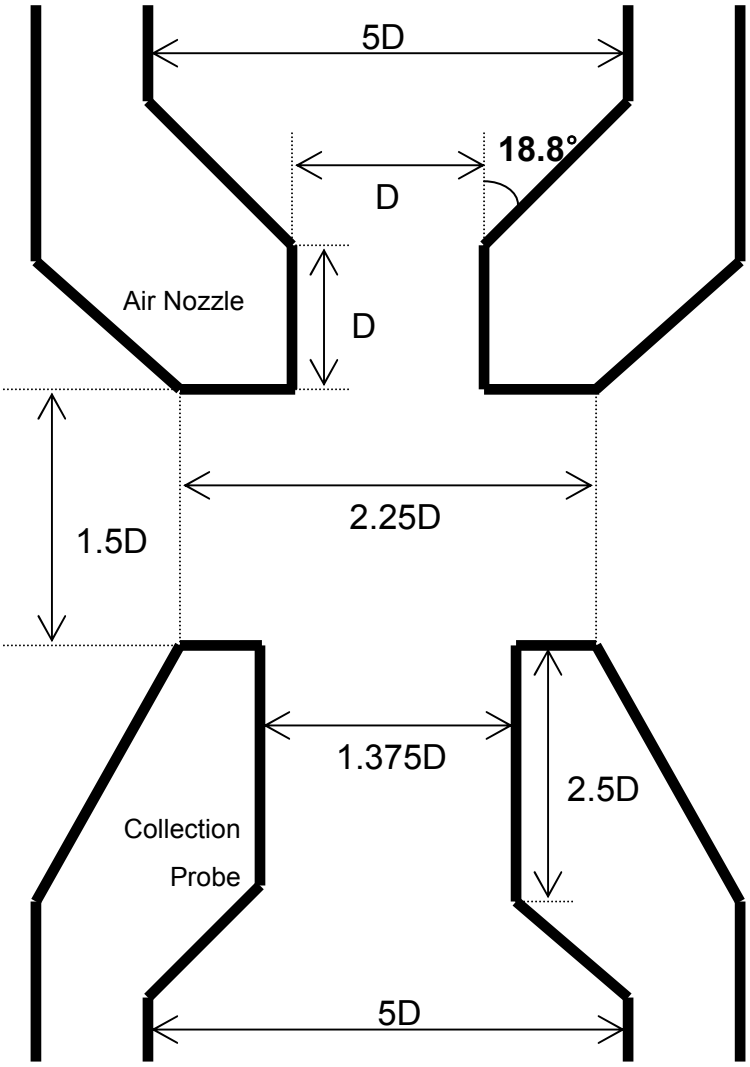

Figure 2. Dimensions of the separation area of a virtual impactor (not to scale).

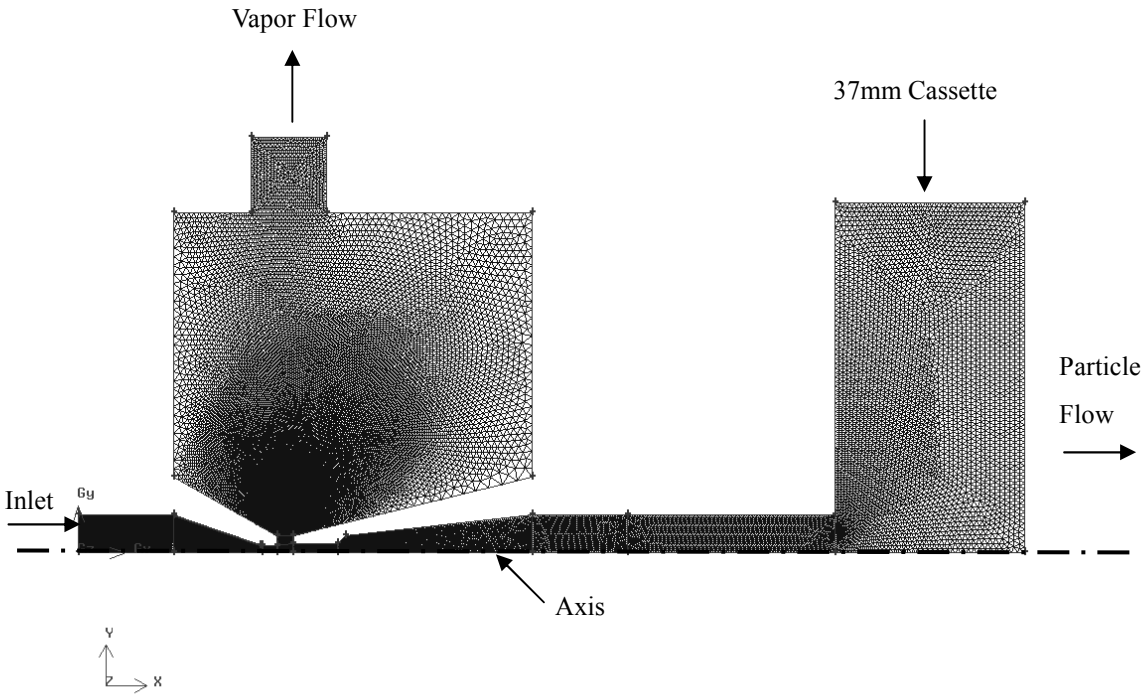

Figure 3. Finite element model volume mesh of the computational domain including a 37 mm cassette.

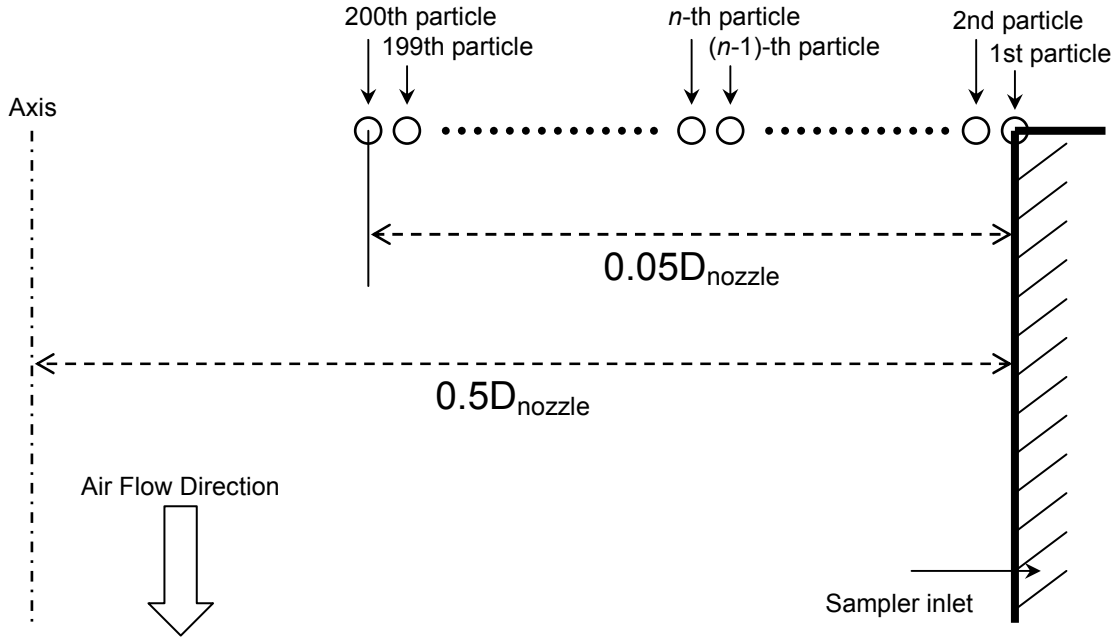

Figure 4. The locations where particles were imposed at the sampling inlet. Drawing is not to scale.

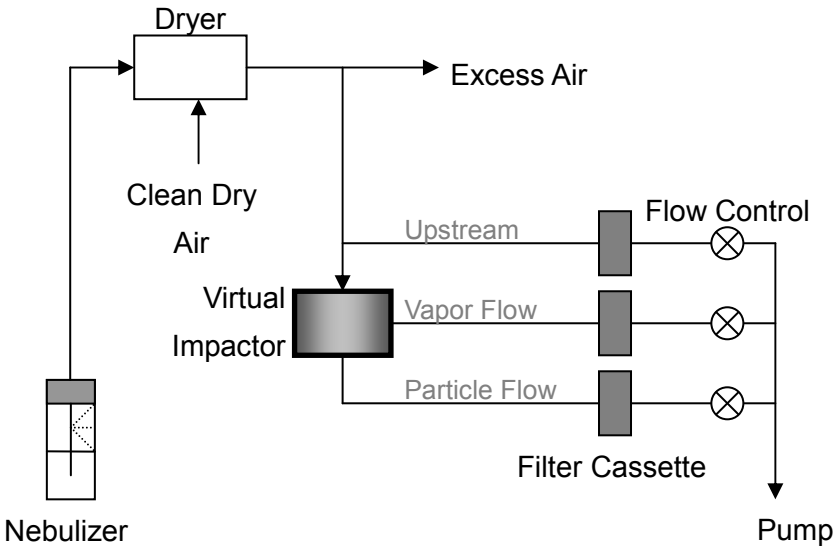

Figure 5. Schematic diagram of experimental setup.

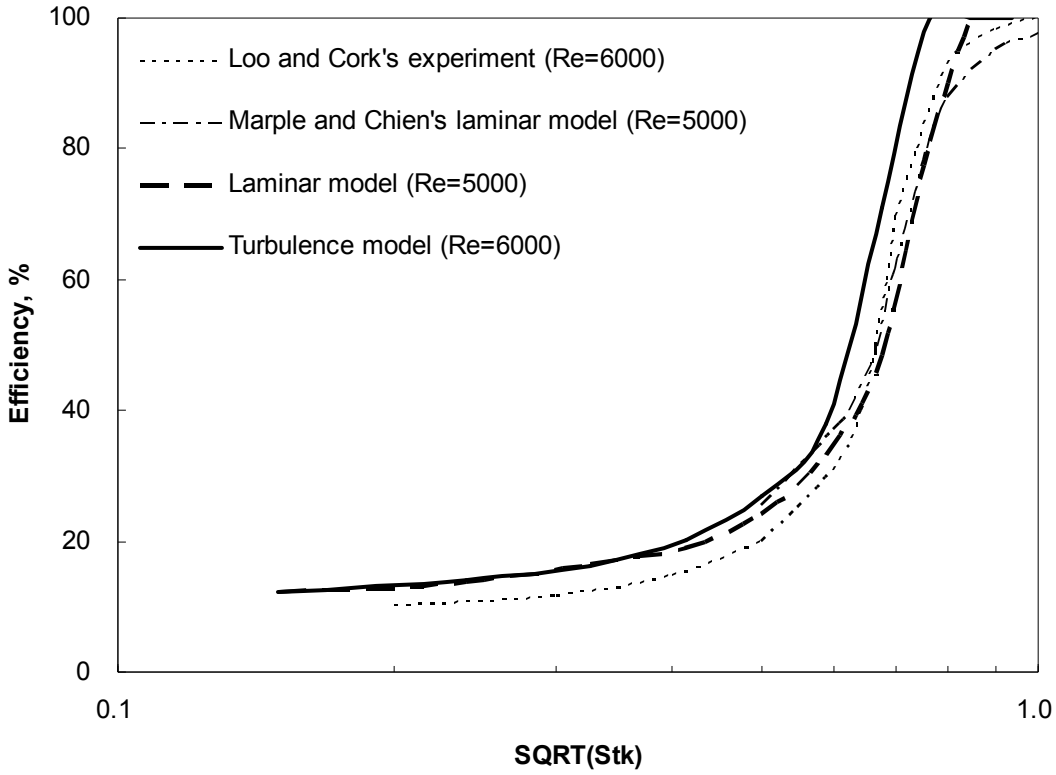

Figure 6. Comparison of numerical model with the results from Loo and Cork (1978) and Marple and Chien (1980). The efficiency curve for the laminar flow model at Re=5000 was closely overlapped with that of Marple and Chien's model. The efficiency curve for the turbulence model at Re=6000 lay slightly to the left side of the experimental result.

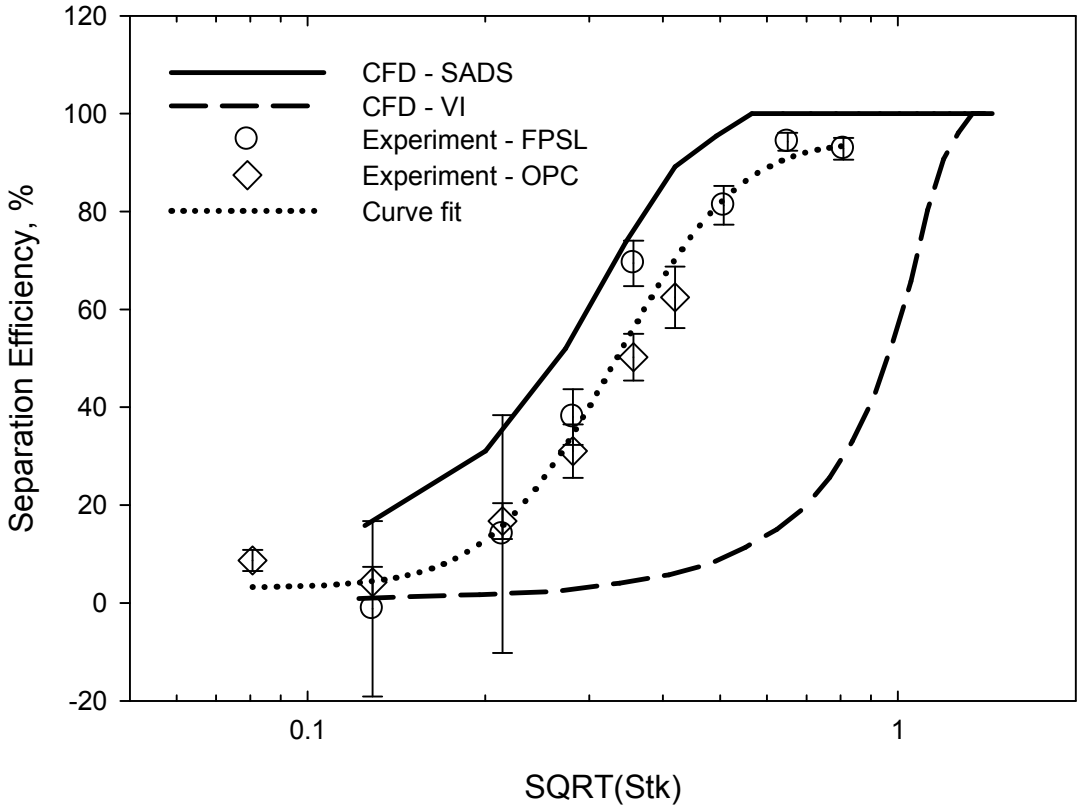

Figure 7. Comparison of numerical results (CFD model) with experimental data. A virtual impactor was simulated in the virtual impactor settings (VI) and in the SADS settings, respectively. Error bars present one standard deviation at each size.

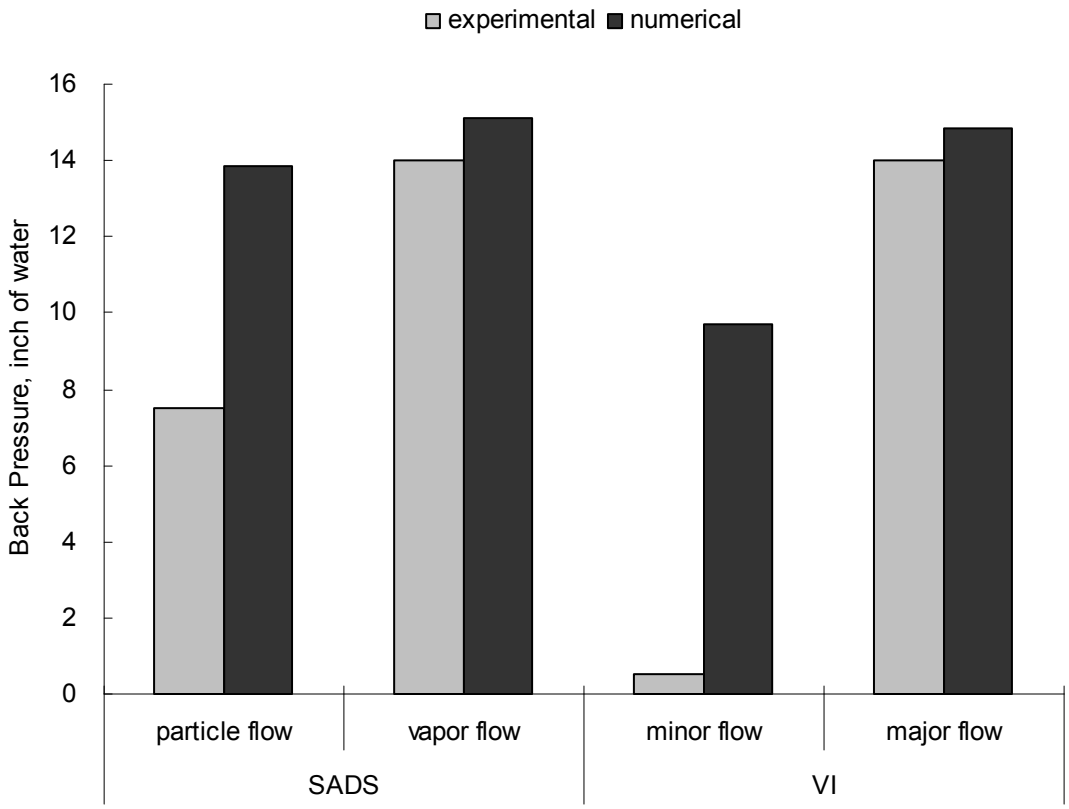

Figure 8. Comparison of back pressures at each outlet of particle flow and vapor flow in SADS settings and virtual impactor settings (VI).

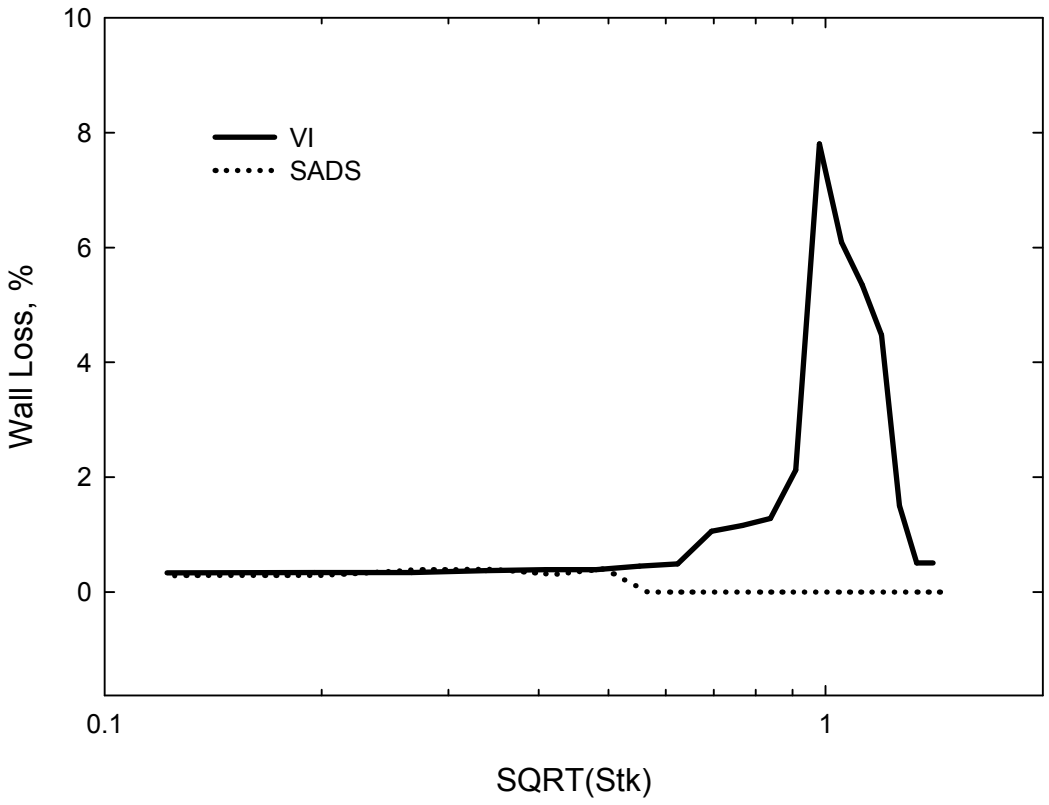

Figure 9. Comparison of wall loss in the numerical model. A virtual impactor was simulated in the virtual impactor settings (VI) and in the SADS settings, respectively.

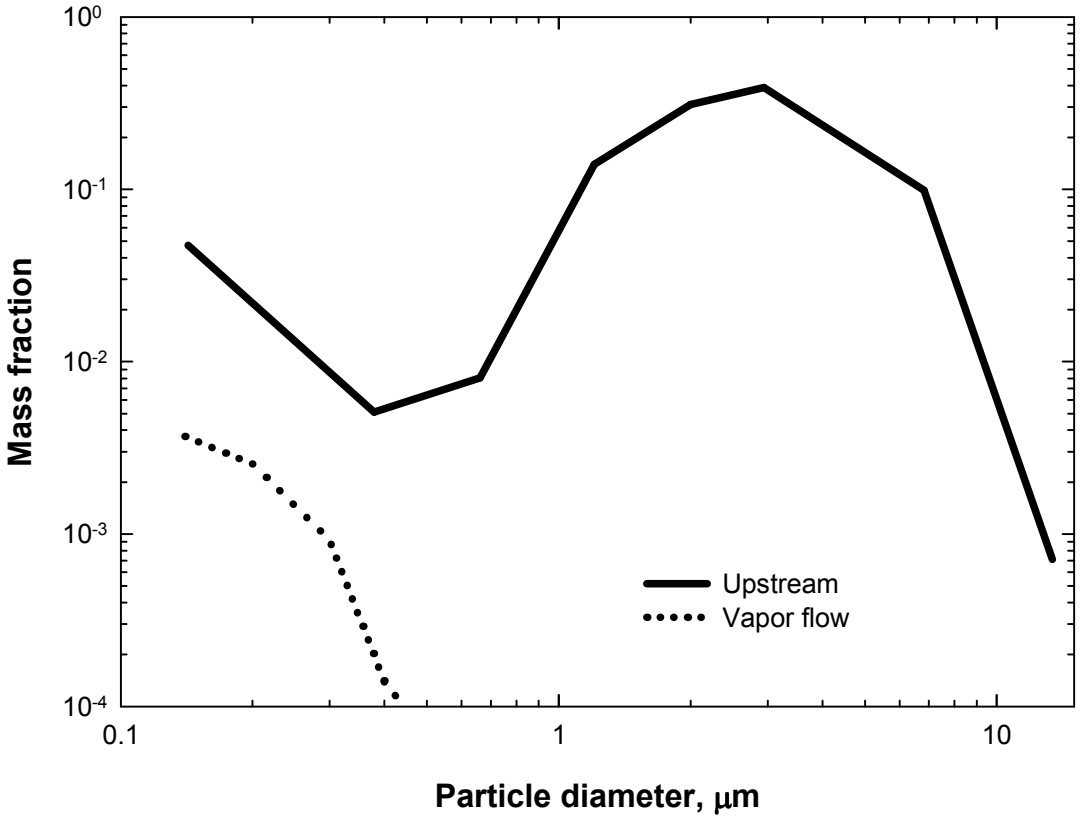

Figure 10. A typical size distribution of mineral oil mist measured by Volckens et al. (1999) (solid line) and the estimated mass fraction that would be lost to the vapor flow (dotted line) in SADS settings sampling.

CHAPTER III

Optimization of the Design of a Semivolatile Aerosol Dichotomous Sampler

ABSTRACT

This paper reports the results of an optimization procedure for a semivolatile aerosol dichotomous sampler (SADS) and experimental confirmation with the optimized sampler. Using the same numerical model adopted in Chapter II, the relationships between four major design and operating parameters significantly affecting the performance of the SADS and four performance parameters were expressed in polynomial equations. Utilizing an optimization procedure, values for the major parameters giving the best performance were determined and used as the base model for optimizing minor parameters. Five minor parameters were then investigated for their possible contribution to better performance of the SADS. The optimal dimensions found were as follows: the diameter ratio between the nozzle and the collection probe was 1.30 and the length ratio of the distance between the nozzle and the collection probe over nozzle diameter was 0.6. Among the minor parameters, only the entrance angle of the nozzle made noticeable improvement at 45°. Experimental tests confirmed that the performance of the new sampler was improved although not as much as expected from the numerical simulation.

INTRODUCTION

Sampling semivolatile aerosols for exposure assessment poses several challenges. Semivolatile aerosols are generated from semivolatile organic compounds (SOCs), which have low vapor pressure between 10^{4} – 10^{-11} atm (Bidleman, 1988). In workplace environments, well known semivolatile aerosols that are associated with adverse health effects include metal removal fluid (MRF) mists, pesticides, asphalt fumes, and environmental tobacco smoke (Woskie et al., 1994; Guidotti et al., 1994; Kriech et al., 2002; Bergman et al., 1996). The compounds in semivolatile aerosols exist in both vapor and particulate form simultaneously at room temperature due to their low volatility (Bidleman, 1988). Sampling only one phase will underestimate the potential exposure to SOC aerosols. In particular, sampling only the particle phase using filtration can significantly bias the exposure due to evaporative loss during sampling (Volckens et al., 1999; Raynor and Leith, 1999; Park et al., 2003). Furthermore, evaluating the vapor and particle phases separately is important because each phase is absorbed into the human body by a different mechanism (Volckens and Leith, 2003).

Another situation in which separation of two phases is important is during sampling of volatile organic compounds (VOCs) coexisting with particles of another

substance. Airborne particles may adsorb or solubilize the VOCs and make the exposure assessment for the VOCs biased (Cohen et al., 1992). Cohen et al. found that the xylene concentrations measured using glass fiber filters followed by sorbent tubes were statistically higher than those measured using only sorbent tubes in paint spray booths.

Conventional methods for sampling SOCs and particles containing VOCs use various filter media or prefiltered sorbent tubes. A high possibility of evaporative loss has been reported for sampling methods using filter media (Raynor and Leith, 1999; Park et al., 2003).

In Chapter II, a semivolatile aerosol dichotomous sampler (SADS) was proposed and tests showed that this new idea has the potential to separate particles and vapor molecules effectively. SADS is a round nozzle virtual impactor for personal sampling. A virtual impactor is a modification to a conventional impactor in which the impaction plate is replaced with a collection probe drawing a fraction of the incoming air (Hounam and Sherwood, 1965). In conventional virtual impactors, typically about 90% of the air moves toward the major flow direction and the remaining 10% of air goes toward the minor flow direction (Figure 1a). In these conditions, the trajectory of a particle with a certain size coming from the air nozzle will follow the vector sum of two vectors, the vector toward the major flow direction and the vector toward the

minor flow direction. The vector toward the major flow direction is stronger because the majority of air flow goes to that direction in virtual impactors. The flow ratio between the major flow and the minor flow is inverted in the SADS (Figure 1b). Because of this inversion, the major and minor flows were redesignated in this paper as ‘vapor flow’ and ‘particle flow’, respectively. For the particle with same size in the same location as in the virtual impactor settings, the direction of the vector on the particle is changed as the flow ratio changes. This change leads to separation of smaller particles using the same device.

Separated particles and vapor molecules can be sampled by attaching various combinations of filter media and sorbent tubes to the outlets of each flow. This gives independence from sampling media so that the SADS can be used in various situations. On the other hand, the sampling media create additional back pressures to the sampling pumps on top of the back pressure from the SADS itself. Because SADS was designed to be used for personal sampling, the back pressure from different sources needs to be carefully considered when sampling strategy is established.

Because particle separation in the SADS still uses the principle of inertial impaction as in virtual impactors, the parameters affecting the performance of virtual impactors may be important in the SADS settings. Marple and Chien (1980) studied the effect of the air nozzle Reynolds number and the ratios between physical

dimensions of virtual impactors on the particle collection efficiency by the numerical solution of the Navier-Stokes equations and of the equations of motion of the particles. Loo and Cork (1988) studied these same factors experimentally. In both studies, the nozzle Reynolds number, the flow split ratio, the ratio between the nozzle diameter and the collection probe diameter, and the nozzle-to-collection probe distance were identified as the most important parameters. Loo and Cork (1988) also reported that the following parameters have a degree of importance: the entrance angle of the air nozzle, the length of the air nozzle throat, the thickness of the rim of the air nozzle, the thickness of the rim of the collection probe, and the polished radius on the inner lip of the collection probe.

The importance of parameters may be different with SADS settings than with virtual impactor settings. Characterizing the effects of the parameters and finding the optimal settings for combinations of parameters are important in developing the best new sampler possible. Numerical modeling can be an efficient way of finding optimal conditions because of its flexibility and cost-effectiveness. In Chapter II, a 2-D axisymmetric numerical model built using Fluent 6.2, a commercial computational fluid dynamics (CFD) code, and was tested and found to be valid.

Dimensional analysis is a conceptual method to understand the relationships among different dimensions and is widely used in scientific studies. In numerical

modeling, this method allows us to simplify equations by reducing the number of variables and to approach situations systemically (Munson et al., 2002). If an equation has *k* variables and *r* reference dimensions, it can be expressed with *k-r* dimensionless products.

In designing particle samplers that depend on inertial forces to collect particles such as cyclones, impactors, and virtual impactors, the dimensions of the devices and operating conditions determine their performance. When either experimental data or numerical models exist, it is possible to put the relationships between independent variables and performance variables into one or more equations and find the most desirable values within constraints. Loo and Cork (1988) tried to find the optimal physical dimensions of a virtual impactor by experiments. Ramachandran et al. (1991) studied cyclone optimization based on an empirical model. Hari et al. (2006) used numerical models to optimize a slit virtual impactor.

When one or more equations are given, several different algorithms are available to find the optimal values within constraints. Optimization algorithms are iterative and there are two different strategies: line search and trust region (Nocedal and Wright, 1999). The Newton search method is one of the most widely used methods in the line search strategy. The search direction of the Newton search method is derived from the second-order Taylor series approximation (Nocedal and Wright,

1999). The single factor method (Cochran and Cox, 1992) is one of the line search methods and finds the optimal value by varying a factor in an iterative manner, which was adopted by Ramachandran et al. (1991). The solver function in Excel software (Microsoft, Redmond, WA) uses the generalized reduced gradient method to find the optimal solution and also provides an option for Newton search method (Fylstra et al., 1998).

The objective of this research was to optimize the physical dimensions and the operating conditions of the SADS to improve the design of the SADS so that it can sample SOCs more accurately.

MATERIALS AND METHODS

Twelve parameters related to the separation of vapor and particles in the SADS were identified. For dimensional analysis and computer simulation, all the parameters were converted into nine dimensionless parameters. Based on the dimensionless parameters, a simulation model was built using commercial CFD software. That model was validated in Chapter II by comparing two sets of the experimental data with its simulation results. Using the model, a full matrix of 4 major dimensionless design and operating parameters each with 3 levels (total of 81 simulations) was simulated and the output data from the modeling runs were collected. Regression curves were obtained for each performance parameter as a polynomial function of the 4 major parameters and the regression equations were used together to find the optimal settings for combinations of design and operating parameters that best meet our design criteria. The best design was the one that had the smallest cutsize, pressure drop, and wall loss, and the steepest slope. Each of the steps in this process will be described in more detail below.

Dimensionless Parameters

Figure 2 shows the nomenclature of the physical design parameters and the

flow parameters which were used in this study. The same simplified 2-dimensional (2-D) axisymmetric model developed in Chapter II was used to build the geometries of the CFD model.

The following twelve variables are related to the separation of vapor and particles in the SADS: (1) the diameter of the air nozzle (D_{nozzle}), (2) the diameter of the collection probe (D_{probe}), (3) the distance between the air nozzle and the collection probe (L), (4) the flow rate at the air nozzle (Q_{nozzle}), (5) the vapor flow rate (Q_{vapor}), (6) the particle density (ρ_p), (7) the fluid density (ρ), (8) the fluid viscosity (μ), (9) the particle diameter (d_p), (10) the vapor flow separation efficiency (η_{vapor}), (11) the pressure drop across the SADS (ΔP), and (12) the wall loss (WL). Here, the vapor flow separation efficiency (η_{vapor}) and the wall loss (WL) were computed from:

$$\eta_{vapor} = \frac{n_{vapor}}{n_{nozzle} \times \left(Q_{vapor} / Q_{nozzle}\right)} \times 100(\%) \quad (1)$$

$$WL = \frac{n_{wall}}{n_{nozzle}} \times 100(\%) \quad (2)$$

where n_{vapor}, n_{nozzle}, and n_{wall} are the number of particles collected in the vapor flow, in the upstream flow, and on the wall, respectively. Both terms are functions of particle diameter.

Among the 12 variables, D_{nozzle}, ρ, and μ were considered constants. Then, using the Buckingham pi theorem, these variables were expressed in the form of nine

dimensionless groups (Perry, 1973): (1) $\frac{D_{probe}}{D_{nozzle}}$, (2) $\frac{L}{D_{nozzle}}$, (3) Stokes number (Stk), (4) $\frac{\rho_p}{\rho}$, (5) η, (6) Reynolds number (Re), (7) $\frac{Q_{vapor}}{Q_{nozzle}}$, (8) $\frac{\Delta PD_{nozzle}}{\mu V_{nozzle}}$, and (9) WL.

Here, Stokes number and Reynolds number are expressed as:

$$Stk = \frac{\rho_p V_{nozzle} C_C d_p^2}{9\mu D_{nozzle}} \tag{3}$$

$$Re = \frac{\rho V_{nozzle} D_{nozzle}}{\mu} \tag{4}$$

$$V_{nozzle} = \frac{4Q_{nozzle}}{\pi D_{nozzle}^2} \tag{5}$$

where ρ_p is the particle density, V_{nozzle} is the mean fluid velocity at the nozzle throat, C_C is the Cunningham slip correction (Hinds, 1999), d_p is the particle diameter, and μ is the absolute viscosity of the fluid. Using these 9 dimensionless parameters, 3 dependent parameters may be expressed as functions of the others:

$$\eta_{vapor} = \varphi_1\left(\frac{D_{probe}}{D_{nozzle}}, \frac{L}{D_{nozzle}}, \frac{Q_{vapor}}{Q_{nozzle}}, Re, Stk, \frac{\rho_p}{\rho}\right) \tag{6}$$

$$WL = \varphi_2\left(\frac{D_{probe}}{D_{nozzle}}, \frac{L}{D_{nozzle}}, \frac{Q_{vapor}}{Q_{nozzle}}, Re, Stk, \frac{\rho_p}{\rho}\right) \tag{7}$$

$$\frac{\Delta PD_{nozzle}}{\mu V_{nozzle}} = \varphi_3\left(\frac{D_{probe}}{D_{nozzle}}, \frac{L}{D_{nozzle}}, \frac{Q_{vapor}}{Q_{nozzle}}, Re\right) \tag{8}$$

These functions were used in the CFD modeling and optimization procedures. ρ_p/ρ was not varied in this study because the aerodynamic diameter (ρ_p=1.0) was used and incompressible fluid was assumed.

Based on the Chapter II study and the literature, we identified 4 major

parameters which are the main factors that can cause significant effects on the performance of the sampler. The major parameters were simulated for the full factorial for each parameter and were used for the optimization procedure. Table 1 shows each parameter range compared with previous studies.

- **D_{probe}/D_{nozzle}**: This value stands for the ratio between the nozzle diameter and the collection probe diameter. The designated values of these parameters were 1.6, 1.2, and 0.8. Particle losses near the cutoff size are strongly dependent on this parameter (Loo and Cork, 1988). These authors identified this parameter as one of the most critical parameters as well as axial misalignment between the acceleration nozzle and collection probe and a polished radius on the inner lip of the collection probe in virtual impactors. Because this is a theoretical study, we assumed that there was no misalignment of axes. The polished radius was categorized as a minor parameter because it mainly affects the wall loss of particles which was expected to be a small fraction in SADS settings from the study in Chapter II.
- **L/D_{nozzle}**: This term stands for the ratio of the distance between the inlet nozzle and the collection probe to the nozzle diameter. In this study, the designated values of this parameter were 1.4, 1.0, and 0.6.

- **Q_{vapor}/Q_{nozzle}**: Values of 0.025, 0.05, and 0.1 were modeled. This flow ratio was the main difference from virtual impactors. Therefore, this was one of the most important parameters in the SADS.
- **Re**: The Reynolds number for the fluid inside a pipe is determined by Eq. (4). Because all values except V_{nozzle} are fixed, the Reynolds number depends on the total flow rate at the air nozzle. Values of 1000, 3000, and 5000 were modeled. These values spanned the transition from laminar flow (Re<2000) to turbulent flow (>4000). In this range, the impaction efficiency curves for conventional impactors were found to be quite steep (Marple and Liu 1975). If Re is too large, the pressure drop across the sampler will be excessive. If Re is too small, then particles will not be able to be accelerated enough to have the necessary inertia to be separated. Thus, finding an optimal point was especially important for this parameter.

Numerical Simulation

The same simplified 2-dimensional (2-D) axisymmetric model as the one used in Chapter II was adopted to build the geometries for the CFD model. The computational domain was limited to the inside of the SADS. Sampler geometries and meshes and flow field solutions were achieved using GAMBIT 2.1 and FLUENT 6.1

(FLUENT Inc., Lebanon, NH), respectively. Uniform velocity was assumed at the inlet. The two outlets had outflow boundary conditions and their split ratio varied according to Q_{vapor}/Q_{nozzle}. The pressure at the inlet was assumed to be 1 atm. Turbulence in the computational domain was modeled using the standard k-ε model. The initial turbulence kinetic energy (TKE) was set to be zero. When the residual of mass flow rate reached less than 0.01% of the inlet mass flow rate, convergence was declared. The residual of mass flow rate is the summation of the absolute values of mass flow rate difference for each node between iterations. The calculation of trajectories of particles was accomplished using the same Lagrangian method as in Chapter II.

Separation efficiency was also calculated in the same way as in Chapter II. Two hundred spherical particles were imposed with equal inter-particle distance from the inlet wall to $0.05D_{nozzle}$ away. The fate of the n-th particle away from the wall decided the fate of any particle entering in the circular area between the n-th and (n-1)-th particles. The flow rate was proportional to the size of the annular area between the n-th and (n-1)-th particles at the inlet, because uniform velocity was assumed at the inlet boundary. The diameters of imposed particles were between 0.1 and 1.0 μm.

At first, all combinations of 2 geometrical parameters (D_{probe}/D_{nozzle} and L/D_{nozzle}), for a total of 9 geometries, were built. Then, all combinations of 2

operational parameters (Q_{vapor}/Q_{nozzle} and Re), for a total of 9, were simulated on 9 geometries. A grand total of 81 simulations were performed.

Statistical Analysis and Optimization

In the optimization procedure, instead of $\frac{\Delta PD_{nozzle}}{\mu V_{nozzle}}$ and Stk, the corresponding dimensional parameters ΔP and d_p were used for intuitive understanding of the resulting data. Pressure drop was redefined as the average pressure drop at the particle flow outlet because additional pressure drop from sampling media was expected to be larger than that at the vapor flow due to relatively high flow rate. Vapor flow separation efficiency, η_{vapor}, was characterized by two different components, the particle diameter of 50% cutsize and the slope of the efficiency curve. The particle diameter of 50% cutsize, d_{50}, was defined to be the corresponding particle diameter showing 50% separation efficiency. The slope of the efficiency curve was calculated by doubling the distance between d_{75} and d_{50} on logarithmic scale. The maximum wall loss was selected from the relationship between wall loss and particle diameter for each simulation. These four dependent variables -- d_{50}, slope of the efficiency curve, maximum wall loss, and pressure drop -- were calculated for each simulation.

Regression equations for the effect of the four major dimensionless design and

operating parameters on each dimensionless performance parameter had the following form:

$$\ln\left(\left[\text{Performance variable}\right]_i\right) = C_i + \sum\left(K_{ij}\ln\left(\left[\text{Major Parameter}\right]_j\right)\right) \quad (9)$$

where i and j are the indices of performance variables and major parameters, respectively, C_i is constant for each equation, and K_{ij} is constant for each major parameter in each equation. To obtain polynomial equations from 81 combinations of simulation results, multiple regression equations for the natural log of each dependent variable were calculated using SAS statistical software (version 9.1.3, SAS Institute, Cary, NC).

After calculating the polynomial equations, the optimal conditions to best meet our best design criteria were calculated using the solver function in Microsoft Excel (Microsoft, Redmond, WA). Using a Newton search method, the solver function found the minimum of a given function within constraints. The best design was the one that had the smallest cutsize, pressure drop, and wall loss, and the steepest slope. Because each parameter covered a different range of numbers, they were normalized to the averages of the three levels for each parameter. Also, the importance of each parameter was considered. The 50% cutsize was the most important parameter and the pressure drop acted as a constraint. So the 50% cutsize was weighted by a factor of 10 while other parameters were weighted by 1. In

weighted optimization procedures, the weights describe which parameter is more or less important for the decision maker (Jahn and Krabs, 1988). The entire optimization equation can be expressed as follows:

$$I = WF_{d_{50}} \frac{d_{50}}{\overline{d_{50}}} + WF_{slope} \frac{slope}{\overline{slope}} + WF_{WL} \frac{WL}{\overline{WL}} + WF_{\Delta P} \frac{\Delta P}{\overline{\Delta P}} \quad (10)$$

where I is the quantity needs to be minimized and WF is the weighing factor for each parameter. The barred value is the average of each parameter. The minimal values and maximal values of major parameters were used in the numerical simulations as their own constraints for the solver. A new CFD model was built based on the optimized parameters and its performance was compared with the values estimated from the polynomial equations.

The SADS was designed to use for personal sampling so that the total back pressure including those coming from filter media and sorbent tubes should fall in the range which personal sampling pumps can handle for at least several hours. Most personal pumps can handle back pressures up to 7500 Pa (30 in. w.g.) at 2.0 lpm for 8 hours. Our measurements indicate that the back pressure from filter media was lower than 500 Pa (2 in. w.g.) and the back pressure from two activated carbon tubes (226-09, SKC Inc., Eighty Four, PA) connected in parallel was less than 3700 Pa (15 in. w.g.) at a combined flow of 2 lpm. These values would increase as chemicals are captured by the media during sampling. Therefore the maximum back pressure that

can be allowed across the SADS itself is about 3300 Pa. Two levels of back pressure were modeled: 1490 Pa (6 in. w.g.) and 2490 Pa (10 in. w.g.), which correspond to approximately 50% and 75% of the maximum back pressure allowance, respectively.

Minor Parameters

The following 5 minor parameters were modeled individually using the optimal dimensions chosen from the optimization procedure. For each parameter, the value giving the minimum 50% cutsize was adopted. The other 3 performance parameters were not considered because their values were not changed substantially by changing the minor parameters.

- **θ (The effects of the entrance angle)**: In their theoretical study, Marple and Chien (1980) indicated fewer losses for 45° than for 30° entrance angles in virtual impactors. This was due to the particles being thrown closer to the center line for the large angle values, making the collection of particles in the probe slightly easier. Loo and Cork (1988) recommended a range of 40° to 50° for virtual impactors. Entrance angles of 30°, 45°, and 60° were modeled.
- **T_{throat}/D_{nozzle} (The length of the air nozzle throat)**: The effects of this parameter on the particle collection efficiency and the sampling loss in virtual impactors were reported as negligible in a theoretical study and an

experimental study (Marple and Chien 1980; Marple and Liu 1974). Loo and Cork (1988) recommended a range of 0.8 – 1.2 for virtual impactors. Ratios of 0.0, 0.5, and 1.0 were evaluated.

- **T_{nozzle}/D_{nozzle} (The thickness of the rim of the air nozzle)**: Loo and Cork (1988) described this parameter as moderately influential and recommended values between 0.5 and 0.75 for virtual impactors. Thicknesses of 0.01, 0.5, and 1.0 were modeled.
- **T_{probe}/D_{nozzle} (The thickness of the rim of the collection probe)**: Loo and Cork (1988) used 0.36 for this parameter and described that this should be small enough to allow the dispersion of the radial air streams. On the other hand, a sharp rim can slightly increase the cutsize of a sampler. Thicknesses of 0.0, 0.5, and 1.0 were evaluated.
- **R/T_{probe} (The polished radius on the inner lip of the collection probe)**: Loo and Cork (1988) used 0.82 for this parameter and described that this is essential in minimizing the loss peak near the cutsize. Radii of 0.0, 0.5 and 1.0 were modeled.

Experimental Comparison

A new SADS was built based on the physical dimensions found from the

optimization procedure and tested for its performance. The experimental method was similar to the one used in Chapter II. Figure 3 shows the experimental setup. Six different monodisperse particle suspensions having physical diameters ranging from 0.05 to 0.50 μm were nebulized and classified using an Electrostatic Classifier (TSI Model 3071, Shoreview, MN). The counts of particles were measured upstream of the sampler and at the vapor flow using a P-Trak (TSI Model 8525, Shoreview, MN) and a Condensation Particle Counter (CPC) (TSI Model 3022, Shoreview, MN), respectively. Separation efficiency (η) was calculated for flow ratio Q_{vapor}/Q_{nozzle} = 0.025 and 0.1. The combined flow rate was 2.0 lpm at which the corresponding Re was 3501. Flow rates were adjusted from those found to be optimal to allow for effective control of the flows. For each size of particle, experiments were repeated 3 times and averages and standard deviations were calculated.

RESULTS

From the results of the numerical simulations, four polynomial equations were obtained using regression analysis in SAS as follows:

$$d_{50} = 998 \cdot (DR)^{-0.601} \exp\left(2.08 \cdot \ln^2(DR)\right)(LR)^{0.178}(Re)^{-0.940}(FR)^{-0.667} \quad (11)$$

$$slope = 0.0892 \cdot (DR)^{0.126} \exp\left(-0.454 \cdot \ln^2(DR)\right)(LR)^{-0.0448}(Re)^{0.0834}(FR)^{0.350} \quad (12)$$

$$loss = 0.793 \cdot (DR)^{1.04} \exp\left(-2.81 \cdot \ln^2(DR)\right)(LR)^{1.25} \exp\left(2.94 \cdot \ln^2(LR)\right) (Re)^{0.0649}(FR)^{-0.294} \quad (13)$$

$$\Delta P = 0.000778(DR)^{-2.95} \exp\left(3.74 \cdot \ln^2(DR)\right)(LR)^{0.0395}(Re)^{1.88}(FR)^{0.0686} \quad (14)$$

where DR, LR, FR represent D_{probe}/D_{nozzle}, L/D_{nozzle}, and Q_{vapor}/Q_{nozzle} respectively. Table 2 showed the p-values of independent parameters in the regression analyses.

The calculation results of variables d_{50}, slope, internal loss, and pressure drop from Eqs. (11)-(14) were compared to the results from numerical simulations in Figure 4. The results from numerical simulations were well correlated with the estimations from the polynomial equations for each parameter. The correlations for 50% cutsizes and pressure drops were stronger than those for slope and maximum wall loss.

Using Eq. (11), the effects of D_{probe}/D_{nozzle} and L/D_{nozzle} on d_{50} (Figure 5) and the effects of Q_{vapor}/Q_{nozzle} and Re on d_{50} (Figure 6) were estimated. The diameter ratio

between the nozzle and the collection probe shows a second order relationship in Figure 5 so that local minima exist for that parameter. The optimal values for four dependent variables were calculated from those polynomial equations for two different pressure drops (Table 3). In both cases the optimal physical dimensions found were identical.

With the optimal dimensions, FR=0.1, and Re=3501, the entrance angle was the only factor among the minor parameters found to have noticeable effect on the performance parameters through the numerical model (Figure 7). The angle that showed the smallest d_{50} was 45º so that this angle was adopted for the optimal design. Table 3 shows the final dimensions of the SADS and its expected performance parameters when flow rate at the inlet is 2.0 lpm (Re=3501). The simulation results from the new CFD model built based on the optimization procedure showed good agreement with the expected values from the polynomial equations. d_{50}, slope of the curve, wall loss, and pressure drop were 0.113 μm and 0.096 μm, 0.37 and 0.40, 0.78% and 0.87%, 2490 Pa and 2490 Pa, for the numerical model and polynomial equations, respectively.

The SADS was built based on physical parameters determined in the numerical simulations and optimization procedure (Figure 8). The D_{nozzle} was 0.8 mm and other dimensions were determined to be proportional to it accordingly. The

separation efficiency of the SADS was tested and compared with that from the numerical simulation with the same settings (Figure 9). The SADS was operated at 2.0 lpm. d_{50} at $Q_{vapor}/Q_{nozzle} = 0.025$ was smaller than that at $Q_{vapor}/Q_{nozzle} = 0.1$. However, the difference of d_{50} between two flow ratios was smaller than estimated from numerical simulation. The slope was sharper when Q_{vapor}/Q_{nozzle} was larger. At $Q_{vapor}/Q_{nozzle} = 0.1$, the d_{50} and the slope of the efficiency curve were 0.247 μm and 0.17, respectively. d_{50} was larger and the slope of the efficiency curve was sharper than expected from the modeling and optimization procedures.

DISCUSSION

The diameter ratio D_{probe}/D_{nozzle} of 1.30 for the optimized sampler was similar to that of virtual impactors studied by Marple and Chien (1980) and Loo and Cork (1988), 1.33 and 1.3-1.4, respectively. If the ratio is too small, some fraction of the air flow from the nozzle will behave as in impactors so that particles will deposit on the lip of the collection probe (Figure 10a). If the ratio is too large, air flow from the nozzle will split into two flows and no separation will occur because particles will have enough space to change their trajectories to follow the change of flow (Figure 10c). When the ratio is optimal, a minimal number of particles go to vapor flow direction (Figure 10b). Figures 10a and 10c each have one more particle going toward the vapor flow than Figure 10b does. To compare these particle counts, it should be considered that the interval between particles imposed in the figure was 10 times larger than in the actual numerical simulation. Even considering the difference of the intervals, however, the effect of diameter ratio on d_{50} was moderate over the simulation range as shown in Figure 5.

The optimal distances between the nozzle and the collection probe L/D_{nozzle} found in this study was 0.6, which was quite different from those reported by other studies on virtual impactors. Marple and Chien (1980) and Loo and Cork (1988)

recommended 1.0, and 1.2-1.8 for this ratio, respectively. A likely reason for this difference is the smaller flow rate of the vapor flow in SADS settings compared to that of virtual impactors. The smaller the distance was, the smaller the cutsize was expected to be. This parameter was not decreased further than 0.6 because the wall loss was expected to increase and because polynomial equations are untrustworthy when extrapolated (Cochran and Cox, 1992). From Eq. (13), the minimum wall loss was expected when the distance ratio was near 0.7.

Reynolds number or the throat velocity at the nozzle has been reported as a major parameter affecting the 50% cutsize of virtual impactors and a contributor to the sharper separation efficiency curve (Marple and Chien, 1980; Loo and Cork, 1988; Hari et al., 2006). Those facts were re-confirmed in this study. The effect of Re was larger when the flow split ratio Q_{vapor}/Q_{nozzle} was large (Figure 6). The fact that decreasing Q_{vapor}/Q_{nozzle} decreases the 50% cutsize has been reported by several studies (Marple and Chien, 1980; Loo and Cork, 1988; Xiong et al., 1998; Hari et al., 2006). However, no existing study tested for $Q_{vapor}/Q_{nozzle} < 0.5$.

Among the 5 minor parameters, only the entrance angle at the nozzle showed a noticeable effect when it was altered (Figure 7). The optimal angle found was 45° and this result was similar with studies by Marple and Chien (1980) and Loo and Cork (1988), 45° and 40° – 50°, respectively. The polished radius on the inner lip of the

collection probe R/T_{probe} was reported as a parameter significantly affecting the performance of virtual impactors (Loo and Cork, 1988). In this study, however, this parameter did not make a noticeable difference. This can be partially explained from the fact that in this model the wall loss is a relatively small in SADS settings compared with that in virtual impactor settings. The fact that only a small fraction of air flows to the vapor flow direction in SADS settings can be another reason because, in this case, a smaller space near the inner lip of the collection probe is required for particle separation.

The major design and operating parameters had 3 levels so that up to second order relationships have been observed as shown in Eqs. (11)-(14). Increasing the number of levels might give us more confidence in the equations or reveal higher order relationships. However, that would require more computation time. Adding one more level to each major parameter would increase the computational time by more than a factor of 3. Four or five levels may be advisable when the ranges of factors are wide and the optimal point is poorly known in factorial experiments (Cochran and Cox, 1992). In this study the ratios between the minimum and the maximum of each range were equal to or smaller than 5.

A discrepancy between the CFD model results and experimental tests was found (Figure 9), and the difference was larger than found in Chapter II. In particular,

the effect of flow ratio Q_{vapor}/Q_{nozzle} from the experiments was found to be smaller than expected from the CFD model. One reason for this discrepancy may be the turbulence model. The standard k-ε model adopted in this study was one of the simplest turbulence models and a static model not including the time variable in flow field equations. Therefore, this model could not encompass all the dynamics of turbulence that might happen in the calculation domain. In their visualization study, Han and Moss (1997) showed that the flow inside the nozzle, inside the collection probe, and the space between them was laminar; whereas the vapor flow direction was turbulent when Re was between 2000 and 6000. Even considering that this could be changed as the flow split ratio was changed in SADS settings, the area where the flow split happens might still be turbulent. The particle separation zone which was expected to be the outer surface of the air column between the nozzle and the probe in SADS fell into the turbulent region (Han and Moss, 1997). Simplified initial conditions and boundary conditions in the CFD model can be another reason for the discrepancy in Figure 9. Initial conditions and boundary conditions frequently affect results significantly in CFD modeling (Munson et al., 2002).

Another contributor to the discrepancy between the results of CFD modeling and experimental tests may be the non-axisymmetric structure of the real SADS. A 2-D axisymmetric model was adopted instead of a 3-D model because the 2-D model

costs less computational time and less effort to build the mesh. A more dense mesh could be added to the separation zone by choosing a 2-D model. In the 2-D axisymmetric model, the outlet for the vapor flow had the shape of circumferential slit. However, the built SADS had a tube type outlet in one direction (Figure 8). This may have caused non-axisymmetric flow at the separation zone. In a preliminary study testing the same SADS, fluorescent PSL particles were used to evaluate the separation efficiency of SADS. After sampling, we found that particles deposited on the lip of the air nozzle in a non-axisymmetric pattern.

Through the optimization procedure, a personal sampling device for semivolatile aerosols with a very low cutsize was produced. d_{50} decreased from 0.373 μm to 0.247 μm. The cutsize is important because a low one means that a superior separation of vapor from aerosols can be achieved. The slope of the efficiency curve became sharper from 0.31 to 0.17 in terms of the doubled distance between d_{75} and d_{50} on logarithmic scale. Wall loss was expected to remain at a similar level to that of the previous version.

CONCLUSIONS

Dimensional analysis and numerical simulations revealed the relationships between design and operating parameters and performance parameters. The diameter ratio between the air nozzle and the collection probe and the flow split ratio between vapor flow and particle flow had significant effects on all the performance parameters of SADS. Using the equations defining the relationships, the optimization procedure improved the modeled performance of the SADS. Experiments on a SADS built according to the optimal design indicated that the built SADS had a lower cutpoint than previous versions, although not as low as the model had anticipated. The experiments indicate that the instrument will separate particles and vapor effectively for particles larger than 0.25 μm in diameter.

REFERENCES

Bidleman TE. (1988) Atmospheric processes – wet and dry deposition of organic compounds are controlled by their vapor-particle partitioning. Environ Sci Technol; 22 361-367.

Bergman TA, Johnson DL, Boatright DT, Smallwood KG, Rando RJ. (1996) Occupational exposure of nonsmoking nightclub musicians to environmental tobacco smoke. Am Ind Hyg Assoc J; 57 746–752.

Cochran WG, Cox GM. (1992) Experimental Designs. 2nd ed. New York: John Wiley & Sons. p. 356-357.

Cohen BS, Brosseau LM, Fang CP, Bower A, Snyhder C. (1992) Measurement of air concentrations of volatile aerosols in paint spray applications. Appl Occup Environ Hyg; 7 514-521.

Fylstra D, Lason L, Watson J, Waren A. (1998) Design and use of Microsoft Excel solver. Interfaces; 28 29-55.

Guidotti TL, Yoshida K, Clough V. (1994) Personal exposure to pesticide among workers engaged in pesticide container recycling operations. Am Ind Hyg Assoc J; 55 1154-1163.

Hari S, Hassan YA, McFarland AR. (2006) Optimization studies on a slit virtual

impactor. Part Sci Technol; 24 105-136.

Han R, Moss OR. (1997) Flow visualization inside a water model virtual impactor. J Aerosol Sci; 28 1005-1014.

Hinds WC. (1999) Aerosol Technology: Properties, Behavior, and Measurement of Airborne Particles. 2nd ed. Wiley-Interscience Publication, John Wiley & Sons, Inc., New York, NY. p 49.

Hounam RF, Sherwood RJ. (1965) The cascade centripeter: a device for determining the concentration and size distribution of aerosols. Am Ind Hyg Assoc J; 26 122-131.

Jahn J, Krabs W. (1988) Applications of multicriteria optimization in approximation theory. In Stadler W, editor. Multicriteria optimization in engineering and in the sciences. New York: Springer. p. 64. ISBN 0306427435, 9780306427435

Kriech AJ, Kurek JT, Wissel HL, Osborn LV, Blackburn GR. (2002) Evaluation of worker exposure to asphalt paving fumes using traditional and nontraditional techniques. Am Ind Hyg Assoc J; 63 628-635.

Loo BW, Cork CP. (1988) Development of high efficiency virtual impactors. Aerosol Sci Technol; 9 167-176.

Marple VA, Chien CM. (1980) Virtual impactors: a theoretical study. Environ Sci Technol; 14 976-984.

Marple VA, Liu BYH. (1975) On fluid flow and aerosol impaction in inertial impactors. J Colloid interface Sci; 53 31-34.

Munson BR, Young DF, Okiishi TH. (2002) Fundamentals of Fluid Mechanics. Danvers, MA: John Wiley & Sons, Inc. ISBN 0 471 44250 X.

Nocedal J, Wright SJ. (1999) Numerical optimization. New York: Springer. p. 19-27. ISBN 0-387-98793-2

Park D, Kim S, Yoon C. (2003) Loss of straight metalworking fluid samples from evaporation during sampling and desiccation. Am Ind Hyg Assoc J; 64 837-841.

Perry RH. (1973) Chemical Engineer's Handbook. 5th ed. Columbus: McGraw-Hill Book Company, p. 2-81-83.

Ramachandran G, Leith D. (1991) Cyclone optimization based on a new empirical model for pressure drop. Aerosol Sci Technol; 15 135-148.

Raynor PC, Leith D. (1999) Evaporation of accumulated multicomponent liquids from fibrous filters. Ann Occup Hyg; 43(3) 181-192.

Volckens J, Boundy M, Leith D, Hands D. (1999) Oil mist concentration: a comparison of sampling methods. Am Ind Hyg Assoc J; 60 684-689.

Volckens J, Leith D. (2003) Partitioning theory for respiratory deposition of semivolatile aerosols. Ann Occup Hyg; 47(2) 157-164.

Woskie SR, Smith TJ, Hammond SK, Hallock MH. (1994) Factors affecting worker

exposures to metal-working fluids during automotive component manufacturing. Appl Occup Environ Hyg; 9 612-21.

Xiong JQ, Fang C, Cohen BS. (1998) A portable vapor/particle sampler. Am Ind Hyg Assoc J; 58 614-621.

Table 1. The ranges of simulation parameters and recommended values for the virtual impactors and the SADS

		Simulation range	Chapter II study	Marple and Chien (1980)	Loo and Cork (1988)
Major parameters	D_{probe}/D_{nozzle}	0.8 – 1.6	1.375	1.33	1.3 – 1.4
	L/D_{nozzle}	0.6 – 1.4	1.5	1.0	1.2 – 1.8
	Q_{vapor}/Q_{nozzle}	0.025 – 0.1	0.1 – 0.14	0.9	0.9
	Re	1000 – 5000	3500	100 – 500	7700
Minor parameters	θ[a]	30° – 60°	19°	45°	40° – 50°
	T_{throat}/D_{nozzle}	0.0 – 1.0	1.0	(n/a)[c]	0.8 – 1.2
	T_{nozzle}/D_{nozzle}	0.0 – 1.0	0.625	(n/a)	0.5 – 0.75
	T_{probe}/D_{nozzle}	0.0 – 1.0	0.44	(n/a)	0.36
	R[b]$/T_{probe}$	0.0 – 0.5	0.0	(n/a)	(n/a)

[a] The entrance angle

[b] The polished radius on the inner lip of the collection probe

[c] not available

Table 2. p-values of independent parameters in regression analysis

Independent parameters	p- value for each dependent variable			
	$\ln(d_{50})$	ln(slope)	ln(wall loss)	ln(pressure drop)
Intercept	<0.0001	<0.0001	0.6247	<0.0001
$\ln(D_{probe}/D_{nozzle})$	<0.0001	0.0151	<0.0001	<0.0001
$\ln^2(D_{probe}/D_{nozzle})$	<0.0001	0.0093	<0.0001	<0.0001
$\ln(L/D_{nozzle})$	<0.0001	0.0976	<0.0001	0.0017
$\ln^2(L/D_{nozzle})$	-	-	<0.0001	-
ln(Re)	<0.0001	<0.0001	0.2414	<0.0001
$\ln(Q_{nozzle}/Q_{vapor})$	<0.0001	<0.0001	<0.0001	<0.0001

Table 3. Optimal values for independent parameters and corresponding dependent parameters from numerical modeling

	Pressure drop		
	Theoretical optimums		Practical application of the optimization
	1500 Pa (6 in. w.g.)	2500 Pa (10 in. w.g.)	2864 Pa (11.5 in. w.g.)
D_{probe}/D_{nozzle}	1.30	1.30	1.30
L/D_{nozzle}	0.60	0.60	0.60
Re	2515	3298	3501
Q_{nozzle}/Q_{vapor}	39	39	9
d_{50}, μm	0.050	0.038	0.096
Slope	0.65	0.67	0.40
Wall loss, %	0.55	0.56	0.87

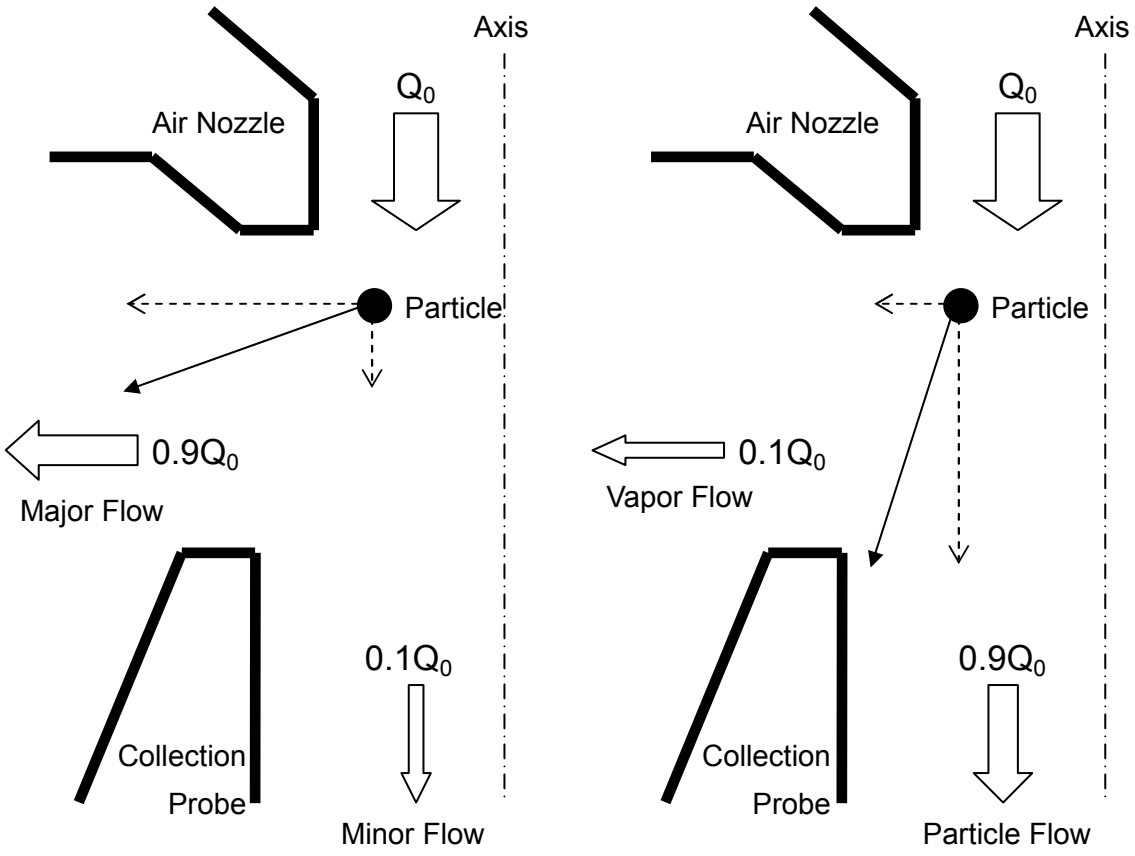

(a) Virtual Impactor (b) SADS

Figure 1. Diagram illustrating the principle of decreasing the cutsize in the SADS settings as compared to the virtual impactor settings.

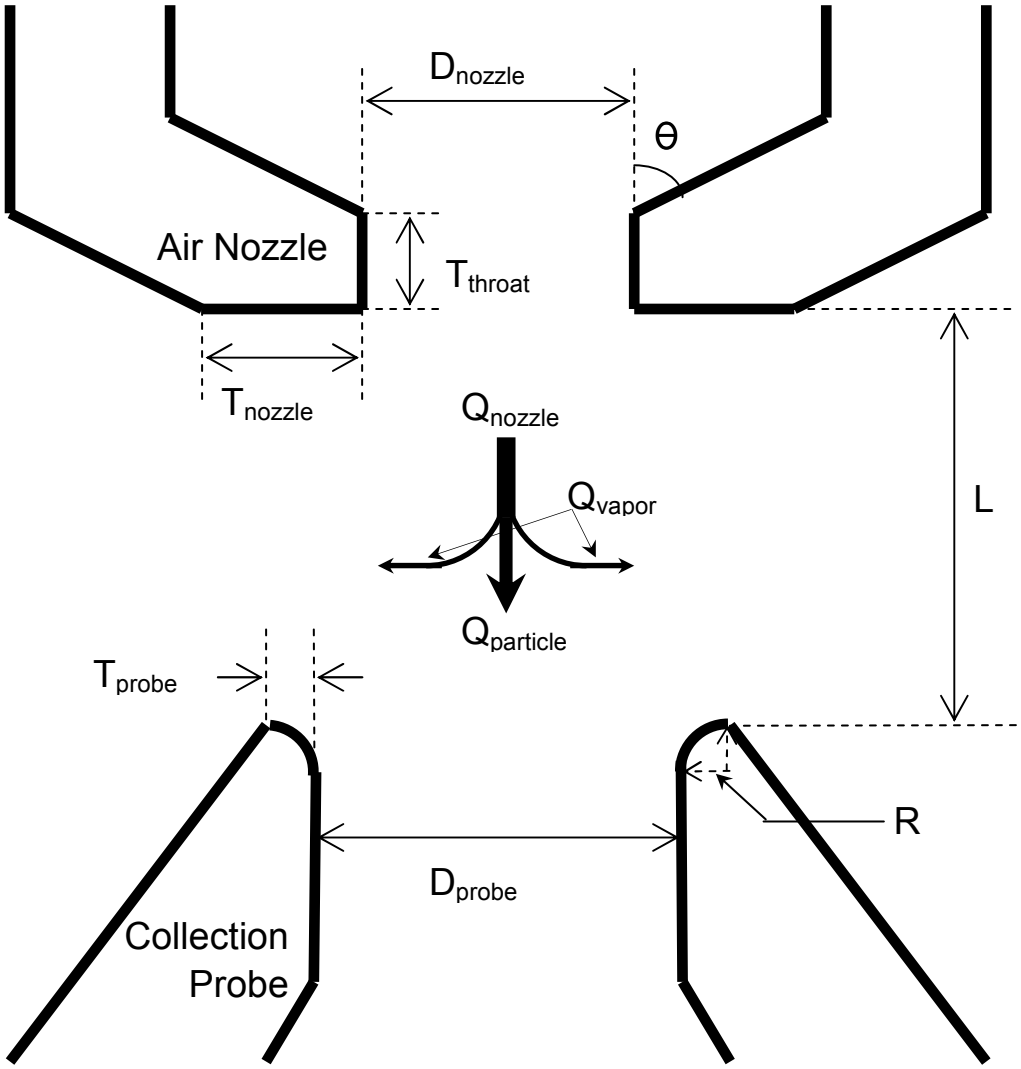

Figure 2. Dimensions of the separation area of a virtual impactor (not to scale)

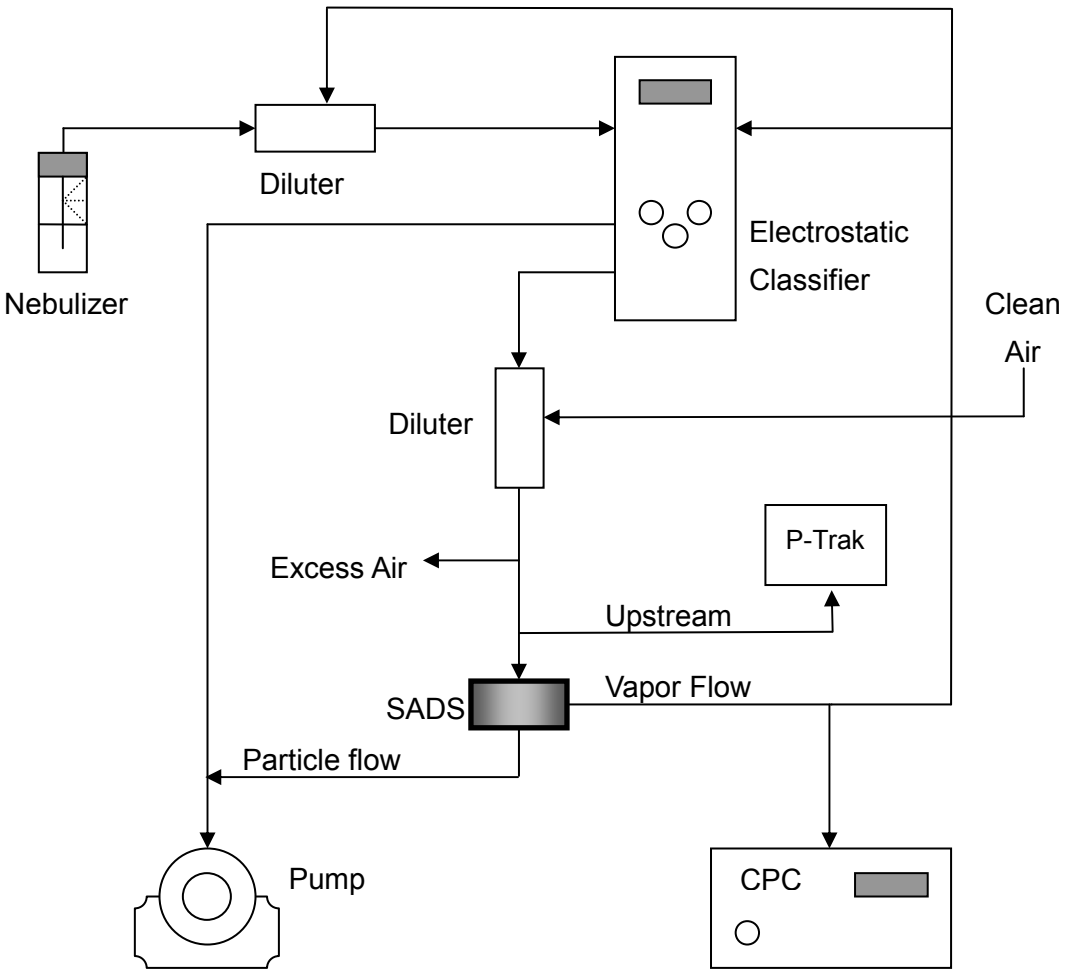

Figure 3. Schematic diagram of experimental setup.

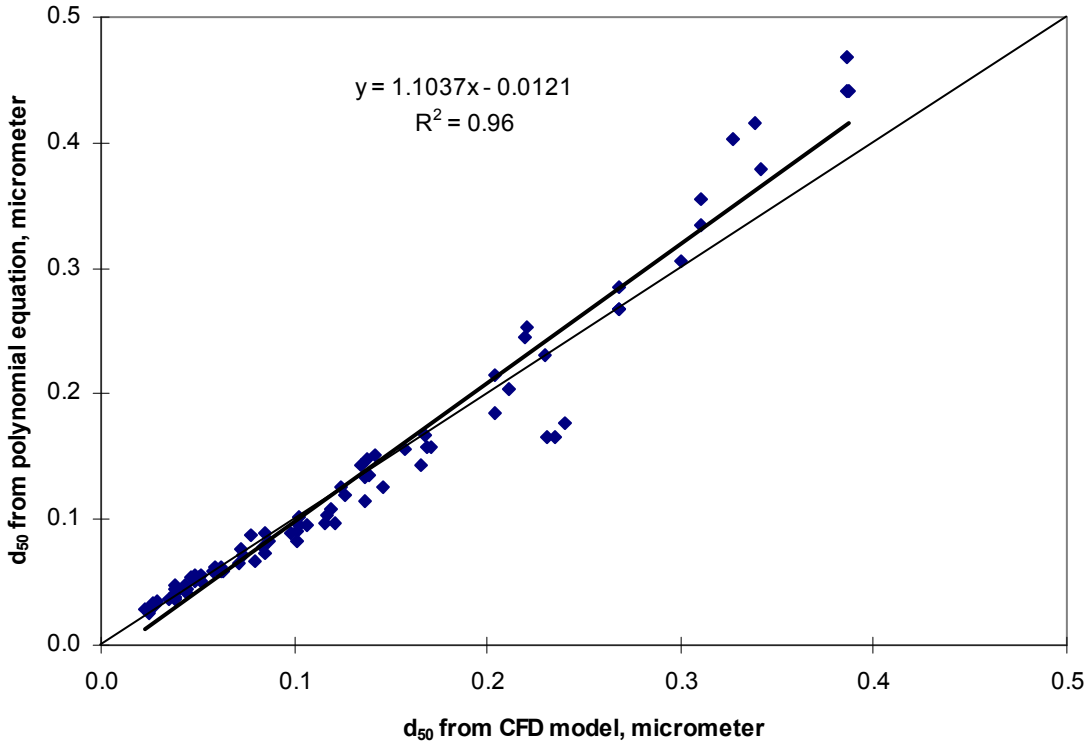

(a) d_{50}

Figure 4. Comparison between estimated values from polynomial equations and simulated values from CFD model for each dependent variable.

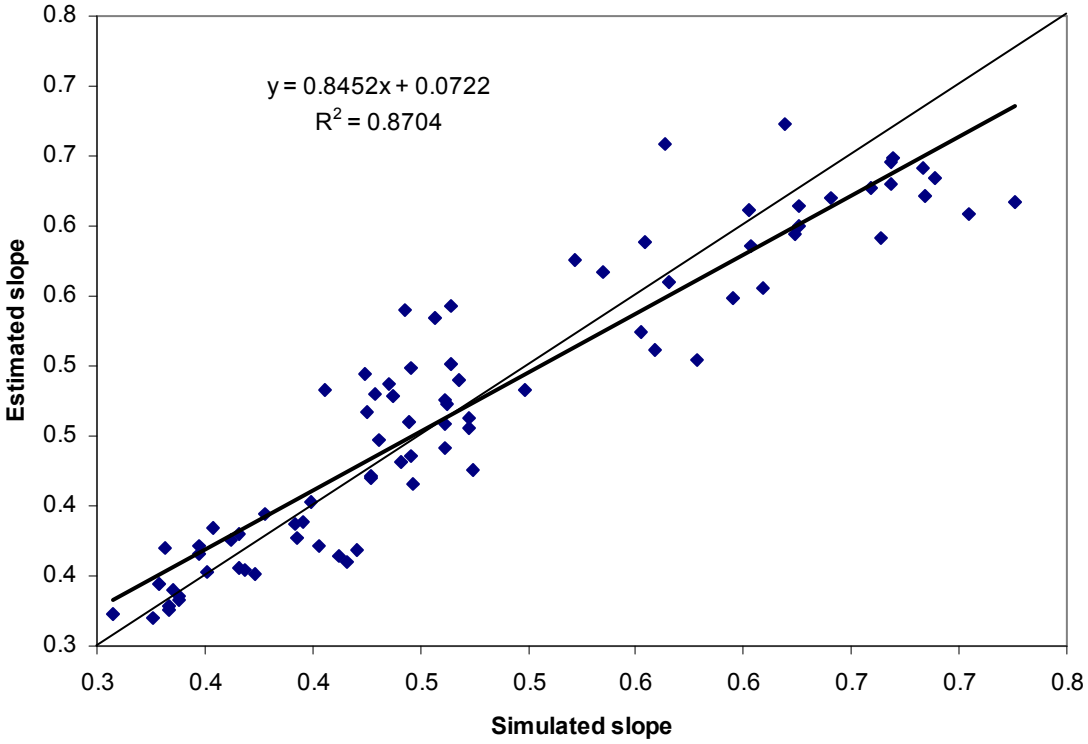
y = 0.8452x + 0.0722
R2 = 0.8704
Estimated slope
Simulated slope
0.3
0.4
0.4
0.5
0.5
0.6
0.6
0.7
0.7
0.8

(b) Slope

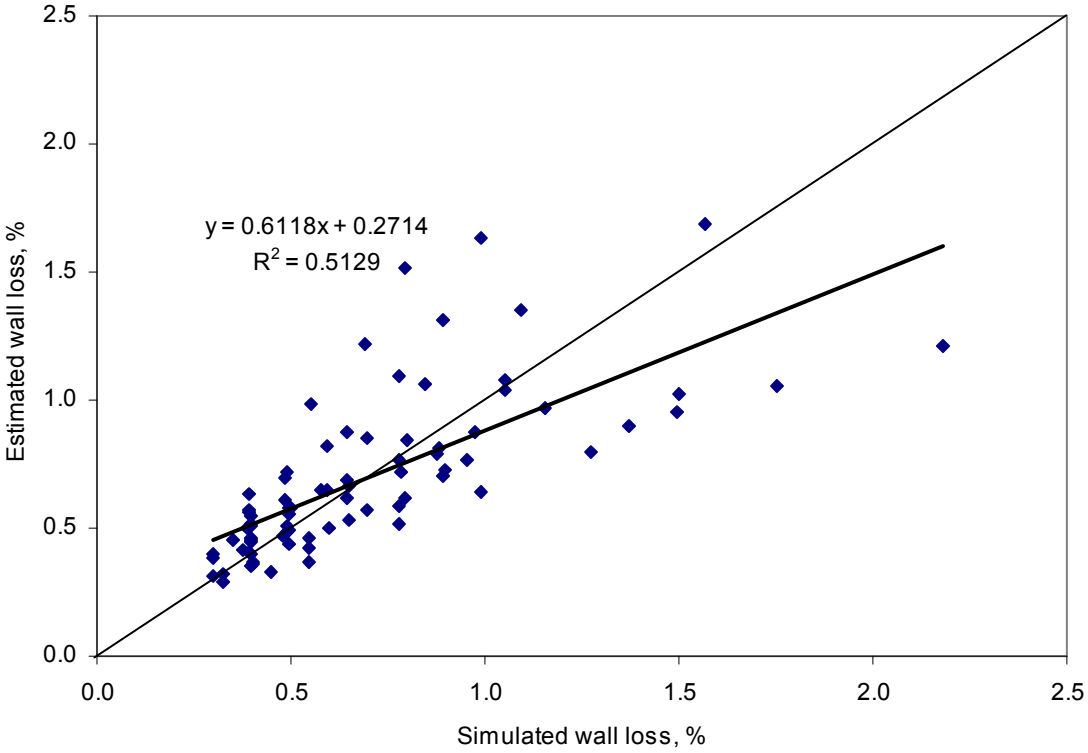
y = 0.6118x + 0.2714
R2 = 0.5129
Estimated wall loss, %
Simulated wall loss, %
0.0
0.5
1.0
1.5
2.0
2.5

(c) Wall loss

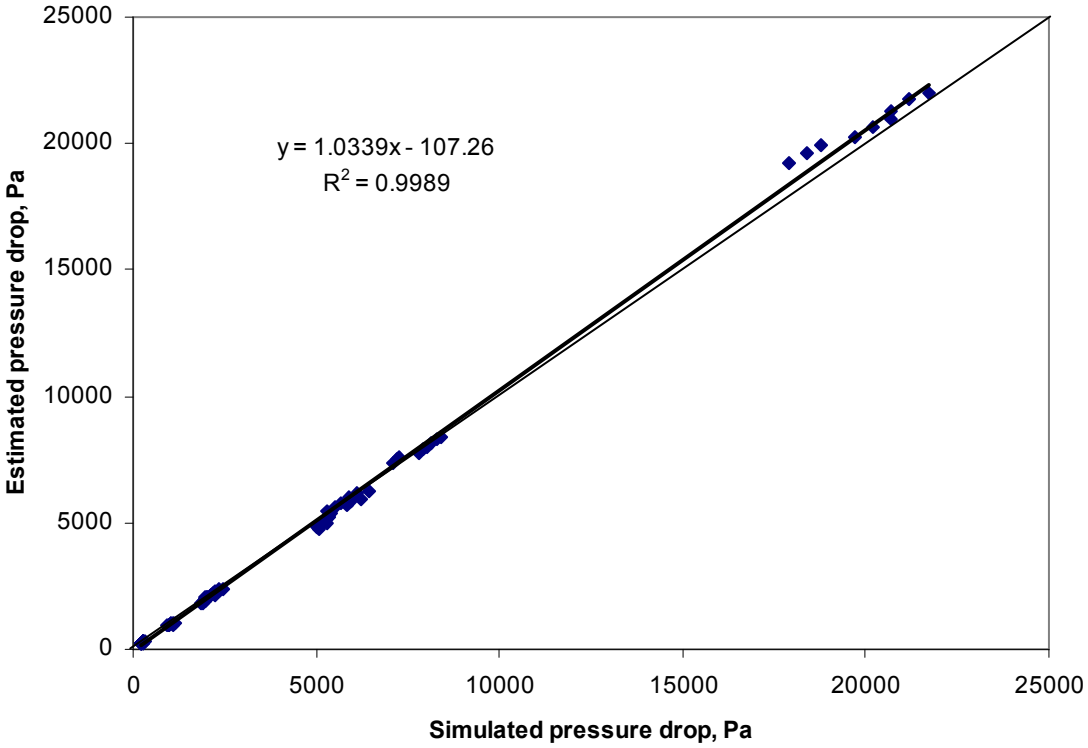

(d) Pressure drop

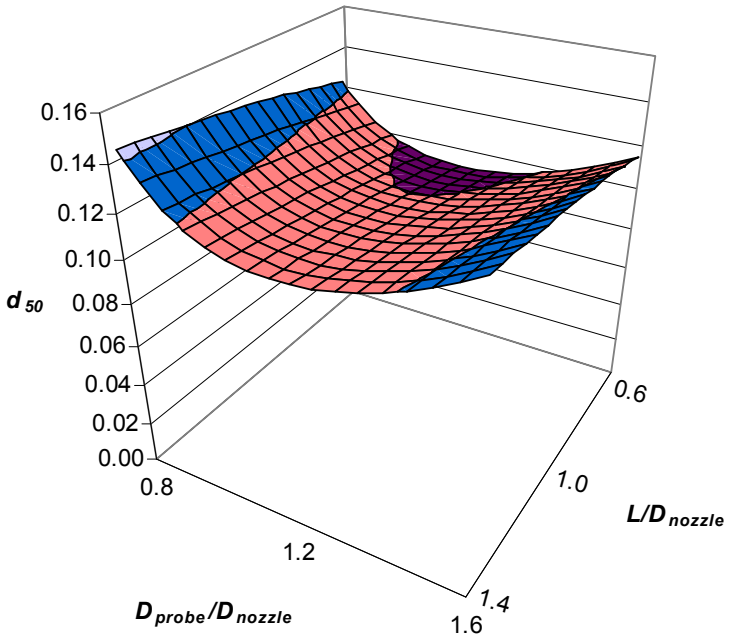

Figure 5. The effect of the physical parameters (D_{probe}/D_{nozzle} and L/D_{nozzle}) on the cutsize of the SADS when Re = 3501 and Q_{vapor}/Q_{nozzle} = 0.1.

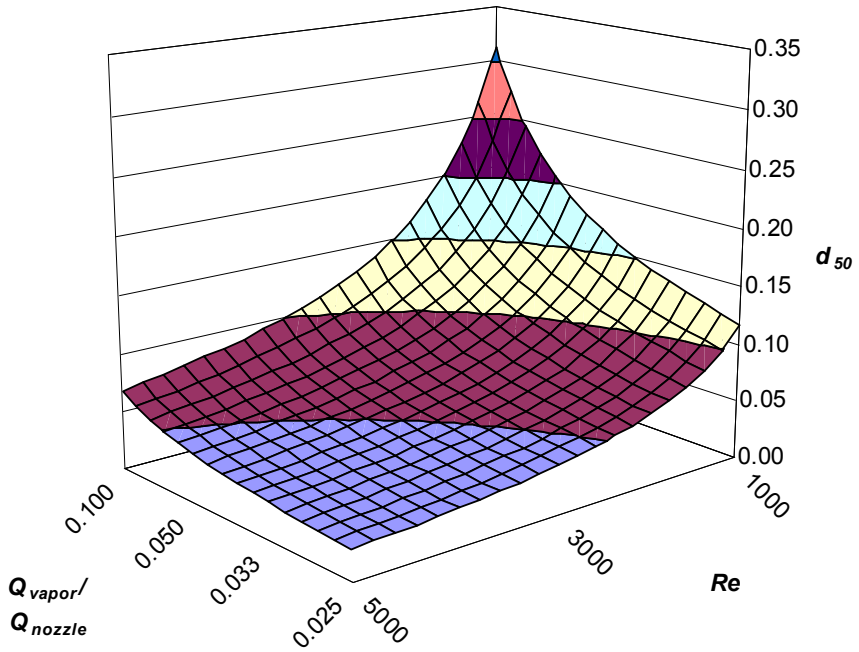

Figure 6. The effect of the operational parameters (Q_{vapor}/Q_{nozzle} and Re) on the cutsize of the SADS when D_{probe}/D_{nozzle} = 1.3 and L/D_{nozzle} = 0.6.

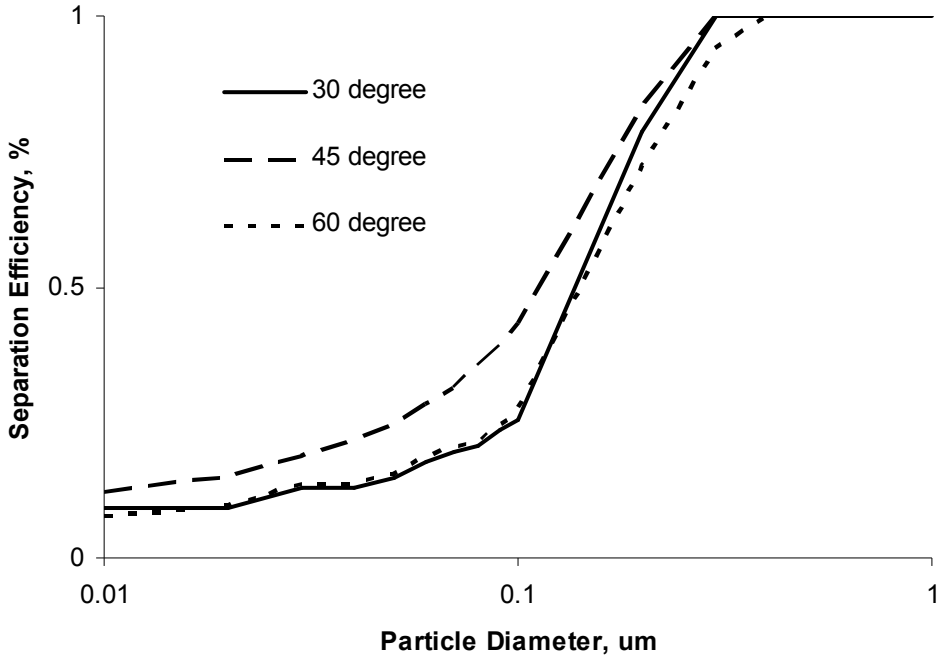

Figure 7. Effect of the entrance angle at the air nozzle through the numerical model when Re = 3501 and Q_{vapor}/Q_{nozzle} = 0.1.

Figure 8. The SADS (lower left) built according to the optimization procedure has the outer shape of 37 mm cassette (lower right) and consists of two pieces, the air nozzle (upper left) and collection probe (upper right).

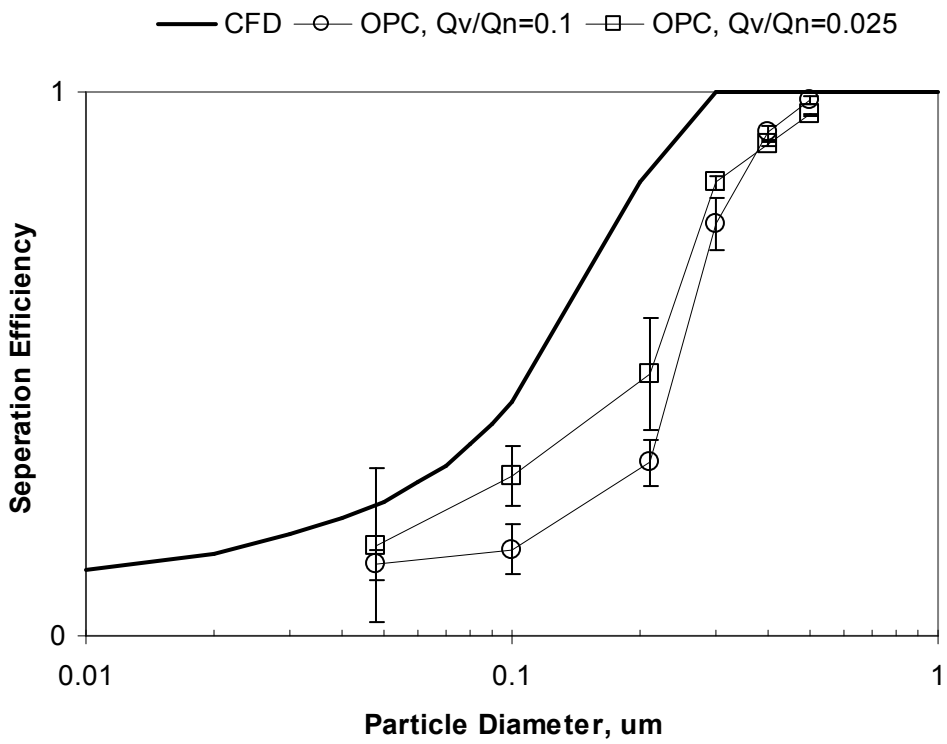

Figure 9. Comparison of numerical results (CFD model) with experimental data when Re = 3501. In the CFD modeling, Q_{vapor}/Q_{nozzle} was 0.1 and in the experimental results, Q_{vapor}/Q_{nozzle} was 0.1 (○) and 0.025 (□), respectively. Error bars present one standard deviation at each size.

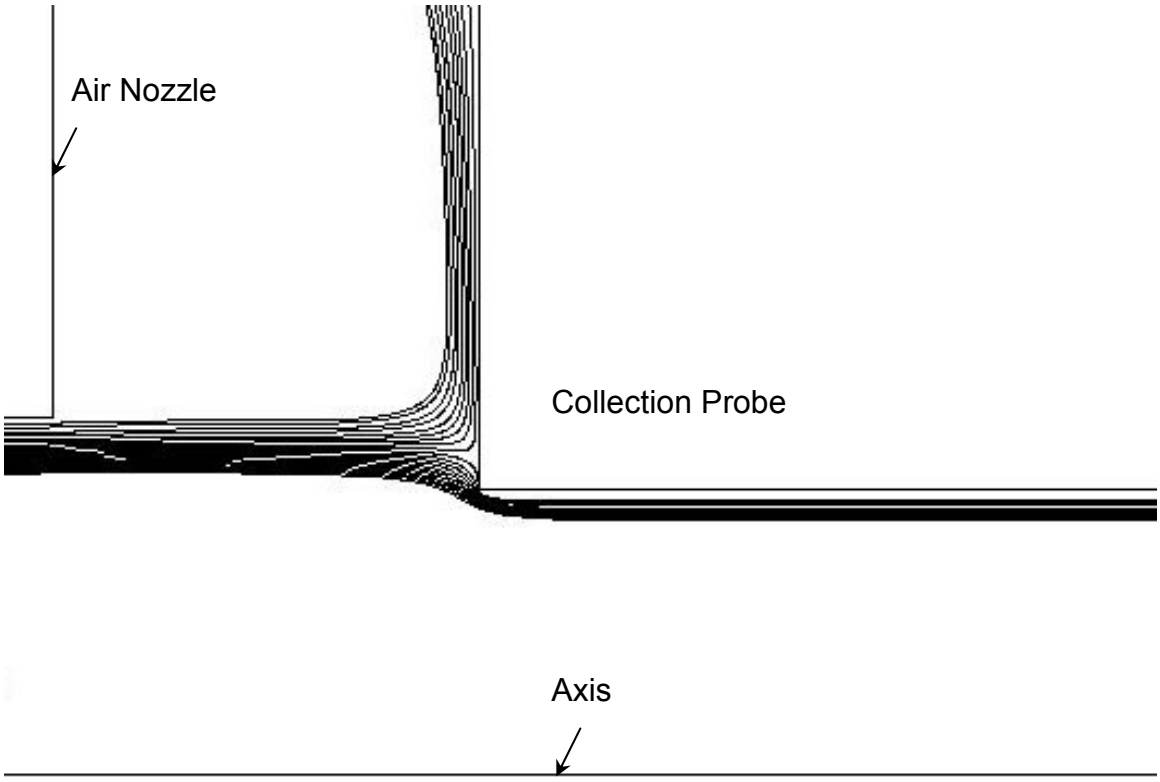

(a) $D_{probe}/D_{nozzle} = 0.8$

Figure 10. The trajectories of 0.1 μm diameter particles when D_{probe}/D_{nozzle} was 0.8, 1.3, and 1.6, respectively. Other dimensions and operational conditions were fixed at $L/D_{nozzle} = 0.6$, $Q_{vapor}/Q_{nozzle} = 0.1$, and Re = 3000.

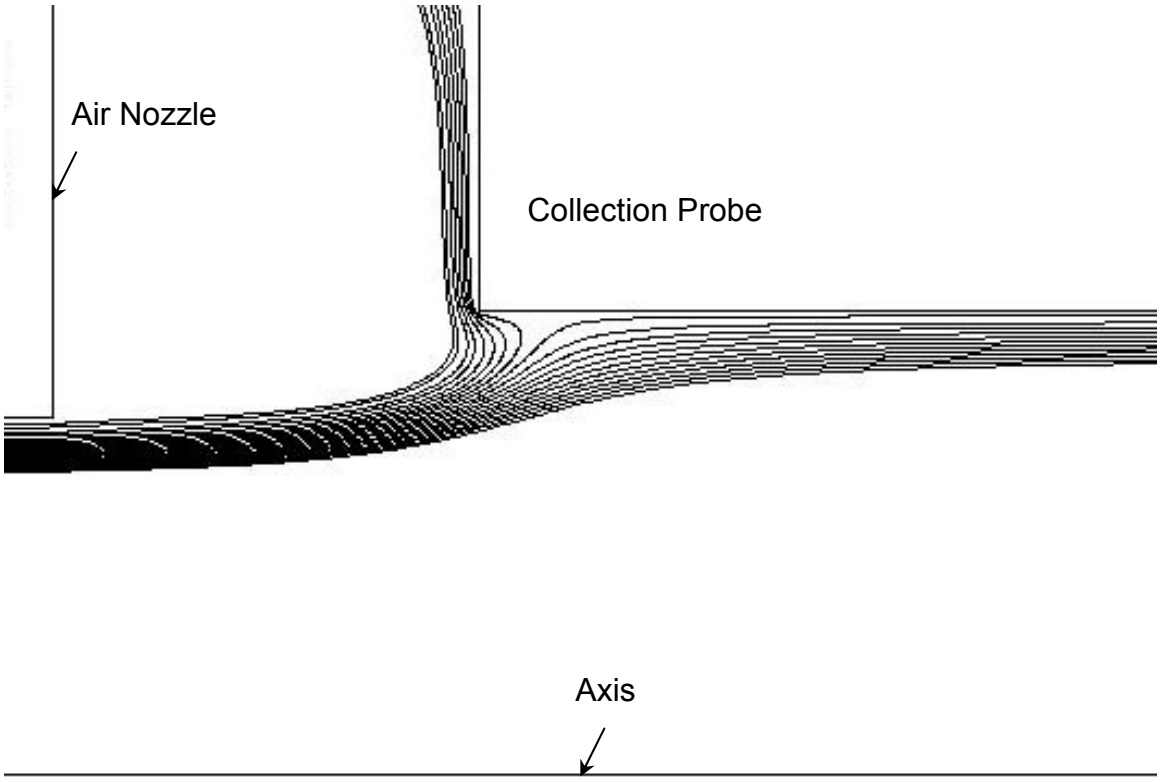

(b) $D_{probe}/D_{nozzle} = 1.3$

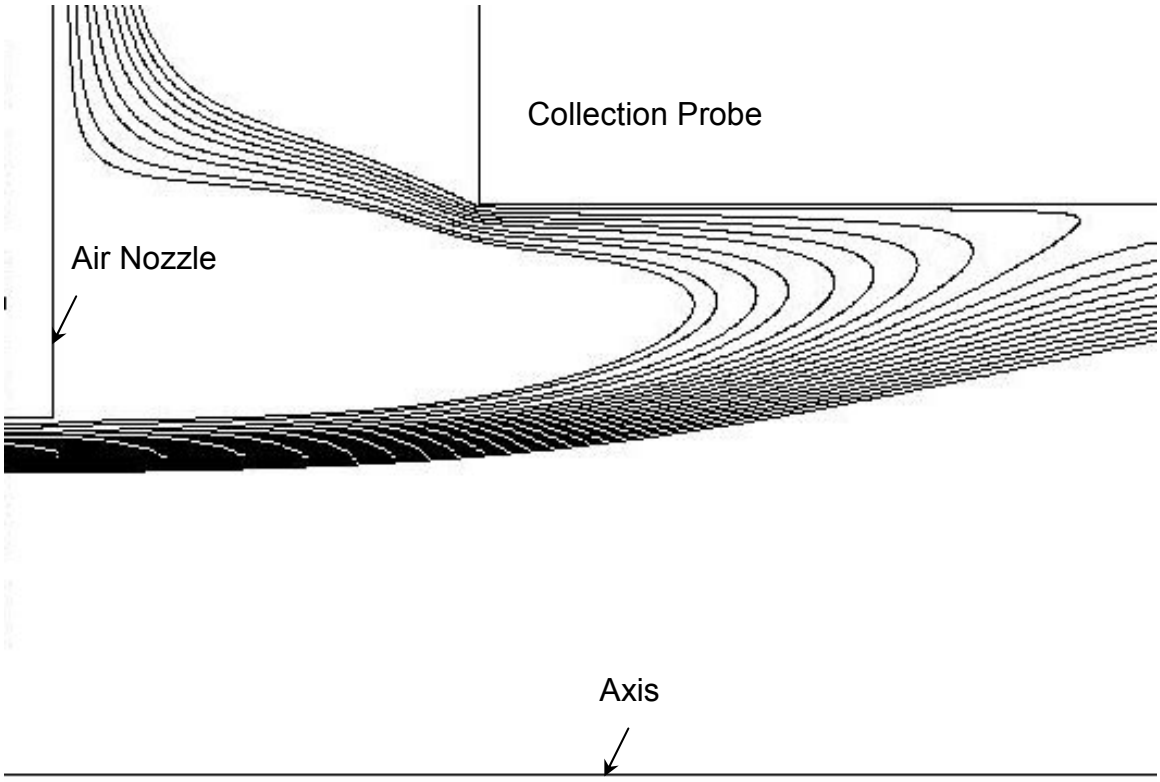

(c) $D_{probe}/D_{nozzle} = 1.6$

CHAPTER IV

EVALUATING AIRBORNE SEMIVOLATILE ORGANIC COMPOUNDS USING A SEMIVOLATILE AEROSOL DICHOTOMOUS SAMPLER

ABSTRACT

The Semivolatile Aerosol Dichotomous Sampler (SADS) was tested and its sampling performance was compared with existing vapor and particle sampling methods: filtration, electrostatic precipitation, and vapor adsorption. Seven different test fluids were used to generate test droplets, and their concentrations and composition in each phase were evaluated using gas chromatography. The amount of wall loss inside the SADS was also evaluated. Combined vapor and particle concentrations for each test aerosol were not statistically different from one another as a function of test method. However, the particle concentrations estimated using the SADS were statistically higher than those from the other methods. The wall losses of hexadecane and *bis*(2-ethylhexyl) sebacate (BEHS) were 0.25% and 26.5% of combined vapor and particle concentrations in the SADS sampling, respectively. In the tests of a chemical mixture, a similar pattern of vapor/particle concentration ratio was observed. For commercial metalworking fluid (MWF) droplets, compounds having low molecular weight were more prevalent in the vapor phase than those compounds with high molecular weight. The compositions of the particle phase were similar to those of the original fluids. Because it can avoid evaporative losses and yield more accurate concentrations than a common filtration method, SADS worked

better than the filtration method and suggested higher particle concentrations than other methods.

INTRODUCTION

Semivolatile aerosols are airborne particles and vapor molecules generated from substances having relatively low vapor pressure between $10^{4} – 10^{-11}$ atm (Bidleman, 1988). Due to their low vapor pressure, they exist in the vapor and particle phases simultaneously. Metalworking fluid (MWF) mists, pesticides, asphalt fumes, and environmental tobacco smoke are well-known potentially hazardous semivolatile aerosols in workplaces (Woskie et al., 1994; Guidotti et al., 1994; Kriech et al., 2002; Bergman et al., 1996).

The mechanisms by which the human body is exposed to particles are different from vapors. Particles deposit inside the lung according to their diameters whereas vapor molecules are absorbed into the lung according to their tissue solubility (Volckens and Leith, 2003). When a semivolatile aerosol consists of more than one compound having different vapor pressures, each phase has a different composition. Evaluating only one phase can bias the exposure assessment for that aerosol.

Many standard personal sampling methods for semivolatile aerosols depend on filtration (NIOSH, 1998). Sampling methods based on filtration are subject to evaporation loss due to continuous aspiration of air during sampling. This evaporation leads to inaccurate measurements of oil mist concentration (Raynor and Leith, 1999;

Simpson et al., 2000; Park et al., 2003). In some cases, the combination of filter media followed by sorbent tubes has been adopted to capture the evaporated vapor molecules (Volckens et al., 1999; Volckens et al, 2000; Simpson et al., 2000).

Impactors have been used to sample particles and typically have more than one stage to differentiate the sizes of particles. Multiple-stage impactors have been used to evaluate oil mist concentrations (Woskie et al., 1994; Piacitelli et al., 2001). Evaporative loss from impactors occurs due to the pressure drop in impactors and from continuous aspiration of air though impactors (Zhang and McMurry, 1987). The pressure drop through an impactor decreases vapor concentrations in the air and the vapor concentration differential between the surface of the deposit and the airstream drives evaporative mass transfer from the deposit surface to the airstream.

Virtual impactors are impactors in which the impaction plate has been replaced with a collection probe (Hounam and Sherwood, 1965). The dichotomous sampling of virtual impactors has the advantage of instant separation of particles from air and no secondary contamination to the other flow if the cutsize of the virtual impactor is small enough. Cutsize is a hypothetical aerodynamic particle diameter for which all particles greater than this size are collected and all particles less than this size pass through in a particulate sampling device (Hinds, 1999). Most virtual impactors have been developed for ambient sampling with higher flow rate than

possible with personal sampling (Solomon et al., 1983; Sioutas et al., 1994; Haglund and McFarland, 2004). A high flow rate virtual impactor is heavy and requires a large sampling pump to draw air, which prevents its use for personal sampling.

Electrostatic precipitators (ESPs) are known to have less evaporation loss than filtration methods (Leith et al, 1996). In the same paper, however, it was admitted that they still have the possibility of some evaporation loss during sampling. The fact that they require power supplies to provide the high voltage at which they operate adds extra weight to the equipment which workers need to wear for personal sampling. The safety issue with the use of high voltage might limit the use of ESPs in some workplaces. The ozone generated from ESPs can react with the collected aerosol and change it chemically (Kaupp and Umlauf, 1992; Volckens and Leith, 2003).

In principle, particle concentrations can be determined if vapor concentrations can be subtracted from the combined concentrations of vapor and particles. This approach only works if the vapor can be measured accurately. Sorbent tubes, passive samplers, and diffusion denuders are the most common personal sampling methods for vapors. The problem with using sorbent tubes for semivolatile aerosol sampling is that they sample particles along with vapor molecules, which can bias the assumed vapor-only concentration (Fairchild and Tillery, 1977; Brosseau et al, 1992). Passive samplers depend on the diffusion of sampled vapor molecules and have been

recommended for gaseous or volatile compounds. For semivolatile aerosols, passive samplers are not recommended because the attachment of particles to sorbents makes them overestimate vapor concentrations and because some semivolatile compounds do not have enough Brownian motion to diffuse into the passive sampler (Brown and Monteith, 2001). Diffusion denuders sample only the compounds attaching to the coating material inside the samplers and, like passive samplers, require active molecular diffusion of compounds being sampled. For semivolatile aerosols having complex compositions such as MWFs, diffusion denuders may not be an appropriate option (Cheng, 2001). Gunderson and Anderson (1987) studied a personal sampling device in which a diffusion denuder and a filter cassette were connected in series to separate vapor and particles. For sampling semivolatile aerosols, this method had the shortcomings of diffusion denuders and filtration methods together.

In Chapter II, the idea of a semivolatile aerosol dichotomous sampler (SADS) was proposed and tested to demonstrate that the SADS can separate vapor and particles effectively. In Chapter III, the SADS was optimized using numerical simulations to have the best performance within constraints, and the performance of the new optimized SADS was tested using monodisperse solid particles.

The SADS is a round nozzle virtual impactor having an inverted flow ratio as introduced in Chapter II. The inverted flow ratio changes the air flow through the

sampler and the trajectories of particles. The destinations of some particles may be changed from one flow direction to another flow direction due to the inversion.

Because of the inversion of flow ratio, the major and minor flows in the virtual impactor were redesignated in this paper as ‘vapor flow’ and ‘particle flow’ respectively. The dimensions of the optimized SADS are showed in Figure 1. The diameter of the nozzle was 0.8 mm and other dimensions followed the optimization results found from Chapter III. The outer shape has that of 37 mm cassette and its aspiration efficiency was reported by Mark et al. (1994). The expected 50% cutsize of the optimized SADS from experiments was 0.25 μm when the flow rate was 2.0 lpm and flow fraction going to the vapor flow direction was 0.1.

In this paper, we tested the sampling performance of the optimized SADS using real polydisperse semivolatile aerosols in a chamber. The individual concentrations of the vapor and particle phases were evaluated using the SADS and they were compared with other sampling methods such as filtration and electrostatic precipitation. The compositions of each phase for real metalworking fluids were compared using four different sampling methods.

MATERIALS AND METHODS

The optimized SADS was placed inside a chamber along with an electrostatic precipitator, a 37 mm filter cassette sampler, and an activated carbon tube. Semivolatile aerosols generated using single component chemicals having different vapor pressures and the mixture of three of the chemicals were sampled by the four different methods and their vapor and particle concentrations were statistically compared. Petroleum-based oils having multiple components were aerosolized and sampled using the same four methods. Each test was repeated four times. The vapor and particle concentrations were statistically compared and the chemical compositions from each phase were inspected.

The test chemicals and their properties are listed in Table 1. Toluene is volatile and would not be expected to have any particles when sampled. The compounds tetradecane, hexadecane, and *bis*(2-ethylhexyl) sebacate (BEHS) (Sigma-Aldrich Chemical Co., Saint Louis, MO) were used individually and in a mixture in which their mole fraction was 1:1:1. Tetradecane and hexadecane are semivolatile and BEHS is nearly non-volatile. Because tetradecane is more volatile than hexadecane, tetradecane was expected to have a greater proportion in the vapor phase than hexadecane.

Two straight oil MWFs were tested to simulate semivolatile aerosol exposures in workplaces. EDM40 (Master Chemical Co., Perrysburg, OH) and Ilocut 5468 (Castrol, Downers Grove, IL) were selected because they have a significant fraction of semivolatile compounds in their compositions.

Figure 2 shows a schematic of the laboratory setup. Particles from a three-jet Collison nebulizer (BGI Inc., Waltham, MA) were introduced into a 1.01 m^3 chamber. The particle concentration of BEHS was controlled to be approximately 3.0 mg/m^3 using a solenoid valve opened to supply air to the nebulizer for 3 seconds every 3 minutes and was closed for the rest of the time. A high-volume pump exhausted air at a rate of 300 lpm. The temperature during experiments was approximately 23°C. No humidity control was applied to the experiment; building relative humidity was generally controlled well to 45 ± 15%. The mass median diameter of the nebulized BEHS mist was measured using an Andersen Mark II cascade impactor (Graseby Andersen Inc., Smyran, GA) in a preliminary test.

Particle concentrations were monitored using a DustTrak (Model 8520, TSI, Shoreview, MN). The averaging time on the DustTrak was one minute. The DustTrak was located outside of the chamber and connected to the chamber using Tygon tubing. The DustTrak was not calibrated to test particles and used only to monitor the stability of particle concentrations. Sampling began 30 minutes after starting nebulization to

obtain stable concentrations and lasted for 4 hours. After the flows to the samplers were stopped, 30 minutes was given to clear out the particles inside the chamber. Each test condition was replicated four times, and the locations of the samplers were rotated each time.

Sampling media were attached to the two outlets of the SADS. To the vapor flow outlet, an activated carbon tube (226-16, SKC Inc., Eighty Four, PA) was connected. To the particle flow outlet, the assembly of two layers of 37 mm glass fiber filter media (61652, Pall Corporation, East Hills, NY) without support pad and an activated carbon tube were connected in series. The SADS mounted with sampling media was connected to a vacuum pump (Gast, Benton Harbor, MI). The flow rates for the vapor and particle outlets were 0.2 and 1.8 lpm, respectively and were monitored by flowmeters (Model 4140, TSI, Shoreview, MN). Back pressure was measured downstream from the sampling media for each flow direction.

Another sampling train was the ESP with a sorbent tube. An ESP (Aerosol Associates, Chapel Hill, NC) developed for personal sampling was used to sample both phases (Leith et al, 1996). The ESP substrate, a rectangular sheet of aluminum foil measuring 4 cm by 5 cm, was coiled inside the aluminum tube provided by the manufacturer. To the end of the ESP, an activated carbon tube was connected. This sampling train was connected to the same vacuum pump to which the SADS was

connected. The flow rate for the ESP was 2.0 lpm and was monitored by a flowmeter (Model 4140, TSI, Shoreview, MN).

A 37 mm cassette having two layers of the same 37 mm glass fiber filter media without support pad was connected to a personal sampling pump (Apex, Casella, Bedford, UK). The sampling flow rate was 2.0 lpm and was calibrated before and after each sampling.

The same activated carbon tubes (226-16, SKC Inc., Eighty Four, PA) adopted in the above methods were used to sample the vapor phase of the test aerosols independently. Because sorbent tubes sample not only vapor molecules but also some particles (Fairchild and Tillery, 1977; Brosseau et al, 1992), the front glass wools in activated carbon tubes were expected to collect some particles. The sampling flow rate was 2.0 lpm and air was drawn by calibrated personal sampling pumps (Apex, Casella, Bedford, UK).

After each experimental run, the SADS was immediately disassembled and the interior of the two pieces was washed by 5 ml of carbon disulfide containing 0.02% of *o*-xylene (Sigma-Aldrich Chemical Co., Saint Louis, MO) by volume as an internal standard.

All activated carbon tubes were separated into three sections: front glass wool, activated carbon granules from the front section of the tube, and activated carbon

granules from the back section of the tube. Each section was placed individually into 15ml vials and 5ml of carbon disulfide (Fisher Scientific, Pittsburgh, PA) was added to extract compounds. Each vial was agitated manually for 30 sec, allowed to stand for one hour, and transferred to another vial prior to analysis. The back section was used to check the breakthrough of the activated carbon tube. If more than 10% of a chemical was found in the back section, that sample was discarded. The mass found from the glass wool was considered to have existed as particles at the moment of sampling. One blank sample of activated carbon tube was prepared for each test to detect any contamination during experiments. Carbon disulfide containing an internal standard was used for desorption.

The aluminum substrates mounted in the ESP were immediately separated from the ESP after each run and were placed into 100ml vials. After adding 5 ml of carbon disulfide to each vial and capping tightly, vials were agitated vertically by hand for 20 seconds. The glass fiber filter media assembled in 37 mm cassettes went through the same procedure as the aluminum substrates except that they were agitated horizontally. The same carbon disulfide containing 0.02% of o-xylene by volume was used.

Known amounts of four chemicals were injected into unused activated carbon tubes using a microsyringe and analyzed to evaluate the desorption efficiencies of

each chemical from the sorbent. The chemical compositions of the original MWFs were analyzed by injecting small amounts of original fluids into carbon disulfide containing 0.02% of o-xylene.

The standard curves for the four individual chemicals were obtained by adding known amounts of each chemical to the standard solutions and analyzing them with samples at the same conditions. The range of the calibration standards was wider than the range of samples. An ASTM D5307 crude oil quantitative standard (Supelco, Bellefonte, PA) was used as a standard for MWF analysis because the chemical compositions of the two test MWFs were not available. This standard contains sixteen normal alkanes ranging from n-decane ($C_{10}H_{22}$) to n-tetratetracontane ($C_{44}H_{90}$) with the same weight percentage for each alkane. Then, based on the fact that each component has the same weight percentage in the crude oil standard, the sixteen alkanes were calibrated.

All samples were analyzed using gas chromatography. A Hewlett Packard (HP) Model 6850A gas chromatograph with a flame ionization detector (GC/FID) and an HP-1 (30 m×0.25 mm i.d.×0.25 μm film thickness, methyl siloxane) capillary column were used in the GC-FID analyses. The GC operating conditions for the single chemicals and the three-way mixture were as follows: 2 μl of each extract was injected in splitless mode, injector temperature 300°C, 350°C at the detector, oven

temperature started at 100°C, 100–220°C at 6°C/min, and no hold at the start or at the end. For the straight MWFs, only the temperature program was changed as follows: 100°C for 2 min, 100–325°C at 15°C/min, and 325°C for 8 min. Data acquisition and analysis were performed with the HP-GC Chemstation software. All the quantities analyzed were adjusted to the internal standard concentrations and the desorption efficiencies of each chemical.

For other compounds of which peaks were not identified by the sixteen alkanes from the crude oil standard, each peak was assigned to an alkane by GC retention time: the integrated area for each unidentified peak was added to the area of the alkane peak with the closest retention time (Raynor et al., 2000).

For the SADS, the airborne vapor concentration (C_{vapor}) and the airborne particle concentration ($C_{particle}$) were determined based on measured values of the masses collected on the filter (M_{filter}) and the two ACTs (M_{ACTv} and M_{ACTp}), sampling time (t), and each flow rate (Q_{vapor} and $Q_{particle}$), under the assumption of complete particle separation, as:

$$C_{vapor} = \frac{M_{ACTv}}{t \times Q_{vapor}} \quad (1)$$

$$C_{particle} = \frac{\left(M_{filter} + M_{ACTp}\right) - \left(\frac{Q_{particle}}{Q_{vapor}}\right) M_{ACTv}}{t \times \left(Q_{vapor} + Q_{particle}\right)} \quad (2)$$

$$M_{ACT} = M_{GC}\left(\frac{100}{DE}\right)\left(\frac{IS_{CS_2}}{IS_{sample}}\right) \quad (3)$$

$$M_{filter} = M_{GC}\left(\frac{IS_{CS_2}}{IS_{sample}}\right) \quad (4)$$

where M_{GC} is the mass integrated from GC analysis, DE is desorption efficiency (%) for each chemical, and IS_{CS2} and IS_{sample} are the concentrations of internal standard of original carbon disulfide solution and each sample, respectively.

The vapor concentrations measured by other methods were calculated using Eqs. (1) and (3). The particle concentrations were calculated as follows:

$$C_{particle} = \frac{M_{substrate}}{t \times Q_{particle}} \quad (5)$$

$$M_{substrate} = M_{GC}\left(\frac{IS_{CS_2}}{IS_{sample}}\right) \quad (6)$$

where $M_{substrate}$ is the mass collected on the substrate of each particle sampling method.

The concentrations of each phase for each sampling method were added for each repeat to obtain the combined vapor and particle chemical concentrations. For each test aerosol, the combined vapor and particle concentrations and the concentrations of each phase measured by the four sampling methods were compared using analysis of variance (ANOVA) to determine if there was any statistically significant difference among sampling methods. The compositions of each phase and the original fluid for the two test MWFs were also compared.

The back pressure at each outlet of SADS was measured using Magnehelic gauges (Dwyer Instruments, Michigan City, IN) in which the reference tab was open to room air.

RESULTS

The mass median diameter of generated BEHS particles and their geometric standard deviation were 2.90 μm and 1.17, respectively. The particle concentrations of BEHS inside the chamber stayed constant with mild variation over sampling time (Figure 3). The particle concentrations of BEHS measured by DustTrak were higher than those from the other four methods.

The desorption efficiencies for toluene, tetradecane, hexadecane, and BEHS were 98.9 ± 1.2% (mean ± SD), 76.4 ± 12.4%, 74.3 ± 11.8%, and 33.1 ± 3.7%, respectively. The correction for the internal standard was minimal for activated carbon tube samples and was less than 10% of the original amounts for wall loss evaluation procedure.

Figure 4 shows the vapor and particle concentrations of the four single chemicals measured by the four different methods. For tetradecane and hexadecane the combined vapor and particle concentrations were not statistically different among sampling methods except the 37 mm glass fiber filter method which did not evaluate vapor concentrations (Figure 4b and 4c). For hexadecane, the average particle concentrations measured by the SADS and an electrostatic precipitator were 77.3% and 1.46% of the combined vapor and particle concentrations and for tetradecane they

were 51.2% and 0.02%, respectively. The combined vapor and particle concentrations of BEHS including the wall loss fraction were statistically different among sampling methods ($p<0.020$) (Figure 4d). The combined vapor and particle concentrations measured by activated carbon tubes were lower than others for BEHS. The combined vapor and particle concentrations of each chemical increased as the vapor pressures of chemicals increased.

The wall loss of hexadecane was 0.25% in the SADS sampling. The wall loss in the BEHS test was 26.5% of combined vapor and particle concentrations in the SADS sampling (Figure 4c and 4d). Out of total wall loss, 25% came from the air nozzle and the rest was found from the collection probe. No wall loss was found from other chemicals.

The results for the mixture of tetradecane, hexadecane, and BEHS showed similar patterns found from the tests for individual chemicals except that the combined vapor and particle concentrations were lower than those from the individual tests (Figure 5). In this test, concentrations showed larger variation among sampling methods than the individual chemical test. The average particle concentration measured by the SADS and the ESP were 55.1% and 0% of combined vapor and particle concentrations for tetradecane (Figure 5a). The same fractions for hexadecane were 71.4% and 4.7%, respectively (Figure 5b). The combined vapor and particle

concentrations of BEHS including the wall loss fraction were statistically different among sampling methods ($p<0.001$) (Figure 5c). The wall loss for BEHS in the SADS method was 19.6%.

The results for EDM 40 showed similar patterns found from the tests for the individual compounds. The average particle concentration measured by the SADS and the ESP were 52.4% and 0.838% of combined vapor and particle concentrations for EMD 40 (Figure 6a). However, the results for Ilocut 5486 showed a higher fraction of particle concentrations than those for EDM 40 (Figure 6b). The average particle concentration measured by the SADS and the ESP were 63.5% and 39.6% of combined vapor and particle concentrations for Ilocut 5486. This difference can be explained by the chemical compositions of two MWFs. Chemical compositions at each phase of the two straight oil MWFs are illustrated in Figure 7. EDM 40 consisted of lighter alkanes than Ilocut 5486. The vapor phase has more light chemicals than particle phase in both cases. The chemical compositions of the particle phase were similar to the original fluids.

The chemical compositions of vapor phase and particle phase measured by each method for Ilocut 5486were compared in Figure 8. Significantly higher percentages of chemicals were found over the range of C18 – C28 in the activated carbon tube method compared with other methods for vapor phase. The GF and ESP

measured higher percentages of C18-C28 in particles than SADS.

The back pressures at the outlet of the vapor flow and particle flow were 4400 ± 130 (mean ± SD) Pa (18 ± 0.5 in. w.g.) and 6500 ± 300 (1 SD) Pa (26 ± 1.2 in. w.g.), respectively. Most personal sampling pumps can handle back pressures up to 7500 Pa (30 in. w.g.) at 2.0 lpm for 8 hours.

DISCUSSION

When a SOC consists of one component, a significant fraction of the chemical can be expected to exist in the vapor phase if the chemical's saturated vapor concentration (SVC) is greater than its total airborne concentration. The SVC for toluene was reported as 110 g/m^3, which was significantly higher than the total concentrations measured in this study (Yaws, 1994). Accordingly, no particle was detected. The SVCs for tetradecane and hexadecane are 90.8 mg/m^3 and 12.4 mg/m^3, respectively (Yaws, 1994). The total concentrations of two chemicals measured in this study were equal to 6.3% and 26% of their SVCs. Because these concentrations were lower than their SVCs, a significant fraction of each chemical, 47.9% and 22.4% respectively, were found as vapor in SADS sampling (Figure 4b and 4c). In case of BEHS, no vapor was detected due to its extremely low vapor pressure (Figure 4d).

For multicomponent SOCs, according to Raoult's Law, vapor concentrations for mixtures of similar compounds are proportional to their mole fractions. In this study, the mole fraction of the test mixture was 1:1:1 and the vapor fractions of three mixture chemicals were similar with those from individual chemical tests in SADS sampling as 44.9% and 22.9% for tetradecane and hexadecane, respectively (Figure 4 and 5). For sampling methods other than SADS, the particle fractions of hexadecane

were higher in the mixture tests (Figure 5b) than those in the individual chemical tests (Figure 4c). Hexadecane might be dissolved in BEHS droplets in the mixture tests and avoided total evaporation while the same chemical evaporated almost completely by air passing through the sampler in single chemical tests. In MWF experiments, the vapor fractions of the chemicals from dodecane (C12) to hexadecane in EDM 40 are roughly proportional to their mole fractions in the original fluid (Figure 7a). For Ilocut 5486, however, tetradecane has an exceptionally high vapor fraction, for which a reason was not identified (Figure 7b).

When VOC molecules coexist with airborne particles, sorbent tubes collect a significant amount of particles on their front glass wools and sorbents (Figure 4d). Figure 8a indicates that the activated carbon tubes capture more particles than the other two methods because the compounds in the range of C18 – C28 mostly exist as particle due to their low vapor pressure. Therefore, when vapor and particles coexist and vapor molecules can be attached to the particles, the true vapor concentrations can be evaluated more accurately by using SADS than by using sorbent tubes only. Cohen et al. (1992) estimated that paint droplets could contain up to 50 percent of airborne solvent in a paint spray booth by comparing the solvent concentrations measured using prefiltered sorbent tubes and sorbent tubes alone. In the same situation, SADS might be able to measure more accurate vapor concentrations by separating the

particles containing solvents. The percentage of solvent contained inside the paint particles might have been larger than what Cohen et al. (1992) estimated because the solvent attached to the particles captured in sorbent tubes could cause the vapor concentrations to be overestimated.

In all experiments, SADS measured significantly higher concentrations than the filtration method which is similar to the current standard method for oil mist sampling in the industrial hygiene field (NIOSH, 1998). Attaching sorbent tubes to the outlet of the filter cassette would make it possible to estimate the overall oil mist concentrations. However, SADS could estimate the overall concentrations and the individual concentrations of each phase at the same time. Figure 6 indicates that when MWFs mists were sampled only using sorbent tubes, the front glass wools should be analyzed together with sorbents. In Figure 8b, the chemical compositions of particle phase shows that the particles captured by either glass fiber filter or ESP lost more volatile compounds during sampling and that only less volatile compounds (C18 – C28) remained on their substrates after sampling. However, SADS could estimate the real compositions at the moment of sampling due to its instant dichotomous separation.

In their study sampling MWFs using an ESP and filter media, Volckens et al. (1999) found significant differences in the particle fraction between two methods. In

this study, those two methods showed similar level of particle concentrations for Ilocut 5486 (Figure 6b) as well as for other test aerosols. Part of the reason may be found from the particle generation method. In this study, mist was generated in a cyclical pattern, which created fluctuation of aerosol concentrations inside the test chamber as shown in Figure 3. Raynor et al. (2000) reported that fluctuations in concentrations and low concentrations can lead to poor measurements in filter sampling for oil mists. These problems can be applied to the ESP method also because ESPs are not dichotomous samplers. SADS is not affected by fluctuating concentrations because it separates particles instantly. This can be a considerable strength of SADS.

The particles smaller than the cutsize of SADS were expected to go to the vapor flow as well as to the particle flow and contributed to an overestimation of the vapor concentrations. The fraction of this mass depends on the size distribution of airborne particles. In the individual chemical test with BEHS, that portion was 1.35% (Figure 4d) and in the mixture chemical test, the same portion for BEHS was 2.04% (Figure 5c). Raynor et al. (1996) showed that the average size of multicomponent semivolatile oil droplets increases with time due to evaporation while the distribution narrows. Because BEHS does not evaporate, however, the particles from the three-way mixture in this study were expected to keep certain minimum sizes after more

volatile components evaporated. Therefore, the size distribution might be smaller in the mixture and the percentage smaller than the cutsize of SADS might increase. A smaller size distribution can make more particles flow to vapor flow.

When the average size of semivolatile aerosols is close to or below the cutsize of SADS, 0.25 μm, the vapor concentration will be significantly overestimated and, accordingly, the particle concentration will be underestimated from Eq. (2). On the other hand, if the average sizes of semivolatile aerosols are larger than the cutsize of SADS, SADS can be used effectively. For example, the aerodynamic mass median diameters (MMDs) for straight oil mist were measure from 6.4 to 7.7 μm and MMDs for soluble oil mist varied between 6.9 and 8.0 μm (Woskie et al., 1994). In another study on MWFs, the overall mean MMD of oil mist was determined to be 5.3 μm (Piacitelli et al., 2001). In these conditions, sampling using SADS will enable effective measurement of both phases.

The wall loss in SADS sampling for BEHS was larger than the estimated fraction from the CFD model. Approximately 20% and 16% wall loss was found in SADS sampling in the single BEHS tests and in the mixture chemical tests, respectively. The difference also can be explained by the probable difference of the size distributions between the two test aerosols as discussed above. Because the wall loss is a function of particle size, a change in size distribution may result in a change

in the amount of wall loss. For other semivolatile particles, negligible amounts of wall loss were found on the air nozzle and the collection probe. Any particles deposited on wall in these instances might evaporate due to continuous aspiration.

Virtual impactors are subject to significant wall losses for liquid particles near the cutpoint (Hering, 2001). Loo and Cork (1988) suggested experimentally determined criteria for minimizing these losses. The same criteria might not be able to be applied to SADS because it has the inverted flow ratio. In other virtual impactor-type dichotomous samplers, the wall loss fraction varied. The mean wall loss of the Portable Vapor/Particle Sampler was 2.2% (Xiong et al., 1998). The wall losses of the Virtual Impactor Personal Aerosol Sampler on the collection probe were found to be 12.1%, 4.9%, and 0.1% and losses in the major flow cavity of the same sampler were found to be 1.6%, 0.3%, and 0.7% for particles with aerodynamic diameters of 0.77, 0.93, and 1.16 μm (Marple et al., 1995) .

Accurate flow control is important in SADS sampling. Because the vapor flow rate is the denominator of the flow ratio $Q_{particle}/Q_{vapor}$ in Eq. (2) and is significantly smaller than the total flow rate in SADS, error in vapor flow rates will be magnified significantly. Therefore, a flow ratio higher than 9 is not recommended. Xiong et al. (1998) reported that sampling error increases as flow ratio $Q_{particle}/Q_{vapor}$ increases when the vapor concentration is higher than particle concentration. When the

semivolatile aerosol has more volatile compounds, the mass of vapor flow becomes bigger and its error will be multiplied by the factor of flow ratio in Eq. (2). In extreme cases, negative values for particle concentrations can be calculated as can be seen in Figure 4a.

For exact evaluation of the concentrations and identification of chemicals having complex and unknown compositions, GC-MS analysis is required. This might increase the cost of the exposure assessment. In addition, it might not be possible to get the exact concentrations and chemical identifications if the library of the GC-MS does not contain all the compounds in the aerosol.

CONCLUSIONS

The optimized SADS designed in Chapter III was tested using polydisperse semivolatile particles. For individual semivolatile compounds, their mixture, and real MWFs, the particle concentrations measured by SADS were statistically higher than those measured by either a filtration method or electrostatic precipitators. Higher wall loss than estimated from numerical models was found for non-volatile compounds. No wall deposition was reported for semivolatile aerosols. The compositions and the concentrations of each phase of real MWFs could be estimated from GC analysis. The SADS separated vapor and particles and gives individual concentrations for each phase. The SADS worked well in realistic laboratory measurements without depending on the choice of sampling media.

REFERENCES

Bergman TA, Johnson DL, Boatright DT, Smallwood KG, Rando RJ. (1996) Occupational exposure of nonsmoking nightclub musicians to environmental tobacco smoke. Am Ind Hyg Assoc J; 57 746–752.

Brosseau LM, Fang CP, Snyder C, Cohen BS. (1992) Particle size distribution of automobile paint sprays. Appl Occup Environ Hyg; 7 607–612.

Brown RH, Monteith LE. (2001) Gas and vapor sample collectors. In Cohen BS, McCammon CS Jr., editors. Air sampling instruments for evaluation of atmospheric contaminants. Cincinnati: American Conference of Governmental Industrial Hygienists. p. 421-424. ISBN 1 882417 39 9.

Cheng Y-S. (2001) Denuder systems and diffusion batteries. In Cohen BS, McCammon CS Jr., editors. Air sampling instruments for evaluation of atmospheric contaminants. Cincinnati: American Conference of Governmental Industrial Hygienists. p. 577-583. ISBN 1 882417 39 9.

Cohen BS, Brosseau LM, Fang CP, Bower A, Snyhder C. (1992) Measurement of air concentrations of volatile aerosols in paint spray applications. Appl Occup Environ Hyg; 7 514-521.

Fairchild CI, Tillery MI. (1977) The filtration efficiency of organic vapor sampling

tubes against particulates. Am Ind Hyg Assoc J; 38 277-283.

Gunderson E, Anderson CC. (1987) Collection device for separating airborne vapor and particulates. Am Ind Hyg Assoc J; 48(7) 634-638.

Guidotti TL, Yoshida K, Clough V. (1994) Personal exposure to pesticide among workers engaged in pesticide container recycling operations. Am Ind Hyg Assoc J; 55 1154-1163.

Haglund JS, McFarland AR. (2004) A circumferential slot virtual impactor. Aerosol Sci Technol; 38 664–674.

Hering SV. (2001) Impactors, cyclones, and other particle collectors. In Cohen BS, McCammon CS Jr., editors. Air sampling instruments for evaluation of atmospheric contaminants. Cincinnati: American Conference of Governmental Industrial Hygienists. p. 315-354. ISBN 1 882417 39 9.

Hinds WC. (1999) Aerosol Technology: Properties, Behavior, and Measurement of Airborne Particles. 2nd ed. Wiley-Interscience, New York, NY.

Hounam RF, Sherwood RJ. (1965) The cascade centripeter: a device for determining the concentration and size distribution of aerosols. Am Ind Hyg Assoc J; 26 122-131.

Kaupp H, Umlauf G. (1992) Atmospheric gas-particle portioning of organic compounds: comparison of sampling methods. Atmos Environ; 26 2259-2267

Kriech AJ, Kurek JT, Wissel HL, Osborn LV, Blackburn GR. (2002) Evaluation of worker exposure to asphalt paving fumes using traditional and nontraditional techniques. Am Ind Hyg Assoc J; 63 628-635.

Leith D, Leith FA, Boundy MG. (1996) Laboratory measurements of oil mist concentrations using filters and an electrostatic precipitator. Am Ind Hyg Assoc J; 57 1137–1141.

Loo BW, Cork CP. (1988) Development of high efficiency virtual impactors. Aerosol Sci Technol; 9 167-176.

Mark D, Lyons CP, Upton SL, Kenny LC. (1994) Wind tunnel testing of the sampling efficiency of personal inhalable aerosol samplers. J Aerosol Sci; 25 Supplement 1 S339-S340.

Marple VA, Rubow KL, Olson BA. (1995) Diesel exhaust / mine dust virtual impactor personal aerosol sampler: design, calibration and field evaluation. Aerosol Sci Technol; 22 140-150.

NIOSH (1998). NIOSH Manual of Analytical Methods (NMAM). 4th ed., DHHS (NIOSH) Publication 94-113. Available from: URL: http://www.cdc.gov/niosh/nmam/nmammenu.html

Park D, Kim S, Yoon C. (2003) Loss of straight metalworking fluid samples from evaporation during sampling and desiccation. Am Ind Hyg Assoc J; 64 837-841.

Piacitelli GM, Sieber WK, O'Brien DM, Hughes RT, Glaser RA, Catalano JD. (2001) Metalworking fluid exposure in small machine shops: an overview. Am Ind Hyg Assoc J; 62 356-370.

Raynor PC, Cooper S, Leith D. (1996) Evaporation of polydisperse multicomponent oil droplets. Am Ind Hyg Assoc J; 57(12) 1128-1136.

Raynor PC, Leith D. (1999) Evaporation of accumulated multicomponent liquids from fibrous filters. Ann Occup Hyg; 43(3) 181-192.

Raynor PC, Volckens J, Leith D. (2000) Modeling evaporative loss of oil mist collected by sampling filters. Appl Occup Environ Hyg; 15 90-96.

Simpson AT, Groves JA, Unwin J, Piney M. (2000) Mineral oil metal working fluids (MWFs) – development of practical criteria for mist sampling. Ann Occup Hyg; 44 165-172.

Sioutas C, Koutrakis P, Burton PM. (1994) A high-volume small cutpoint virtual impactor for separation of atmospheric particulate from gases pollutants. Particulate Sci Technol; 12 207-221.

Solomon PA, Moyers JL, Fletcher RA. (1983) High-volume dichotomous virtual impactor for the fractionation and collection of particles according to aerodynamic size. Aerosol Sci Technol; 2 455-464.

Volckens J, Boundy M, Leith D, Hands D. (1999) Oil mist concentration: a

comparison of sampling methods. Am Ind Hyg Assoc J; 60 684-689.

Volckens J, Boundy M, Leith D. (2000) Mist concentration measurements II: laboratory and field evaluations. Appl Occup Environ Hyg; 15(4) 370-379.

Volckens J, Leith D. (2003) Partitioning theory for respiratory deposition of semivolatile aerosols. Ann Occup Hyg; 47(2) 157-164.

Woskie SR, Smith TJ, Hallock MF, Hammond SK, Rosenthal F, Eisen EA, Kriebel D, Greaves IA. (1994) Size-selective pulmonary dose indices for metal-working fluid aerosols in machining and grinding operations in the automobile manufacturing industry. Am Ind Hyg Assoc J; 55(1) 20-29.

Xiong JQ, Fang C, Cohen BS. (1998) A portable vapor/particle sampler. Am Ind Hyg Assoc J; 58 614-621.

Yaws CL. (1994) Handbook of Vapor Pressure. Gulf Pub. Co., Houston, TX.

Zhang X, McMurry PH. (1987) Theoretical analysis of evaporative losses from impactor and filter deposits. Atmos Environ; 21 1779-1789.

Table 1. Test compounds and their molecular weight, and vapor pressure

Compound	Molecular weight	Vapor pressure
Toluene	92.1	22 mmHg @ 22 °C[#]
Tetradecane	198.4	0.012 mmHg @ 22 °C[#]
Hexadecane	226.4	0.0012 mmHg @ 22 °C[#]
Bis(2-ethylhexyl) sebacate (BEHS)	426.7	2.8×10^{-6} mmHg @ 22 °C[*]

[#] Yaws (1994)

* Raynor and Leith (1999)

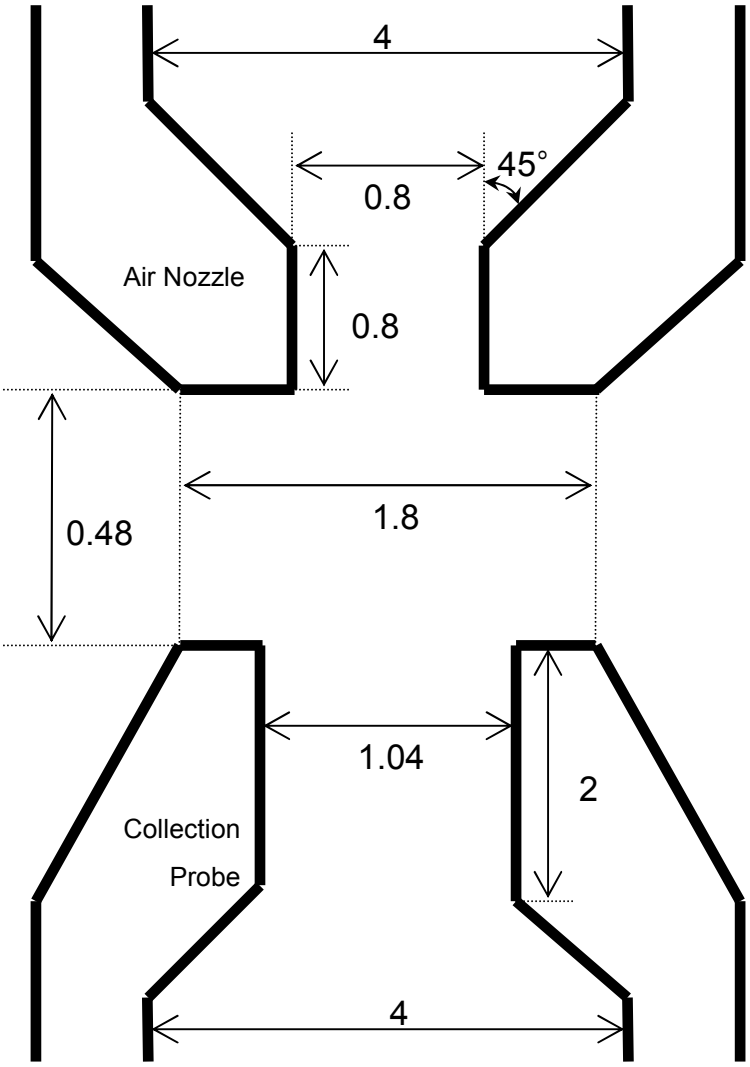

Figure 1. Dimensions of the optimized semivolatile aerosol dichotomous sampler (SADS) in the units of mm.

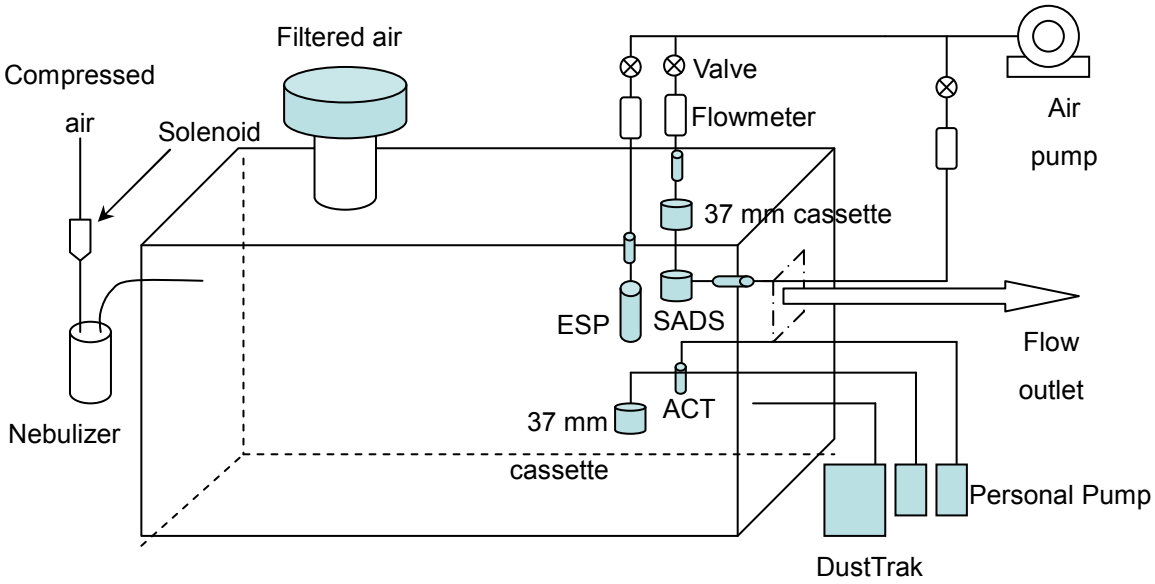

Figure 2. Schematic drawing of the test chamber.

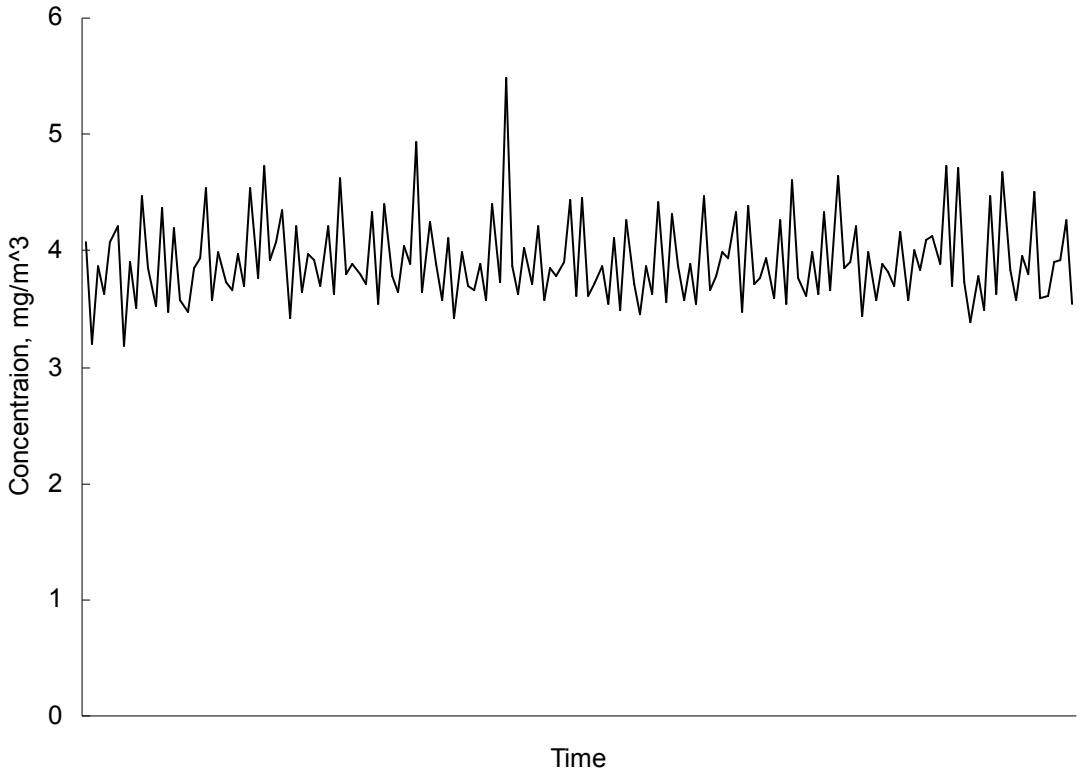

Figure 3. Temporal change of BEHS particle concentrations in the chamber measured using the DustTrak.

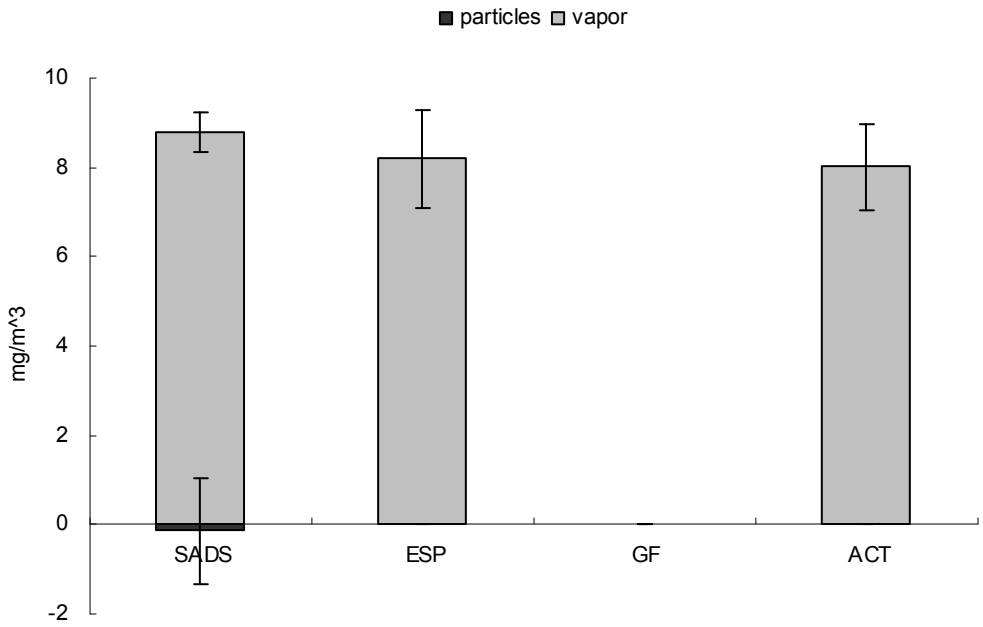

(a) Toluene

Figure 4. Vapor concentrations and particle concentrations of individual chemicals measured by four different methods. Error bars represent one standard deviation for each method.

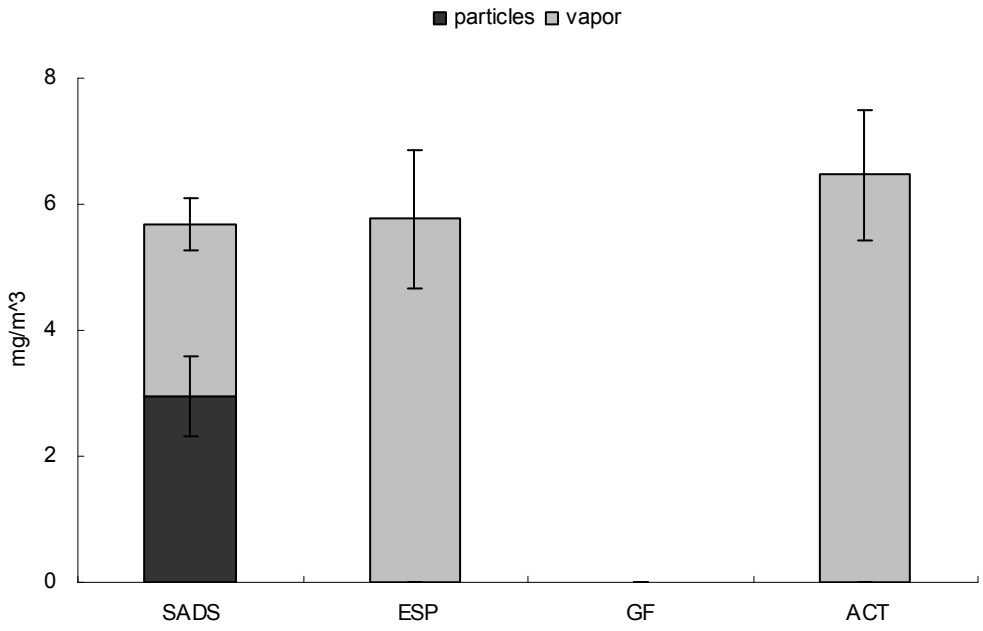

(b) Tetradecane

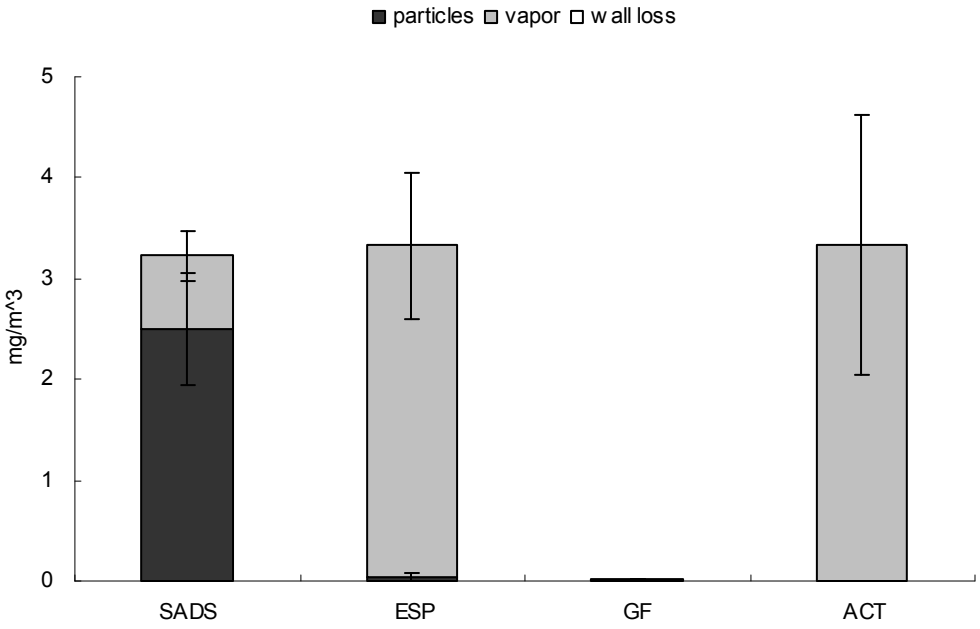

(c) Hexadecane

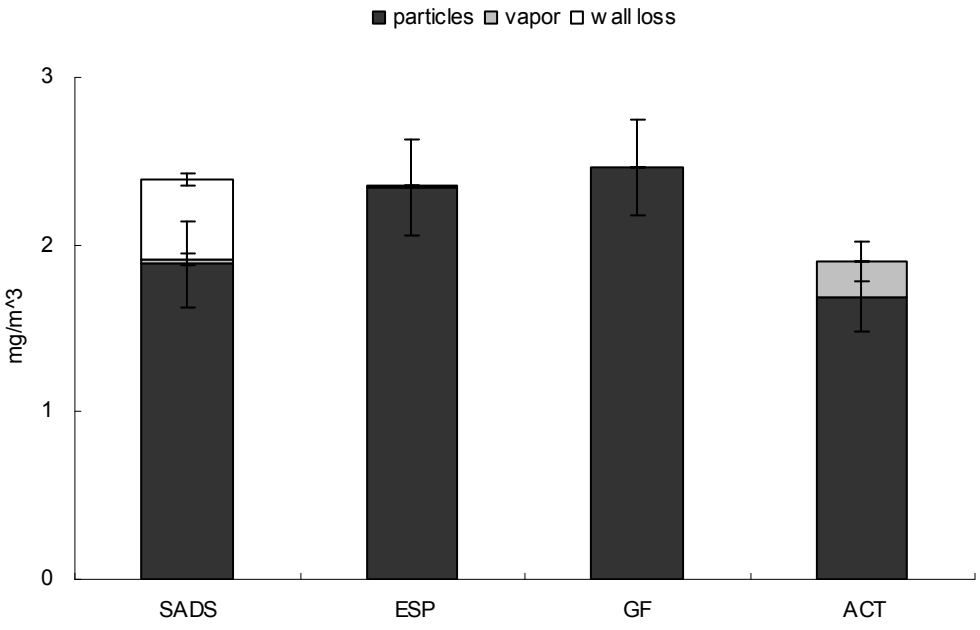

(d) BEHS

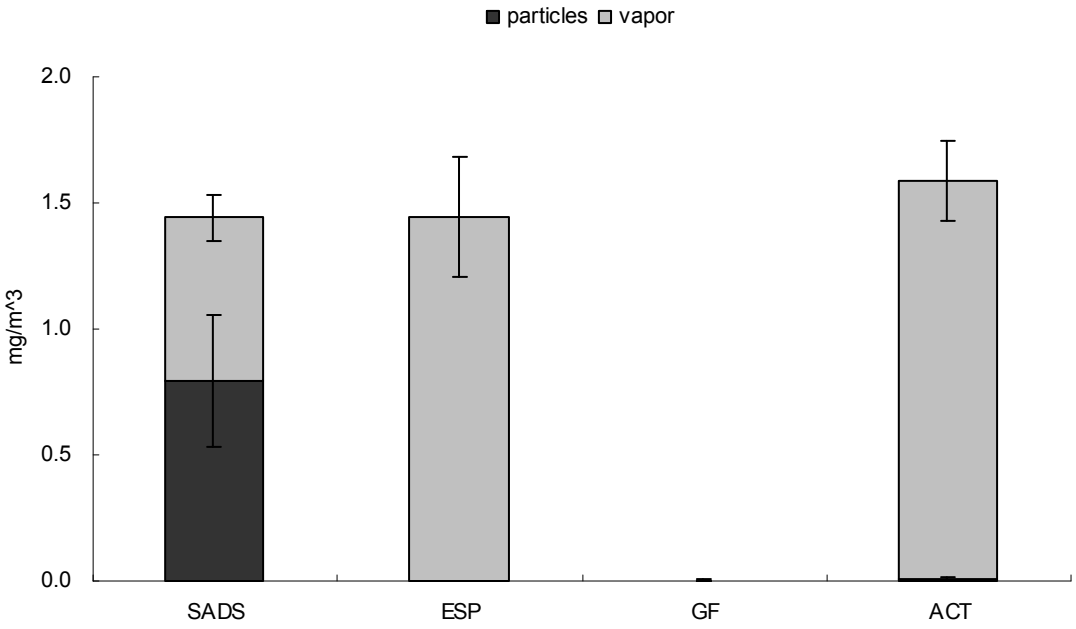

(a) Tetradecane

Figure 5. Vapor concentrations and particle concentrations of the mixture of three chemicals measured by four different methods. Error bars represent one standard deviation for each method.

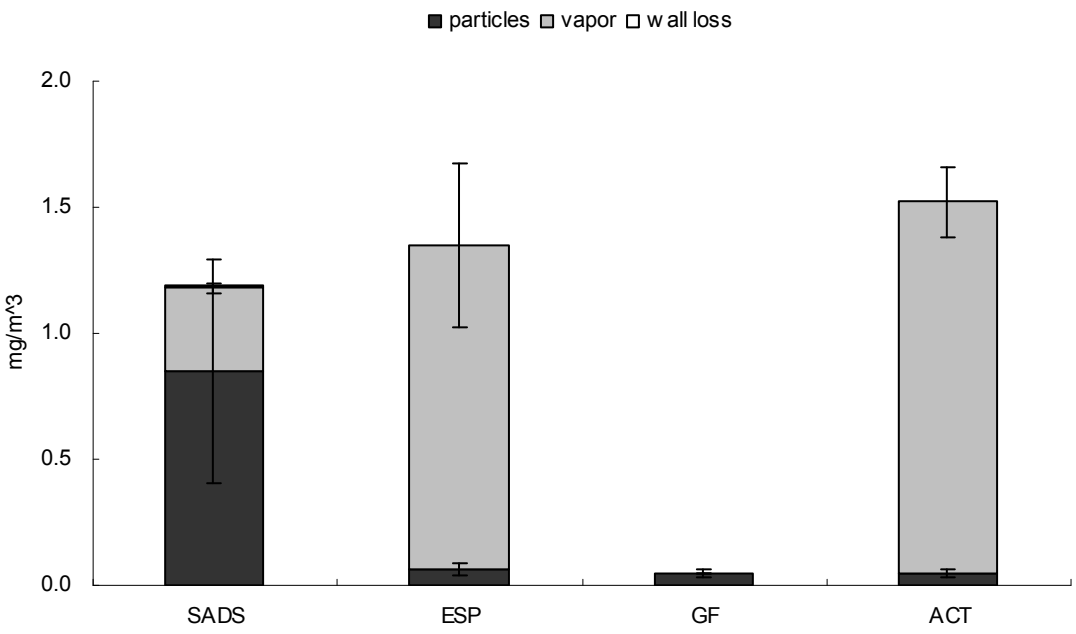

(b) Hexadecane

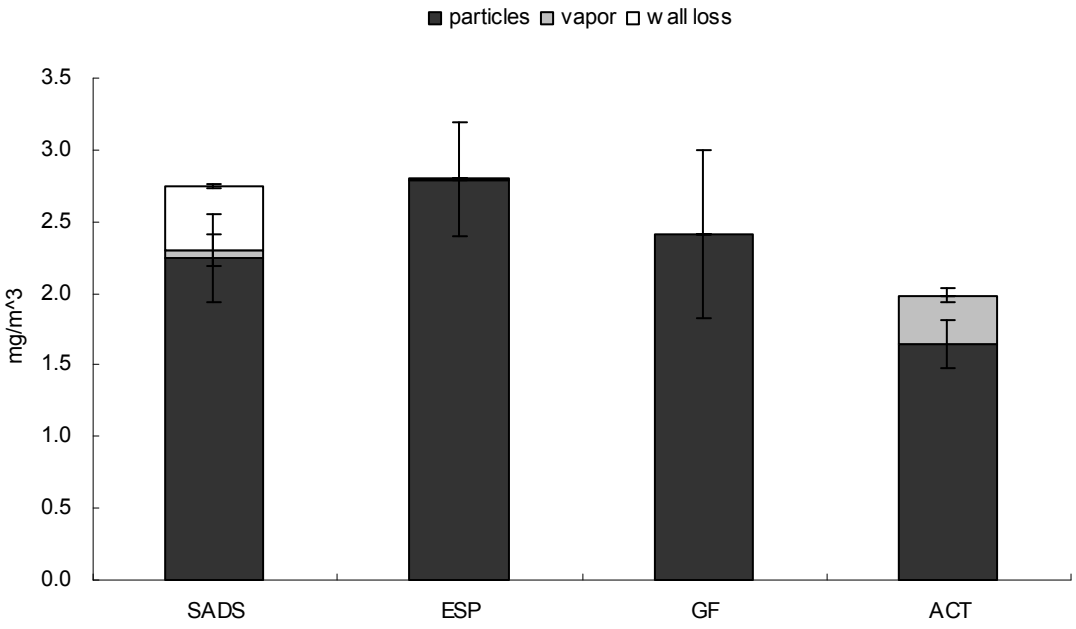

(c) BEHS

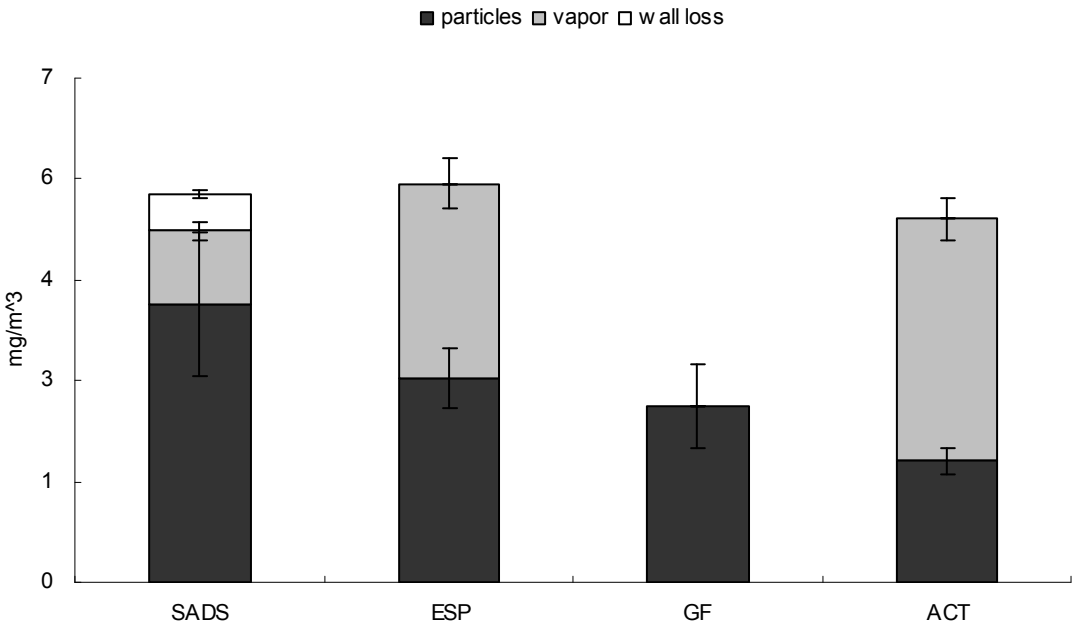

(d) Mixture total

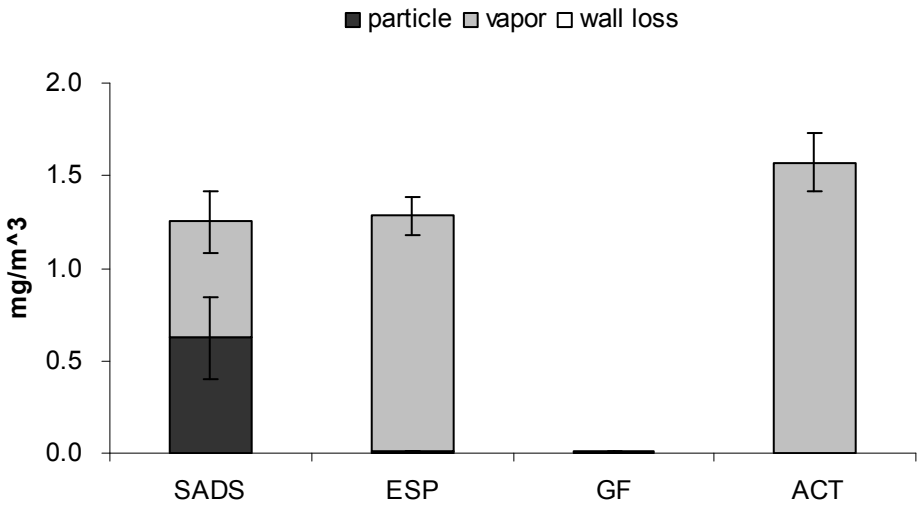

(a) EDM 40

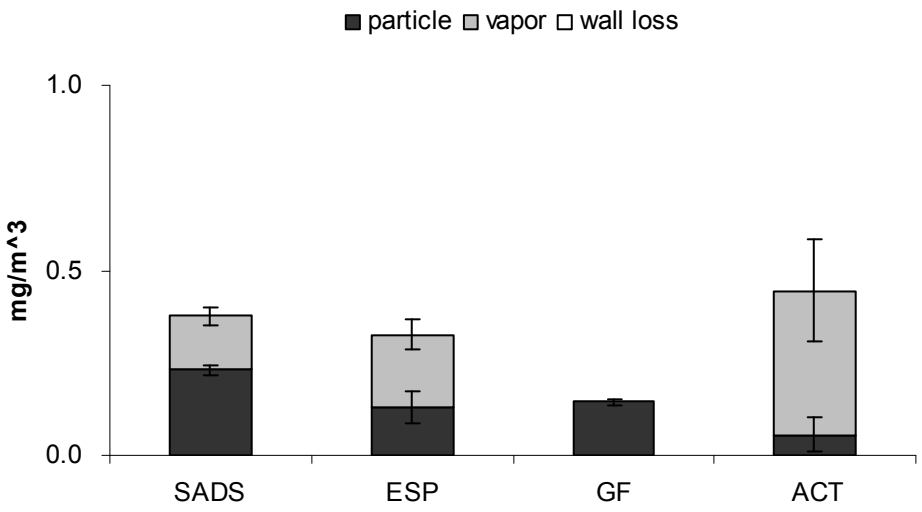

(b) Ilocut 5486

Figure 6. Vapor concentrations and particle concentrations of the two straight oil MWFs measured by four different methods. Error bars represent one standard deviation for each method.

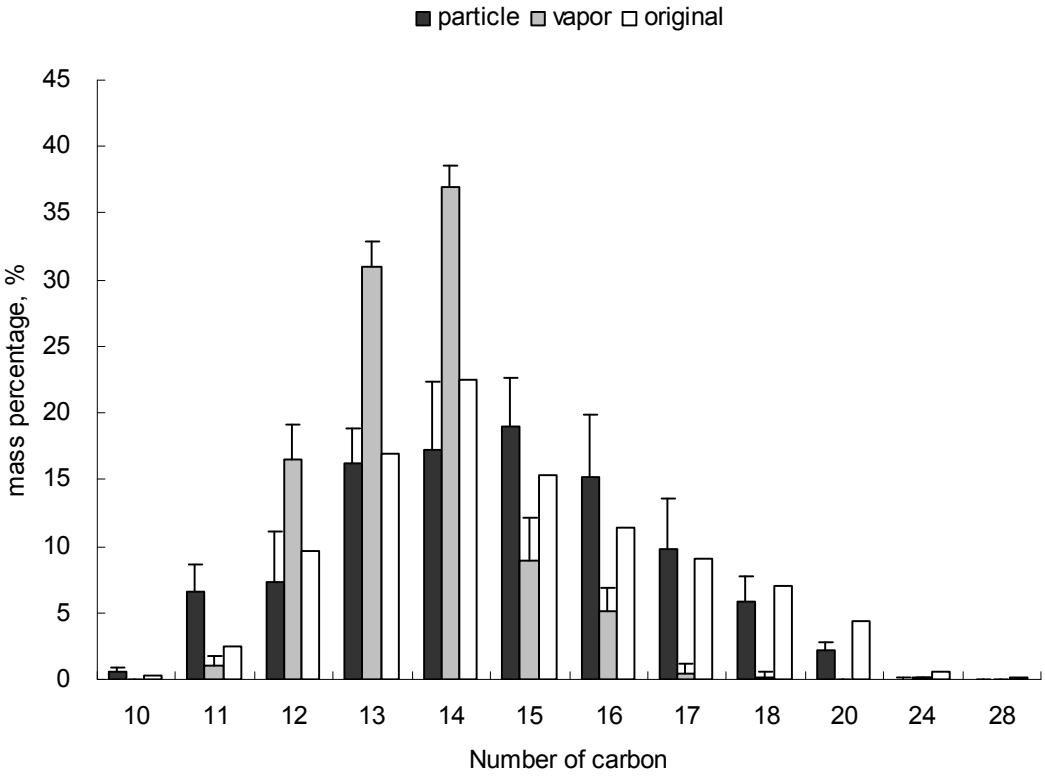

(a) EDM 40

Figure 7. Chemical compositions of vapor phase, particle phase, and original fluid of two straight oil MWFs measured by SADS. Error bars represent one standard deviation for each method.

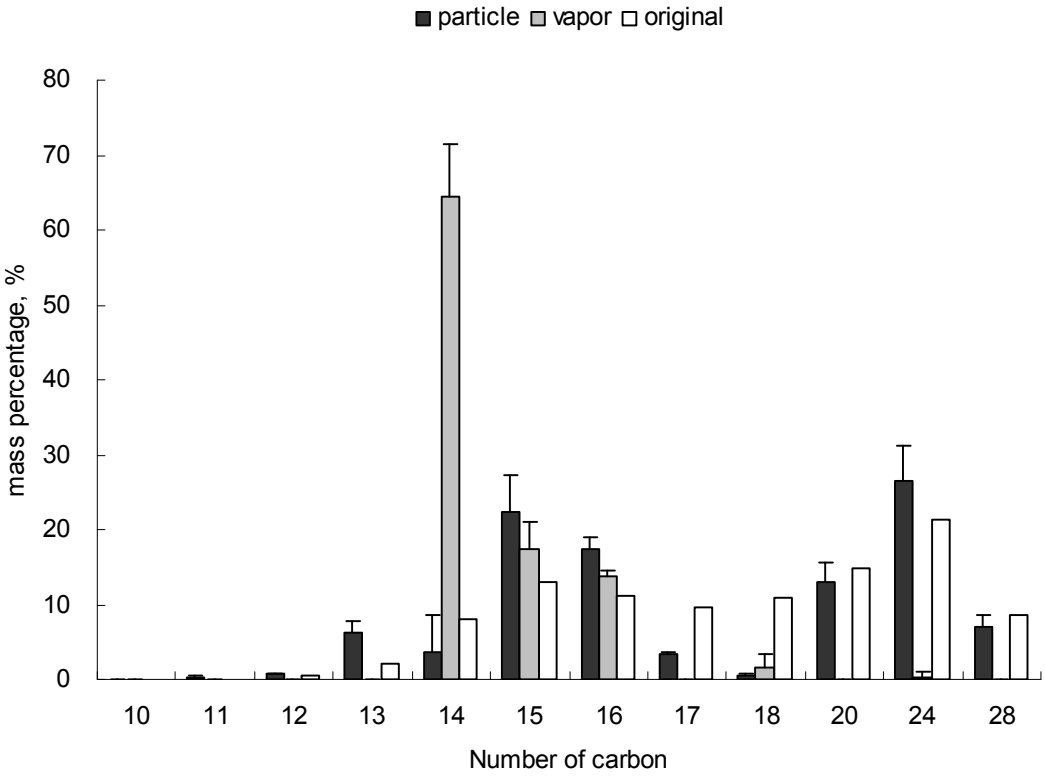

(b) Ilocut 5486

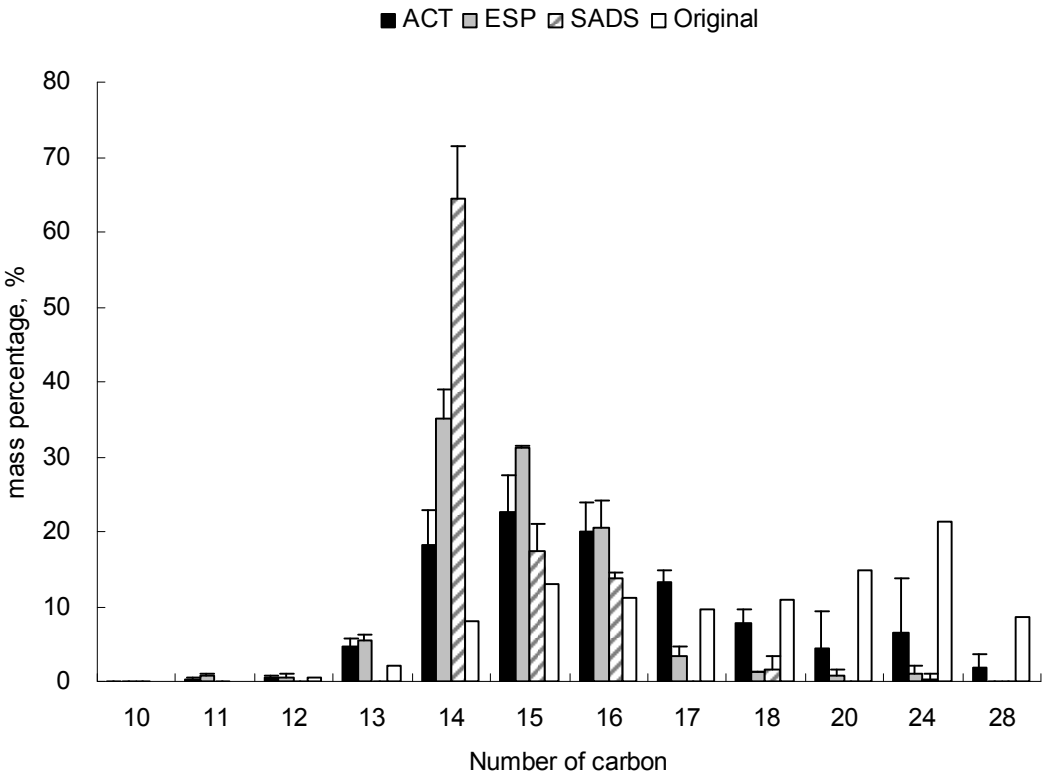

(a) Vapor phase

Figure 8. Chemical compositions of vapor phase (a), particle phase (b),and original fluid of Ilocut 5486 measured by sorbent tubes, GF, ESP, and SADS. Error bars represent one standard deviation for each method.

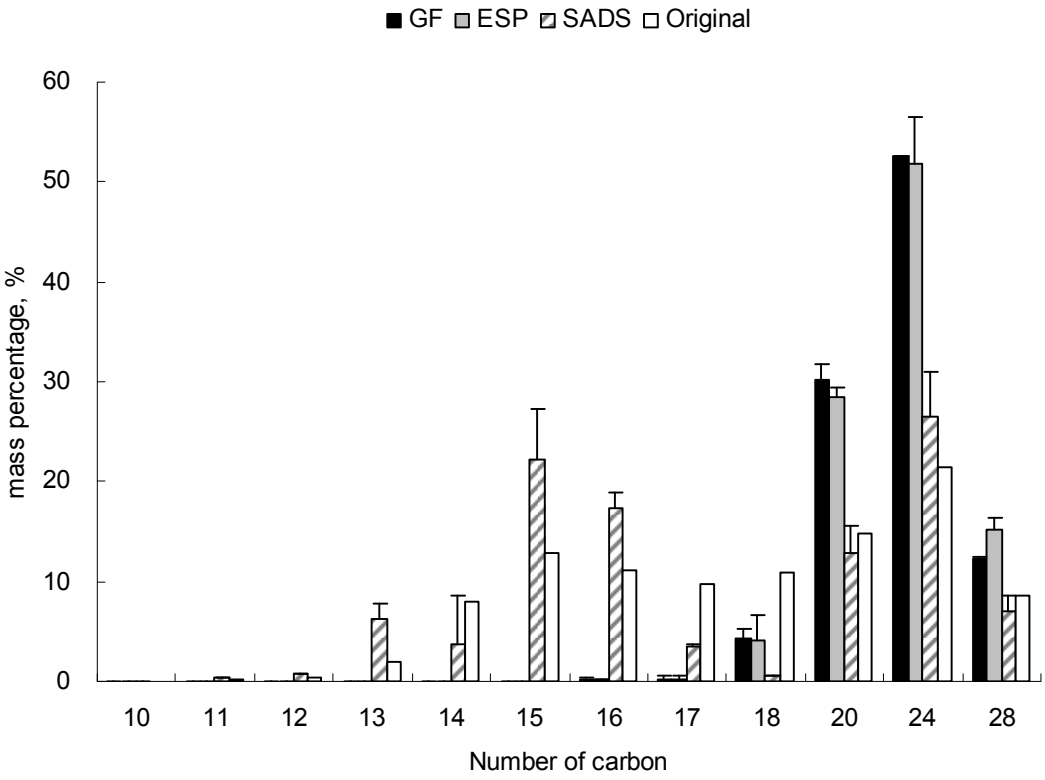

(b) Particle phase

CHAPTER V

Conclusions and Future Directions

5.1 Overall Conclusions

The long-range goal of this research was to evaluate the exposure of workers to particles and vapors more accurately. As a result of this study, SADS was determined to be able to assess each phase of semivolatile aerosols more accurately compared with other existing methods in personal sampling settings. This section draws the following conclusions and summarizes implications regarding the findings of this research.

A new approach to sampling aerosols using a virtual impactor (VI) was attempted using inverted flow ratios. A CFD model for VI and SADS settings was built and validated. The validated model shows that SADS settings provide much smaller cutsize and much smaller wall loss than VI settings. SADS is an approach that can lead to much more accurate sampling of the particle and vapor phases of a semivolatile aerosol.

Dimensional analysis and numerical simulations revealed the relationships between design and operating parameters and performance parameters for the SADS. The diameter ratio between the air nozzle and the collection probe and the flow split ratio between vapor flow and particle flow had significant effects on all the performance parameters of SADS. Using the equations defining the relationships, an

optimization procedure improved the modeled performance of the SADS. Experiments on a SADS built according to the optimal design indicated that the built SADS had a lower cutpoint than previous versions, although not as low as the model had anticipated. The experiments indicate that the instrument will separate particles and vapor effectively for particles larger than 0.25 μm in diameter.

For individual semivolatile compounds, their mixture, and real MWFs, the particle concentrations measured by the optimized SADS were statistically higher than those measured by either a filtration method or electrostatic precipitators. Higher wall loss than estimated from numerical models was found for non-volatile compounds. No wall deposition was observed for semivolatile aerosols. The compositions and the concentrations of each phase of real MWFs could be estimated from GC analysis.

The SADS separated vapor and particles and gave individual concentrations for each phase. The SADS worked well in realistic laboratory measurements without depending on the choice of sampling media.

5.2 Future Directions

Further research will continue with the following issues: i) characterization of wall loss as a function of particle size and the effect of the location of vapor flow outlet on wall loss; ii) comparison of the performance of SADS in steady concentrations and in fluctuating concentrations; and iii) development of a slit nozzle-type SADS to use in atmospheric studies and to lower the cutsize.

Significant amount of wall loss in SADS sampling was not simulated in numerical investigations (Chapter II and III), but detected in experimental data (Chapter IV). The location of the vapor outlet also seems affect the wall loss by making non-uniform flow inside the sampler. This issue should be studied more thoroughly to make SADS a more reliable sampling device for workplaces.

In this study, SADS was tested in fluctuating concentrations. Because of its instant separation of particles and vapor, SADS is expected not to be affected by the fluctuation of aerosol concentrations, which is considered as a substantial strength of SADS. This advantage of SADS needs to be further investigated by comparing with other methods in both steady concentrations and fluctuating concentrations. Other samplers are expected to show higher fraction of particles

when concentrations are steady than when concentrations fluctuate as long as the time-averaged concentrations of semivolatile aerosol are same.

To enable SADS to be used in personal sampling settings, the flow rate through SADS was limited in this study, which also limited the potential of having a lower cutsize. By not constraining the flow rate and by adopting a slit nozzle, SADS will be able to have a lower cutsize and be utilized in atmospheric studies in which the concentrations of contaminants are lower than those in workplaces in general.

APPENDIX

Appendix A: Cunningham Correction Program Used in Chapters II and III

This is a UDF used in Fluent and was provided by Xiaoliang Wang.

```
#include "udf.h"
#include "dpm.h"
#include "surf.h"
#define mfp_r 6.74e-8

DEFINE_DPM_DRAG(Cunningham_correction, Re, p)
{
      /* get the current cell that particle sit in */
      cell_t c = RP_CELL(&((p)->cCell));
      Thread *t = RP_THREAD(&((p)->cCell));

      double drag_force;
      double Dp = P_DIAM(p);
      double w,mfp,Cc;

      mfp = mfp_r;
      Cc = 1.0+2.0*mfp/Dp*(1.257+0.4*exp(-
1.1*Dp/2.0/mfp));

      if (Re < 0.01)
      {
            drag_force = 18.0/Cc;
      }
      else if (Re < 20.0)
      {
            w = log10(Re);
            drag_force = (18.0 + 2.367*pow(Re,0.82-
0.05*w))/Cc ;
      }
      else
      {
```

```
            /* Note: suggested valid range 20 < Re < 260
*/
            drag_force = (18.0 + 3.483*pow(Re,0.6305))/Cc;
      }

      return (drag_force);
}
```

BIBLIOGRAPHY

Alomar A. (1994) Occupational skin disease from cutting fluids. Dermatol Clin; 12(3) 537-546.

Asgharian B, Godo MN. (1997) Transportation and deposition of spherical particles and fibers in an improved virtual impactor. Aerosol Sci Technol; 27 499-506.

Aviado DM. (1996) Cardiovascular Disease and Occupational Exposure to Environmental Tobacco Smoke. Am Ind Hyg Assoc J; 57(3) 285-294.

Barr EB, Hoover MD, Kanapilly GM, Yeh HC, Rothenberg SJ. (1983) Aerosol concentrator. Aerosol Sci Technol; 2 437-442.

Bergman TA, Johnson DL, Boatright DT, Smallwood KG, Rando RJ. (1996) Occupational exposure of nonsmoking nightclub musicians to environmental tobacco smoke. Am Ind Hyg Assoc J; 57 746–752.

Bergstedt BA. (1956) Application of the electrostatic precipitator to the measurement of radioactive aerosols. J Sci Instr; 33 142-148.

Bidleman TE. (1988) Atmospheric processes – wet and dry deposition of organic compounds are controlled by their vapor-particle partitioning. Environ Sci Technol; 22 361-367.

Boulter JE, Cziczo DJ, Middlebrook AM, Thomson DS, Murphy DM. (2006) Design

and performance of a pumped counterflow virtual impactor. Aerosol Sci Technol; 40 969–976.

Brosseau LM, Fang CP, Snyder C, Cohen BS. (1992) Particle size distribution of automobile paint sprays. Appl Occup Environ Hyg; 7 607–612.

Brown RH, Monteith LE. (2001) Gas and vapor sample collectors. In Cohen BS, McCammon CS Jr., editors. Air sampling instruments for evaluation of atmospheric contaminants. Cincinnati: American Conference of Governmental Industrial Hygienists. p. 421-424. ISBN 1 882417 39 9.

Calvert GM, Ward E, Schnorr TM, Fine LJ. (1998) Cancer risk among workers exposed to metalworking fluids: a systematic review. Am J Ind Med; 33 282-292.

Cardello N, Volckens J, Tolocka MP, Wiener R, Buckley TJ. (2002) Technical note: performance of a personal electrostatic precipitator particle sampler. Aerosol Sci Technol; 36(2) 162-165.

Chein H, Lundgren DA. (1993) A virtual impactor with clean air core for the generation of aerosols with narrow size distributions. Aerosol Sci Technol; 18 376-388.

Chemical Substances Threshold Limit Values Committee. (1983) Separate TLVs for vapor and particulate. Ann Am Conf Govt Ind Hyg; 4 153-155.

Cheng Y-S. (2001) Denuder systems and diffusion batteries. In Cohen BS,

McCammon CS Jr., editors. Air sampling instruments for evaluation of atmospheric contaminants. Cincinnati: American Conference of Governmental Industrial Hygienists. p. 577-583. ISBN 1 882417 39 9.

Cheng Y, Tsai C. (1997) Evaporation loss of ammonium nitrate particles during filter sampling. J Aerosol Sci; 28 1553-1567.

Cochran WG, Cox GM. (1992) Experimental Designs. 2nd ed. New York: John Wiley & Sons. p. 356-357.

Cohen BS, Brosseau LM, Fang CP, Bower A, Snyhder C. (1992) Measurement of air concentrations of volatile aerosols in paint spray applications. Appl Occup Environ Hyg; 7 514-521.

CONCAWE. (1986) Health aspects of worker exposure to oil mists. Brussels 86/89.

Conner WD. (1966) An inertial-type particle separator for collecting large samples. J Air Pollut Control Assoc; 16(1) 35-8.

Decker HM, Buchanan LM, Frisque DE, Filler ME, Dahlgren CM. (1969) Advances in large-volume air sampling. Contamination Cot; 8: 13-17.

Ding Y, Koutrakis C. (2000) Development of a dichotomous slit nozzle virtual impactor. J Aerosol Sci; 31(12) 1421-1431.

Dixkens J, Fissan H. (1999) Development of an Electrostatic Precipitator for Off-Line Particle Analysis. Aerosol Sci Technol; 30(5) 438-453.

Durham JL, Wilson WE, Bailey EB. (1978) Application of an SO2 denuder for continuous measurement of sulfur in submicrometer aerosols. Atmos Environ; 12 883-886.

Dzubay TG, Stevens RK. (1975) Ambient air analysis with dichotomous sampler and x-ray fluorescence spectrometer. Environ Sci Technol; 9 663-668.

Eatough DJ, Lewis LJ, Eatough M, Lewis EA. (1995) Sampling artifacts in the determination of particulate sulfate and SO_2(g) in the desert Southwest using filter pack samplers. Environ Sci Technol; 29 787-791.

Fairchild CI, Tillery MI. (1977) The filtration efficiency of organic vapor sampling tubes against particulates. Am Ind Hyg Assoc J; 38 277-283.

Flagan RC. (2001) Electrical techniques. In Baron PA, Willeke K, editors. Aerosol measurement: principles, techniques, and applications. New York: Wiley-InterScience. p. 537-568. ISBN 0 471 35636 0

Fluent Inc. (2005) FLUENT 6.2 User's Guide. Fluent Inc. p. 23-5-11.

Forney LJ, Ravenhall DG, Lee SS. (1982) Experimental and theoretical study of a two-dimensional virtual impactor. Environ Sci Technol; 16 492-497.

Fuchs NA. (1964) The Mechanics of Aerosols. New York: Pergamon Press. p. 151-159.

Fylstra D, Lason L, Watson J, Waren A. (1998) Design and use of Microsoft Excel

solver. Interfaces; 28 29-55.

Garcia AM. (1998) Occupational exposure to pesticides and congenital malformations: a review of mechanisms, methods, and results. Am J Ind Med; 33 232-240.

Guidotti TL, Yoshida K, Clough V. (1994) Personal exposure to pesticide among workers engaged in pesticide container recycling operations. Am Ind Hyg Assoc J; 55 1154-1163.

Gunderson E, Anderson CC. (1987) Collection device for separating airborne vapor and particulates. Am Ind Hyg Assoc J; 48(7) 634-638.

Haglund JS, McFarland AR. (2004) A circumferential slot virtual impactor. Aerosol Sci Technol; 38 664–674.

Han R, Moss OR. (1997) Flow visualization inside a water model virtual impactor. J Aerosol Sci; 28 1005-1014.

Hari S, Hassan YA, McFarland AR. (2006) Optimization studies on a slit virtual impactor. Part Sci Technol; 24 105-136.

Hawthorne SB, Miller DJ, Louie PKK, Butler RD, Mayer GG. (1996) Vapor-phase and particulate-phase pesticides and PCB concentrations in eastern North Dakota air samples. J Environ Qual; 25 594-600.

Hering SV. (2001) Impactors, cyclones, and other particle collectors. In Cohen BS,

McCammon CS Jr., editors. Air sampling instruments for evaluation of atmospheric contaminants. Cincinnati: American Conference of Governmental Industrial Hygienists. p. 315-354. ISBN 1 882417 39 9.

Hinds WC. (1999) Aerosol Technology: Properties, Behavior, and Measurement of Airborne Particles. 2nd ed. Wiley-Interscience, New York, NY.

Hounam RF, Sherwood RJ. (1965) The cascade centripeter: a device for determining the concentration and size distribution of aerosols. Am Ind Hyg Assoc J; 26 122-131.

IARC. (1991) Occupational Exposures in Insecticide Application, and Some Pesticides. Lyon, France. IARC: IARC Monographs on the Evaluation on the Carcinogenic Risks to Humans, Volume 53.

IARC. (1997) Polychlorinated Dibenzo-para-Dioxins and Polychlorinated Dibenzofurans. Lyon, France. IARC: IARC Monographs on the Evaluation on the Carcinogenic Risks to Humans, Volume 69.

Jahn J, Krabs W. (1988) Applications of multicriteria optimization in approximation theory. In Stadler W, editor. Multicriteria optimization in engineering and in the sciences. New York: Springer. p. 64. ISBN 0306427435, 9780306427435

Jensen TE, Hites RA. (1983) Aromatic diesel emissions as a function of engine conditions. Anal Chem; 55 594-599.

Kagawa J. (2002) Health effects of diesel exhaust emissions—a mixture of air pollutants of worldwide concern. Toxicol; 181-182 349-353.

Kaupp H, Umlauf G. (1992) Atmospheric gas-particle portioning of organic compounds: comparison of sampling methods. Atmos Environ; 26 2259-2267.

Kimbrough RD. (1995) Polychlorinated biphyenyls (PCBs) and human health: an update. Crit Rev Toxicol; 25(2) 133-163

Koutrakis P, Sioutas C, Ferguson ST, Wolfson JM. (1993) Development and Evaluation of a glass honeycomb denuder/filter pack system to collect atmospheric gases and particles. Environ Sci Technol; 27 2497-2501.

Kreiss K, Cox-Ganser J. (1997) Metalworking fluid-associated hypersensitivity pneumonitis: a workshop summary. Am J Ind Med; 32 423-432.

Kriech AJ, Kurek JT, Wissel HL, Osborn LV, Blackburn GR. (2002) Evaluation of worker exposure to asphalt paving fumes using traditional and nontraditional techniques. Am Ind Hyg Assoc J; 63 628-635.

Krieger MS, Hites RA. (1992) Diffusion denuder for the collection of semivolatile organic compounds. Environ Sci Technol; 26 1551-1555.

Legraverend C, Guenthner TM, Nebert DW. (1984) Importance of the route of administration for genetic differences in benzo[a]pyrene-induced in utero toxicity and tetratogenicity. Teratology; 29 35-47.

Leith D, Leith FA, Boundy MG. (1996) Laboratory measurements of oil mist concentrations using filters and an electrostatic precipitator. Am Ind Hyg Assoc J; 57 1137–1141.

Li S-N, Lundgren DA. (1997) Effect of clean air core geometry on fine particle contamination and calibration of a virtual impactor. Aerosol Sci Technol; 27 625-635.

Lioy PJ, Daisey JM. (1986) Airborne toxic elements and organic substances. Environ Sci Technol; 20 8-14.

Lippmann M. (2001) Filters and filter holders. In Cohen BS, McCammon CS Jr., editors. Air sampling instruments for evaluation of atmospheric contaminants. Cincinnati: American Conference of Governmental Industrial Hygienists. p. 281-284. ISBN 1 882417 39 9.

Loo BW, Cork CP. (1978) Paper LBL-8204.University of California, Berkeley, California: Lawrence Berkeley Labs.

Loo BW, Cork CP. (1988) Development of high efficiency virtual impactors. Aerosol Sci Technol; 9 167-176.

Mainelis G, Adhikari A, Willeke K, Lee S-A, Reponen T, Grinshpun SA. (2002) Collection of airborne microorganisms by a new electrostatic precipitator. J Aerosol Sci; 33 1417–1432.

Malek RF, Daisey JM, Cohen BS. (1986) The effect of aerosol on estimates of inhalation exposure to airborne styrene. Am Ind Hyg Assoc J; 47 524-529.

Mark D, Lyons CP, Upton SL, Kenny LC. (1994) Wind tunnel testing of the sampling efficiency of personal inhalable aerosol samplers. J Aerosol Sci; 25 Supplement 1 S339-S340.

Marple VA, Chien CM. (1980) Virtual impactors: a theoretical study. Environ Sci Technol; 14 976-984.

Marple VA, Liu BYH. (1974) Characteristics of laminar jet impactors. Environ Sci Technol; 8 648-654.

Marple VA, Liu BYH. (1975) On fluid flow and aerosol impaction in inertial impactors. J Colloid interface Sci; 53 31-34.

Marple VA, Rubow KL, Olson BA. (1995) Diesel exhaust / mine dust virtual impactor personal aerosol sampler: design, calibration and field evaluation. Aerosol Sci Technol; 22 140-150.

Marple VA. (1970) A fundamental study of inertial impactors. PhD Thesis, Mechanical Engineering Department, University of Minnesota: Particle Technology Laboratory Publ. No. 144.

Marple VA. (2004) History of Impactors—The First 110 Years. Aerosol Sci Technol; 38 247–292.

Masuda H, Nakasita S. (1988) Classification performance of a rectangular jet virtual impactor. Effect of nozzle width ratio of collection nozzle to acceleration jet. J Aerosol Sci; 19(2) 243-252.

McFarland AR, Ortiz CA, Bertch Jr RW. (1978) Particle collection characteristics of a single-stage dichotomous sampler. Environ Sci Technol; 12 679-682.

Miller GT. (2004) Sustaining the Earth. 6th ed. Thompson Learning, Inc. Pacific Grove, California. Chapter 9, p. 211-216.

Munson BR, Young DF, Okiishi TH. (2002) Fundamentals of Fluid Mechanics. Danvers, MA: John Wiley & Sons, Inc. ISBN 0 471 44250 X.

National Research Council (NRC). (1986) Environmental tobacco smoke – measuring exposures and assessing health effects. Committee on Passive Smoking in NRC. p. 69-100.

Nebert DW, Jensen NM, Levitt RC, Felton JS. (1980) Toxic chemical depression of the bone marrow and possible aplastic anemia explainable on a genetic basis. Clin Toxicol; 16 99-122.

Nielsen T, Jørgensen HE, Larsen JC, Poulsen LM. (1996) City air pollution of polycyclic aromatic hydrocarbons and other mutagens: occurrence, sources and health effects. Sci Total Environ; 189/190 41-49.

NIOSH (1977). Occupational Exposure to Polychlorinated Biphenyls, USDHEW

(NIOSH) Publication 77-225.

NIOSH (1998). NIOSH Manual of Analytical Methods (NMAM). 4th ed., DHHS (NIOSH) Publication 94-113. Available from: URL: http://www.cdc.gov/niosh/nmam/nmammenu.html

NIOSH (1998). Occupational Exposure to Metalworking Fluids, DHHS (NIOSH) Publication 98-102.

NIOSH (2000). Health Effects of Occupational Exposure to Asphalt, DHHS (NIOSH) Publication 2001-110.

Nocedal J, Wright SJ. (1999) Numerical optimization. New York: Springer. p. 19-27. ISBN 0-387-98793-2

Noone KJ, Ogren JA, Heintzenberg J, Charlson RJ, Covert DS.(1988) Design and calibration of a counterflow virtual impactor for sampling of atmospheric fog and cloud droplets. Aerosol Sci Technol; 8(3) 235-244.

Norseth T, Waage J, Dale I. (1991) Acute effects and exposure to organic compounds in road maintenance workers exposed to asphalt. Am J Ind Med; 20 737-744.

O'Brien DM, Piacitelli GM, Sieber WK, Hughes RT, Catalano JD. (2001) An evaluation of short-term exposures to metalworking fluids in small machine shops. 62(3) 342-348.

Ounis H, Ahmadi G, McLaughlin JB. (1991) Brownian diffusion of submicrometer

particles in the viscous sublayer. J Colloid Interface Sci; 143(1) 266-277.

Pankow JF. (2001) A consideration of the role of gas/particle partitioning in the deposition of nicotine and other tobacco smoke compounds in the respiratory track. Chem Res Toxicol; 14(11) 1465-1481.

Park D, Kim S, Yoon C. (2003) Loss of straight metalworking fluid samples from evaporation during sampling and desiccation. Am Ind Hyg Assoc J; 64 837-841.

Perez C, Soderholm SC. (1991) Some chemicals requiring special consideration when deciding whether to sample the particle, vapor, or both phases of an atmosphere. Appl Occup Environ Hyg; 6(10) 859-864.

Perry RH. (1973) Chemical Engineer's Handbook. 5th ed. Columbus: McGraw-Hill Book Company, p. 2-81-83.

Peters AJ, Lane DA, Gundel LA, Northcott GL, Jones KC. (2000) A comparison of high volume and diffusion denuder samplers for measuring semivolatile organic compounds in the atmosphere. Environ Sci Technol; 34 5001-5006.

Piacitelli GM, Sieber WK, O'Brien DM, Hughes RT, Glaser RA, Catalano JD. (2001) Metalworking fluid exposure in small machine shops: an overview. Am Ind Hyg Assoc J; 62 356-370.

Poon WS, Pui DYH, Lee CT, Liu BYH. (1994) A compact porous-metal denuder for atmospheric sampling of inorganic aerosols. J Aerosol Sci; 25(5) 923-934.

Possanzini M, Febo A, Liberti A. (1983) New design of a high-performance denuder for the sampling of atmospheric pollutants. Atmos Environ; 17(12) 2605-2601.

Ramachandran G, Leith D. (1991) Cyclone optimization based on a new empirical model for pressure drop. Aerosol Sci Technol; 15 135-148.

Ravenhall DG, Forney LJ, Jazayeri M. (1978) Aerosol sizing with a slotted virtual impactor. J Colloid Interface Sci; 65(1) 108-117.

Raynor PC, Cooper S, Leith D. (1996) Evaporation of polydisperse multicomponent oil droplets. Am Ind Hyg Assoc J; 57(12) 1128-1136.

Raynor PC, Leith D. (1999) Evaporation of accumulated multicomponent liquids from fibrous filters. Ann Occup Hyg; 43(3) 181-192.

Raynor PC, Volckens J, Leith D. (2000) Modeling evaporative loss of oil mist collected by sampling filters. Appl Occup Environ Hyg; 15 90-96.

Rosenmann KD, Reilly MJ, Kalinowski D, Watt F. (1995) Occupational asthma and respiratory symptoms among workers exposed to machining fluids. In symposium proceedings of the Industrial Metalworking Environment. p. 143-146.

Rounds SA, Tiffany BA, Pankow JF. (1993) Description of gas/particle sorption kinetics with an intraparticle diffusion model: desorption experiments. Environ Sci Technol; 27(2) 366-377.

Simpson AT, Groves JA, Unwin J, Piney M. (2000) Mineral oil metal working fluids

(MWFs) – development of practical criteria for mist sampling. Ann Occup Hyg; 44 165-172.

Simpson AT, Wright MD. (2008) Diffusive sampling of C7-C16 hydrocarbons in workplace air: uptake rates, wall effects and use in oil mist measurements. Ann Occup Hyg; 52(4) 249-257.

Simpson AT. (2003) Comparison of methods for the measurement of mist and vapor from light mineral oil-based metalworking fluids. Appl Occup Environ Hyg; 18(11) 865-876.

Sioutas C, Koutrakis P, Burton PM. (1994) A high-volume small cutpoint virtual impactor for separation of atmospheric particulate from gases pollutants. Particulate Sci Technol; 12 207-221.

Solomon PA, Moyers JL, Fletcher RA. (1983) High-volume dichotomous virtual impactor for the fractionation and collection of particles according to aerodynamic size. Aerosol Sci Technol; 2 455-464.

Sprince NL, Palmer JA, Popendorf W, Thorne PS, Selim MI, Zwerling C, Miller ER. (1996) Dermatitis among automobile production machine operators exposed to metalworking fluids. Am J Ind Med; 30 421-429.

Tolman RC, Reyerson LH, Brooks AP, Smyth HD. (1919) An electrical precipitator for analyzing smokes. J Am Chem Soc; 41 587-589.

Turpin BJ, Liu S, Podolske KS, Gomes MSP, Eisenreich SJ, McMurry PH. (1993) Design and evaluation of a novel diffusion separator for measuring gas/particle distributions of semivolatile organic compounds. Environ Sci Technol; 27 2441-2449.

Van Vaeck L, Van Cauwenberghe K, Janssens J. (1984) The gas-particle distribution of organic aerosol constituents: measurement of the volatilization artifact in Hi-Vol cascade impactor sampling. Atmos Environ; 18(2) 417-430.

Verma DK, Shaw DS, Shaw ML, Julian JA, McCollin S-A, Tombe KD. (2006) An evaluation of analytical methods, air sampling techniques, and airborne occupational exposure of metalworking fluids. J Occup Environ Hyg; 3(2) 53-66.

Volckens J, Boundy M, Leith D, Hands D. (1999) Oil mist concentration: a comparison of sampling methods. Am Ind Hyg Assoc J; 60 684-689.

Volckens J, Boundy M, Leith D. (2000) Mist concentration measurements II: laboratory and field evaluations. Appl Occup Environ Hyg; 15(4) 370-379.

Volckens J, Leith D. (2002) Electrostatic Sampler for Semivolatile Aerosols: Chemical Artifacts. Environ Sci Technol; 36 4608-4612.

Volckens J, Leith D. (2003) Partitioning theory for respiratory deposition of semivolatile aerosols. Ann Occup Hyg; 47(2) 157-164.

White FM. (1994) Fluid mechanics. 3rd ed., McGraw-Hill. p. 213.

White KLJ, Lysy HH, Holsapple MP. (1985) Immunosuppression by polycyclic aromatic hydrocarbons: a structure-activity relationship in B6C3F1 and DBA/2 mice. Immunopharmacology; 9 155-164.

Wilkening MH. (1962) A monitor for natural atmospheric radioactivity. Nucleonics; 10(6) 36-39.

Wolff MS. (1985) Occupational exposure to polychlorinated biphenyls (PCBs). Environ Health Perspectives; 60 133-138.

World Health Organization. (1996) Diesel fuel and exhaust emissions. International Program on Chemical Safety. Environmental Health Criteria 171, Geneva, Switzerland.

Woskie SR, Smith TJ, Hallock MF, Hammond SK, Rosenthal F, Eisen EA, Kriebel D, Greaves IA. (1994) Size-selective pulmonary dose indices for metal-working fluid aerosols in machining and grinding operations in the automobile manufacturing industry. Am Ind Hyg Assoc J; 55(1) 20-29.

Woskie SR, Smith TJ, Hammond SK, Hallock MH. (1994) Factors affecting worker exposures to metal-working fluids during automotive component manufacturing. Appl Occup Environ Hyg; 9 612-21.

Woskie SR, Smith TJ, Hammond SK, Schenker MB, Garshick E, Speizer FE. (1988) Estimation of the diesel exhaust exposures of railroad workers: I. current

exposures. Am J Ind Med; 13(3) 381-394.

Xiong JQ, Fang C, Cohen BS. (1998) A portable vapor/particle sampler. Am Ind Hyg Assoc J; 58 614-621.

Yaws CL. (1994) Handbook of Vapor Pressure. Gulf Pub. Co., Houston, TX.

Zaebst DD, Clapp DE, Blade LM. (1991) Quantitative determination of trucking industry workers exposures to diesel exhaust particles. Am Ind Hyg Assoc J; 52(12) 529-541.

Zhang X, McMurry PH. (1987) Theoretical analysis of evaporative losses from impactor and filter deposits. Atmos Environ; 21 1779-1789